ACCURACY ASSESSMENT OF FUZZY CLASSIFICATION

EZEILO CHEKWUBE BARTHOLOMEW
March, 2011

SUPERVISORS:
Dr. N.A.S. Hamm
Dr. V.A. Tolpekin

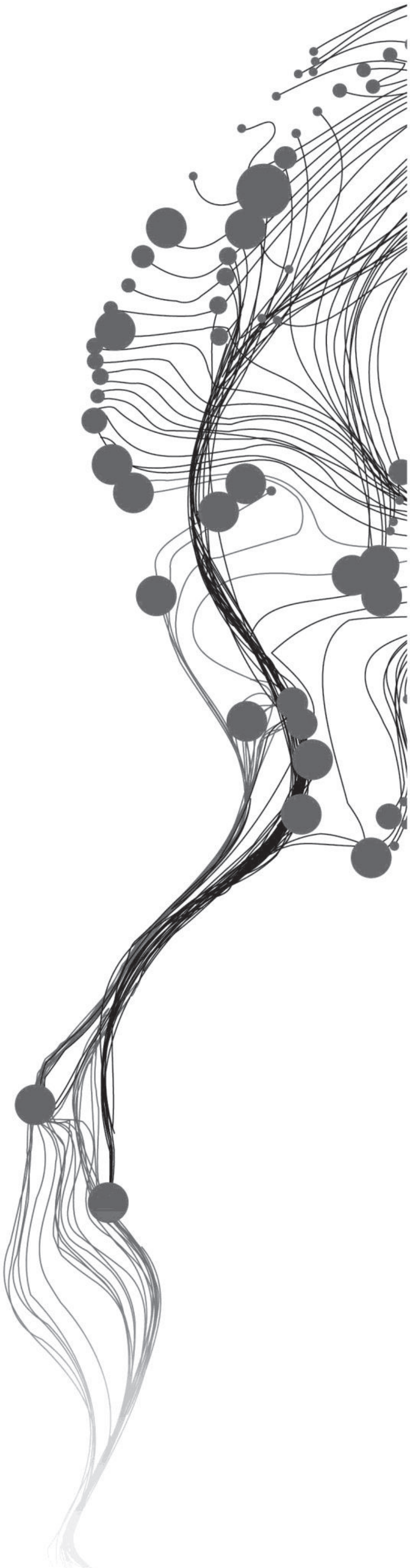

ACCURACY ASSESSMENT OF FUZZY CLASSIFICATION

EZEILO CHEKWUBE BARTHOLOMEW
Enschede, The Netherlands, March, 2011

Thesis submitted to the Faculty of Geo-Information Science and Earth Observation of the University of Twente in partial fulfilment of the requirements for the degree of Master of Science in Geo-information Science and Earth Observation.
Specialization: Geoinformatics

SUPERVISORS:
Dr. N.A.S. Hamm
Dr. V.A. Tolpekin

THESIS ASSESSMENT BOARD:
Prof.Dr.Ir. A. Stein (Chair)
Dr.Ir. G.W.A.M. van der Heijden (External examiner)

ABSTRACT

Remote sensing technology captures information about an object. The wealth of information extractable from an object is dependent on the nature of the object and the technique applied in the extraction. Objects in remote sensing can be divided into two forms: (1) Objects that have definite boundaries - they can be easily identified and described they are referred to as crisp objects; (2) Objects whose boundaries are shrouded in mysteries (indefinite-cannot be easily determined and identified), they are referred to as fuzzy objects. Assessing the accuracy of crisp object can be easily done using the error matrix which is by convention, the traditional way of assessing the accuracy of crisp objects. Defining the boundary of a fuzzy object is difficult and assessing the accuracy as well, has not been standardized; hence, it is the focus of this research.

The fuzziness in an object is as a result of uncertainty, before an attempt is made to characterise the object, there is need to identify the uncertainty in the object. Several forms of uncertainty exist; however, the uncertainty in the fuzzy object of interest was defined as the vagueness that results when the boundary of the object lies within the zone of transition.

The east fork fire burn scar that occurred in April 2004 was the choice of the fuzzy object. MODIS and ASTER images were acquired for classification and generating the reference. MODIS image was classified using four classification techniques (unsupervised crisp (ISODATA), supervised crisp (Maximum likelihood), unsupervised and supervised fuzzy-c-means). Three cases were investigated for each classification scheme, in which 2, 3 and 4 classes were defined as Case A, Case B and Case C respectively. The reference data was generated by using the same classification scheme as MODIS'; the output was degraded to make it comparable with the pixels of the MODIS.

The accuracy of the classifications was judged using the entire image as samples. The conventional error matrix was used to assess the crisp outputs; the fuzzy error matrix was used to assess the fuzzy outputs. The crisp and fuzzy outputs were also assessed by determining the association of each class with the reference this was referred to as correlation coefficient determination.

The results obtained from the crisp assessment was higher than those obtained from the fuzzy assessment, the correlation coefficient values were higher in the fuzzy outputs than for the crisp outputs. Also, the fuzzy outputs gave a better description of the burn scar phenomenon than that obtained from the crisp descriptions.

Key words: Fuzzy objects, Un-supervised and supervised crisp classifications, Un-supervised and supervised fuzzy classifications, Accuracy assessment.

ACKNOWLEDGEMENTS

First and foremost, am grateful to God Almighty, who brought me this far, without him, the essence of my existence and this thesis work, will be worthless, am grateful to you Lord!

I expressed my deepest appreciation to my wonderful supervisors, Dr. N.A.S. Hamm and Dr. V.A. Tolpekin, without them, this piece of work would not have been a success; thank you sirs for all the criticisms, corrections, suggestions and encouragement, I owe the success of this work to you both.

Am also grateful to all the staff of ITC, who in one way or the other helped me to become who I am today: my special greeting goes to the course director, Mr. Gerrit Huurneman, thank you sir for the fatherly role you played in my life here in ITC and most importantly during this research period, am very grateful sir.

I am grateful to my family members, for all their supports, prayers and encouragement; obviously I would not have come this far without them. Thank you so much dad, mum, Sis.Vicky, Chy, Uche, Kechis, Cb and Ogo; I love you all!

Am grateful to you sirs; Rev. Canon Emeka Onwuakpa, Bro. John Udensi, Bro. Ndubuisi, Bro. Prosper and the host of others, indeed God will continue to bless you all for all the investment of prayers you continue to make to God on my behalf.

This is specially for you my sweety! You are simply the best, your prayers, encouragement and positive words to me are just indescribable; love you dear.

Finally, I salute all my friends here in ITC, especially my classmates GFM 2 2009, who in one way or the other touched my life, God bless you all real good!

TABLE OF CONTENTS

LIST OF FIGURES

LIST OF TABLES

1. INTRODUCTION

1.1. Background

Over the years, remote sensing technology has grown to become a tool that is widely embraced and used by people from diverse field of endeavours to acquire information about the environment or Earth related issues that are of interest to them. This information becomes available when the remotely sensed data are processed and presented, often as maps with various themes (Hammen, 1997). The information extracted is usually an approximation of the geographic reality, hence the results obtained are geo-information that are not completely accurate; the degree of inaccuracy varies depending on the image processing and analytical method used, the intended application, the expert knowledge etc (Weng & Lu, 2007).

Image classification is one of the important steps in image processing, that can lead to the production of thematic maps depicting land cover or land use information (Foody, 2008). Classifying remotely sensed data can be very complex due to the various factors that interact during the process, such as the data used for the classification, classifier used, the nature of the study sites etc (Weng & Lu, 2007); these factors influence results obtained from image classification (the description of the Earth's phenomenon of interest is affected); evaluating the outcome of an image classification establishes the quality information of the derived product as well as aid in the better understanding of the phenomenon of interest. The choice of the evaluation approach depends on so many factors; however, the consideration in this research is centred on the evaluation of the classified output of an object whose spatial extent cannot be easily established or defined because its boundary is vague (fuzzy). The proceeding sections and chapters throw more light on this.

1.2. Motivation and problem statement

The use of remote sensors to capture data about our environment, results in different types of objects. According to (Cheng, Molenaar, & Lin, 2001), we can distinguish these objects based on their thematic nature, geometric nature and inherent uncertainties by using three statements: the existential statement- it talks about the thematic and spatial conditions that implies an object exists; the extensional statement- it talks about identifying the geometric elements that describes the spatial extent of an object; the geometric statement- it talks about the identification of the actual shape, size and position of an object from a metric sense (Molenaar & Cheng, 1998). There are several sources of uncertainties, which affect the accurate determination of the spatial extent (Cheng & Molenaar) as well as the thematic interior of remotely sensed objects; as a result, it becomes very difficult defining and describing these objects. Some of these sources of inherent uncertainties were described by (Cheng, 2002), they are: vagueness in determining object boundary; multiple criteria used in delineating objects, this is different from person to person; spatial incompleteness, in which objects are categorized to give them meaning in a particular context, while in another context, they are treated as undefined; time incoherency, in which object definition is subject to a specified period of time and then changes; sampling and measuring error, resulting from data observations etc.

Five categories of objects were described by (Cheng, 2002); they are: (1) Crisp-Crisp (CC) object- This is the only object assumed not to be fuzzy, its boundary points (spatial extent) and its thematic interiors are well defined and determined, there is no area of confusion between one object and the other, hence no transition zone, each pixel of the object belongs to only one class, the uncertainty in identifying the object is based on error, which is probabilistic in nature and can be modelled; (2) Fuzzy-Fuzzy (FF) object- The boundary points (or spatial extent) and its thematic interior are not clearly defined,(i.e. vague or fuzzy), they have transition zones and it is possible to assign a pixel of the object to more than one class, using fuzzy membership functions to show the degree to which the pixel is a member of each class; (3) The Alpha-Fuzzy (αF) object- this object results by assigning a threshold value α to the boundary of FF-object, in this case, the object has defined boundary points (or spatial extent) described by the α value, but its thematic interior is still fuzzy, these are areas of confusion, characterized by transition zones; (4) Crisp-Fuzzy(CF) object- This object does not overlap with another, areas of transition does not exist, because the boundary points (or spatial extent) of the object is conceptualized to be determined by a given condition (criteria). However its thematic interior is still fuzzy; (5) Fuzzy-Crisp (FC) object- The boundary of this object cannot be defined, resulting in transition zones between the object and another, however, its interior can be clearly defined. From the above, we can see that four categories of fuzzy objects exist (FF, αF, CF and FC) all these have one form of fuzziness or the other in determining their boundary points (spatial extent) and or thematic interiors, resolving this fuzziness using remotely sensed data, is difficult because of the following reasons: Nature is made of geographic entities which are continuous in space, it is not clear where the boundary of objects actually lies, hence, the interpretation of boundary points in remote sensing will differ from one person to another. Objects or entities are heterogeneous, they mix with each other, this results in different people, giving different opinion about their extent (Foody, 1999). Most objects are dynamic and changes with time, this makes it difficult to accurately establish their boundaries, (McNicoll, 1997). Most objects are scale and context dependent, as a result, resolutions plays a big role in revealing or concealing information about them, this makes the definition of the extent of object subjective (Fowler, 1991).

The object of interest in this research work is fuzzy object. Fuzzy object of interest is the burnt scar that resulted from the forest fire that engulfed the Apalachicola National Forest in April 2004. It is located in Florida, United States of America. The need for this research is centred on characterizing the burnt scar using its spatial extent and position within the Apalachicola National Forest in Florida, United States of America. This is necessary because, classifying and assessing the accuracy of this kind of object (fuzzy) is still been investigated; much research work is still needed to be done so as to understand and describe the object better; adequate understanding and description of the burnt scar phenomenon provides useful information that will be beneficial to the government, forest services, fire fighters etc, in damage assessment programme, preventive measures against future forest fire occurrences etc. Furthermore, this research will be a stepping stone, on which further work can be based and developed.

(Green & Congalton, 2009) stated that object classification and the method used is very important, because it influences the validation and the accuracy of our derived product. Most of the research works done so far are mainly centred on the definition and classification of crisp objects. In classifying and assessing the accuracy of crisp object, there is the assumption that the object is unique, homogenous and mutually exclusive; hence, classification results, in assigning object to a class, each of its pixels belongs to one and only one class. However, nature is hardly homogenous; hence,(Lizarazo & Barros, 2010), pointed out that, representing nature as crisp object, will results in the lost of information, because the uncertainty due to unclear definition of the object (vagueness) is not considered. A better approach is to consider it as a fuzzy object; this takes into account the vagueness of the object and expresses it using fuzzy logic, with this a pixel of the object belongs to all the defined classes based on its membership values determined by the membership function used. This is referred to as fuzzy classification.

Fuzzy method of object classification uses fuzzy logic, which originated in the mid-1960s by the work of Lotfi Zadeh, but became a valuable tool for use in fuzzy object classification in the 1990s (Williams, Kessinger, Abernethy, & Ellis, 2009). The fuzzy (soft) method of classifying object, adapts more to nature's reality; hence it is more suitable in handling features with vague or unclear boundaries and or thematic interiors.

Assessing the accuracy of object is still been debated and researched (Foody, 2002; Fuller, Groom, & Jones, 1994); there exist several methods of assessing the accuracy of objects, based on the object's uniqueness; with this, the accuracy components assessed by each method differs (Lark, 1995). No one unique and acceptable measure of accuracy exist, it is dependent on the feature of interest (Stehman, 1997) and the intended application. One school of thoughts, suggested, the need to standardize the accuracy assessment methods and styles of reporting (Smits, Dellepiane, & Schowengerdt, 1999), with the variety of needs and interpretation that exists and the complex nature of the world, a single all-purpose measure of accuracy assessment is not feasible (Foody, 2002).

The accuracy of crisp objects, are mostly assessed and expressed using the confusion matrix (Pontius, 2000), which is a probabilistic measure (Stehman & Czaplewski, 1998) and the kappa coefficient. The method for validating and assessing the accuracy of fuzzy object is yet to be fully popularized by one or more known techniques, unlike crisp object (validation and accuracy assessment has been popularized by the use of the confusion matrix and kappa coefficient). The subject of finding a common method for assessing the accuracy of fuzzy object is still been researched.

The desire for this research work is to classify fuzzy object and assess the accuracy of the derived product, so as to understand and describe the phenomenon better; to achieve this, the burnt scar resulting from the forest fire of April 2004 in the Apalachicola National Forest in Florida, United States of America was used as a case study.

1.3. Research identifications

The research was carried out in order to fulfil the stated objectives and provide answers to the questions raised. The research objectives and questions are stated below.

1.3.1. Research objectives

The major aim of the research is to determine the accuracy measures for fuzzy classification. However, to achieve this, the following sub-objectives and as well as the provision of answers to the following questions were formulated.

The following were the sub-objectives addressed in the research:

- To establish the definition of forest fire burn scar.
- To classify the study area using fuzzy classifier in order to determine burnt scar and un-burnt areas.
- To determine the method to generate the reference data.
- To determine the applicable accuracy assessment technique(s) that can be used to judge the performance of the fuzzy classifier.

1.3.2. Research questions

The following research questions will assist in reaching the stated objectives, they are:

- What are the characteristics elements that defines forest fire burn scar?
- What factors influences the identification of forest fire burn scar?
- What accuracy value is achievable when fuzzy-c-means classifier is used?
- What accuracy assessment technique is appropriate and why?
- What reference data should be used and how can we validate the result produced?

1.4. Research set-up

A summary of the adopted approach in this research is shown in Figure 1.1. The MODIS and ASTER images are acquired for classification and reference data generation purposes respectively. Both images are imported, explored and prepared for further analysis. The MODIS image is classified using hard and soft classification methods, before its accuracy is assessed using the reference data. The reference data is the classified output of ASTER image, which is degraded before making it comparable to the MODIS image.

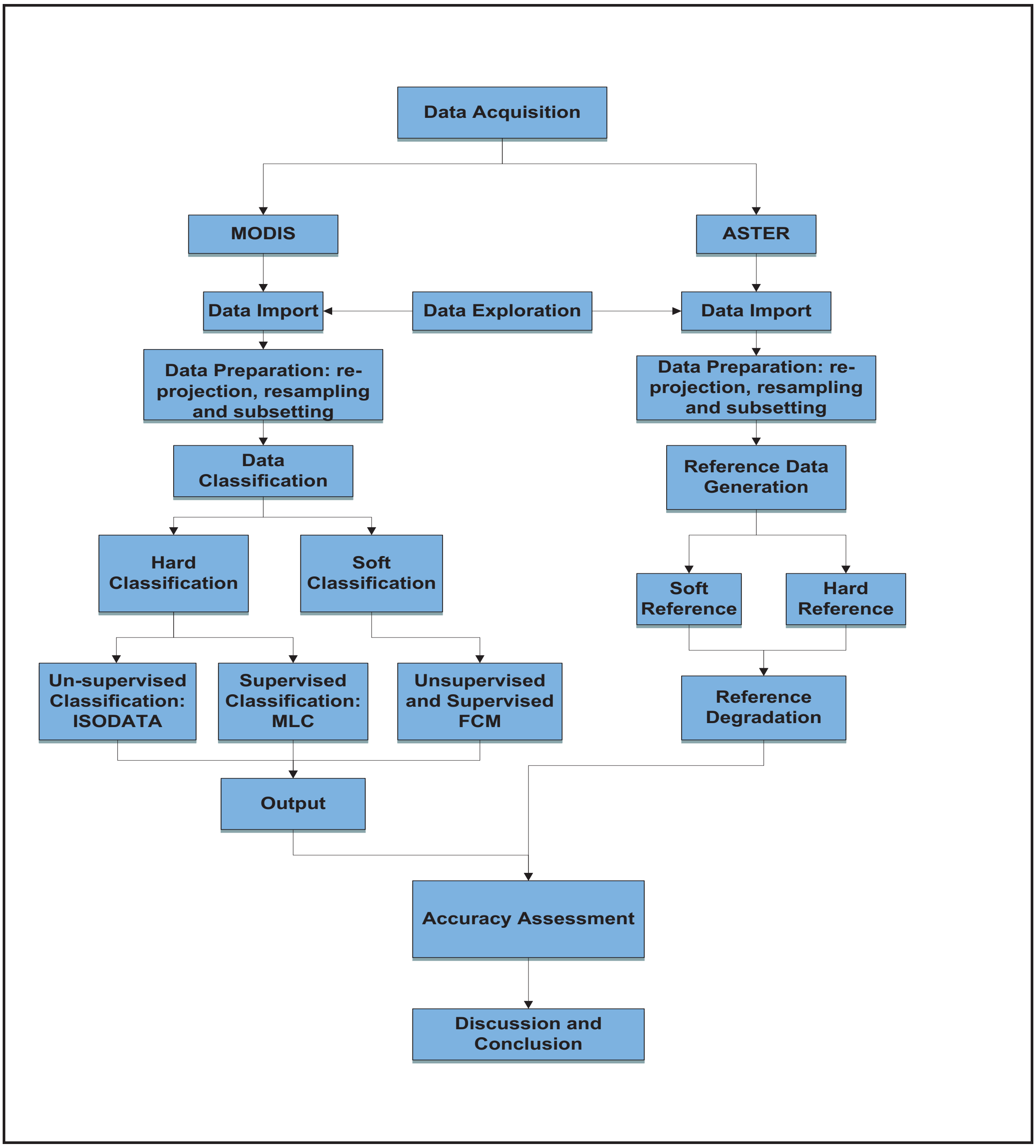

Figure 1.1: Research set-up

1.5. Structure of thesis work

This thesis work is made up of six chapters. In chapter 1, general back ground information as well as the research objectives and research questions were explained. Chapter 2, is made up of literature review, in which the background knowledge of the burn scar was explained, image classifications and as well as accuracy assessment issues were discussed. Chapter 3 explained the study area, data used, data preparation and the software used. Chapter 4 described the adopted methodology. In Chapter 5, the results obtained were presented. In chapter 6, the results were discussed, conclusions and recommendations were made.

2. LITERATURE REVIEW

2.1. Forest fire and burn scar

Forest fire occurrence is a global phenomenon that affects the natural ecosystem, destroying several thousands of hectares of forest, farmland, houses and infrastructures (Ambrosia & Brass, 1988). There is the need to monitor forest fire, assess the extent of damage and proffer solutions on the possible preventive measures to adopt. One of the ways to achieve this, is by doing a post forest fire analysis of an area affected by forest fire, this is referred to as burn scar area.

Burn scar is the damage that results from forest fire engulfment (Key & Nate, 2004). The extent or size of the burn scar is dependent on the nature, spread and severity of the fire. The extent or size of the scar can be studied to provide useful information that can be of assistance in describing and understanding the forest fire phenomena and occurrences. Remotely sensed technique can be applied to capture the data about the forest affected area, this will be processed to produce the burn scar map.

Burn scar is characterized by dark or black patches (pixels) with varying degree of burnt, within the area affected by forest fire; this area contains fully burnt pixels (which will fully belong to the burn scar), partially burnt pixels (which is within the boundary point of the burn scar and un-burnt feature) and pixels that are not burnt (belongs entirely to the un-burnt feature). Using the object model defined by (Cheng, 2002), we can categorise the fully burnt pixels to be part of the interior of the burn scar, while the partially burnt pixel is embedded within the boundary area of the burn scar and the boundary area of the un-burnt feature: this is referred to as the zone of transition from where there is a gradual change from burn scar region to un-burn feature and vice-versa. It is very difficult demarcating this region in order to determine the actual boundary line between these features (Fisher, Arnot, Wadsworth, & Wellens, 2006); the un-burnt pixel lies completely within the interior of the un-burnt feature. The area of confusion lies in determining the label for the pixels within the area of transition. The transition zone results in an unclear definition of the extent of the burn scar, because its boundary cannot be easily defined, uncertainty is introduced by this which is referred to as vagueness (fuzziness) (Atkinson & Foody, 2006). Uncertainty resulting from vagueness (fuzziness) can be modelled using fuzzy logic; this will make a pixel belong to all the classes to a certain degree defined by a membership function that assigns membership values to the pixel in all the classes. Another approach will be to assign the pixel to one and only one class, this will not resolve the transition zone problems, as a result we lose information about the object we have modelled, to guide against information lose so as to have a better description and the understanding of the fuzzy phenomenon, the burn scar was chosen as the fuzzy object of interest. The transitional phenomenon is shown in Figure 1.3.

Figure 2.1: Intergrade phenomenon used to depict area of transition (vagueness): Source:(Fisher, 1997)

Figure 1.3, represents the diagram depicting the zone of transition. Within this zone, it is difficult to determine the boundary of features; this is because it represents a gradual change from one phenomenon to the other.

2.2. Image classification

Image classification is one of the most important aspects in remote sensing for the production of thematic maps. Most image classifiers use the clustering method to classify images. Partitions are created to define groups of pixels. Each group of pixels forms a cluster (class). Clustering tends to group the pixels in a form such that the distributions of pixels and the resulting patterns within an image can be easily recognised and understood (Tso & Mather, 2001). Partitioning of an image can result in hard (clusters do not overlap) or fuzzy clusters (natural way to represent Earth features- clusters can overlap).

2.2.1. Hard clustering

Hard clustering is the conventional method of partitioning an image into a finite number of clusters c, that are mutually exclusive from each other. It is formulated from the classical set theory and can be mathematically, stated below with the following assumptions:
Let $Y = \{y_1, y_2, \ldots, y_N\}$ be a sample of N observations in $\mathbf{R}^n$ (n-dimensional Euclidean space); y_k = k-th feature vector; y_{kj} the j-th feature of y_k; c is an integer, defined by: $2 \leq c < n$. Therefore, a hard c-partition of Y, results in c-tuple $(Y_1, Y_2, \ldots Y_c)$ of subsets Y that satisfies the conditions below (Bezdek, 1981):

$$Y_i \neq \phi;\ 1 \leq i \leq c; \quad (2.1)$$

$$Y_i \cap Y_j = \phi;\ 1 \leq i \neq j \leq c, \quad (2.2)$$

$$\bigcup_{i=1}^{c} Y_i = Y \quad (2.3)$$

$$\phi \subset Y_i \subset Y;\ 1 \leq i \leq c, \quad (2.4)$$

$\bigcup$, $\bigcap$ represents union and intersection respectively, ϕ = empty set.

The interpretation of the above equation is thus: Y is the total number of clusters created within a given image, each cluster is identified by its name Y_i. Equation (2.1) explains the fact that each created cluster cannot be empty, it must contain pixels. More so, the number of clusters created starts from 1 to a finite number. Equation (2.2) explains the fact that each created cluster is unique and contains pixels with distinct positions. This means two clusters cannot overlap, hence their intersection results in null. In other words, they must be disjoint. Equation (2.3) states that when we combine the clusters (union), it should result in Y, which is the whole image. Equation (2.4), states clearly that each of the cluster is not empty and must be a subset of the whole image Y.

In hard clustering, pixels are assigned only one membership value (0 or 1) as defined by the membership function. Membership refers to the condition by which a pixel belongs to a cluster, this condition is expressed by a membership function which is a graph that maps a pixel to obtain either the value of 1 or 0. When a pixel belongs to a cluster, its membership value is 1; when it does not belong to a cluster is membership value is 0. This can be mathematically stated below:
If the partitions in an image are represented in matrix form $\mathbf{U} = [\mu_{ik}]_{c \times N}$. The ith row of the matrix contains the membership values as defined by the membership function μ_i of the ith subset Y_i of Y. Thus the following equation is stated (Bezdek, 1981).

$$\mu_{ik} \in \{0, 1\}; \quad 1 \leq i \leq c; \quad 1 \leq k \leq N; \tag{2.5}$$

$$\sum_{i=1}^{c} \mu_{ik} = 1; \quad 1 \leq k \leq N, \tag{2.6}$$

$$0 < \sum_{k=1}^{N} \mu_{ik} < N; \quad 1 \leq i \leq c, \tag{2.7}$$

$$\mu_i(y_k) = \mu_{ik} \begin{cases} 1; & y_k \in Y_i \\ 0; & \text{otherwise} \end{cases} \tag{2.8}$$

The explanation for the above equations is stated thus: Equation (2.5), expresses the fact that the membership value a pixel can get is either 0 or 1 in a cluster. Equation (2.6), expresses the fact that the sum total of the membership value of a pixel in the entire clusters is 1. Equation (2.7), states that the sum total of the membership value of a pixel in the entire image must be greater than 0. However, equation (2.8), confirms the fact that, once a pixel has been identified to belong to a cluster, it takes full membership value in that cluster, which is 1 and in any other cluster, its membership value will be 0 (no membership in that cluster). Thus, it is confirmed that in hard clustering, a pixel, belongs entirely to only one cluster with full membership value of 1 and 0 membership values in other clusters. A simple diagram illustrates this further;

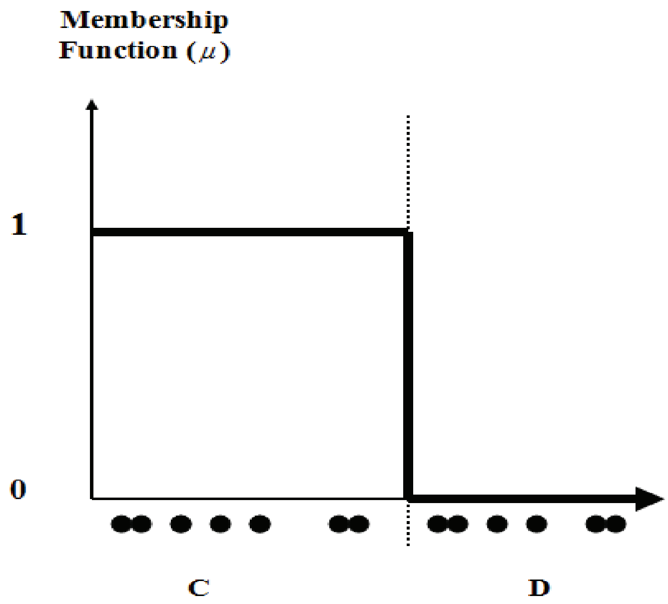

Figure 2.2: A hard clustering membership value.

Figure 2.2, shows a membership function for two partition C and D, it can be noticed that the pixels in cluster C, belong entirely to cluster C and each have a membership value of 1, neither of them, obtained any value from cluster D. In cluster D, none of its pixel, obtained value in cluster C.

Combining equation (2.1-2.8), a summary of the hard clustering space is thus (Bezdek, 1981):

$$\mathbf{T}_{\text{space}} = \left\{ \mathbf{U} \in \mathbf{R}^{c \times N} \;\middle|\; \mu_{ik} \in \{0, 1\}, \forall\, i,k;\ \sum_{i=1}^{c} \mu_{ik} = 1;\ \forall\, k;\ 0 < \sum_{k=1}^{N} \mu_{ik} < N,\ \forall\, i \right\}$$

Hard clustering algorithm can change the pixel position of a pixel to suit the iterative processes, but still, a one-pixel-one-cluster relationship is maintained. Hard clustering does not allow cluster overlap, however, most features of interest on the Earth surface are never distinct, they overlap with the neighbouring features. If a classifier used to describe this feature of interest results in hard classification, then some information about the feature will be lost, since the overlapping area will not be considered as such. Figure 2.3, is a simple diagram that shows the distinct nature of clusters in hard clustering below.

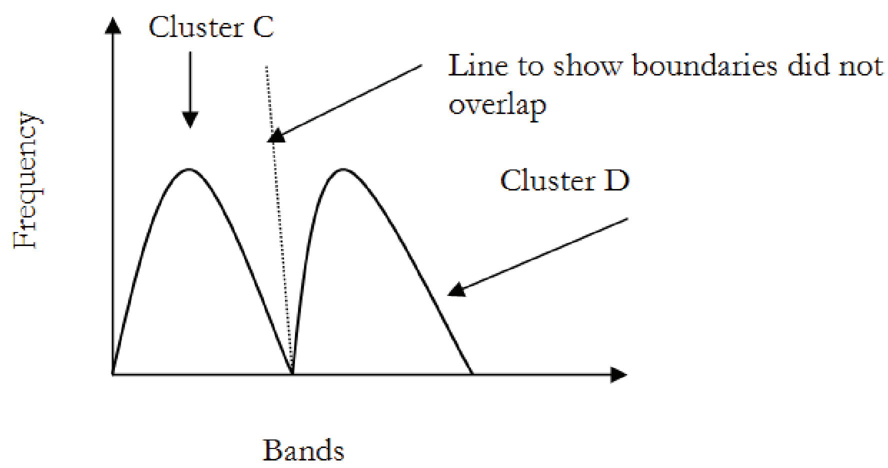

Figure 2.3: A simple diagram to illustrate the distinct nature of clusters boundaries in hard clustering.

The above diagram shows clusters C and D. It is distinctly shown that cluster C and cluster D, did not overlap. In other words, the boundary of C does not overlap with that of D. Boundaries of clusters with hard clustering, follows this trend.

To understand and describe burnt scar phenomenon, hard and fuzzy clustering classifiers were used. In this section, the hard clustering method is described; they are:

- Hard clustering classifier:
  - Unsupervised classifier-Iterative self-organising data analysis technique (ISODATA).
  - Supervised classifier-Maximum Likelihood Classifier (MLC).

2.2.1.1. Unsupervised classifier-Iterative self-organising data analysis technique (ISODATA)

Iterative self-organizing data analysis technique (ISODATA) is an unsupervised crisp clustering classification techniques. The process is initialized by the human operator, assigning three different parameters to the process, these are: the maximum number of clusters needed (N), the convergence threshold (T) and the maximum number of iterations to be performed (M). Once this is done, the process creates random cluster centres in which each pixel is assigned to base on the shortest distance to mean centre criteria. The standard deviation within each cluster is computed as well as the distance between clusters, merging of clusters results when the distance between clusters are less than the defined threshold or split when the one or more standard deviation is greater than the defined threshold. The iteration is again performed using the new cluster centres; again the split and merge criteria is applied, depending on which condition is met, to create new set of cluster centres; the iterative procedures continues until the average inter-class distance falls below the defined threshold, the average change in the inter-centre distance between iterations is less than the threshold or when the number of iterations is reached. During the duration of the process, clusters having less than the required number of pixels are removed, while lone pixels are either reclassified or ignored (Memarsadeghi, Netanyahu, & LeMoigne, 2006; Richards, 1993).

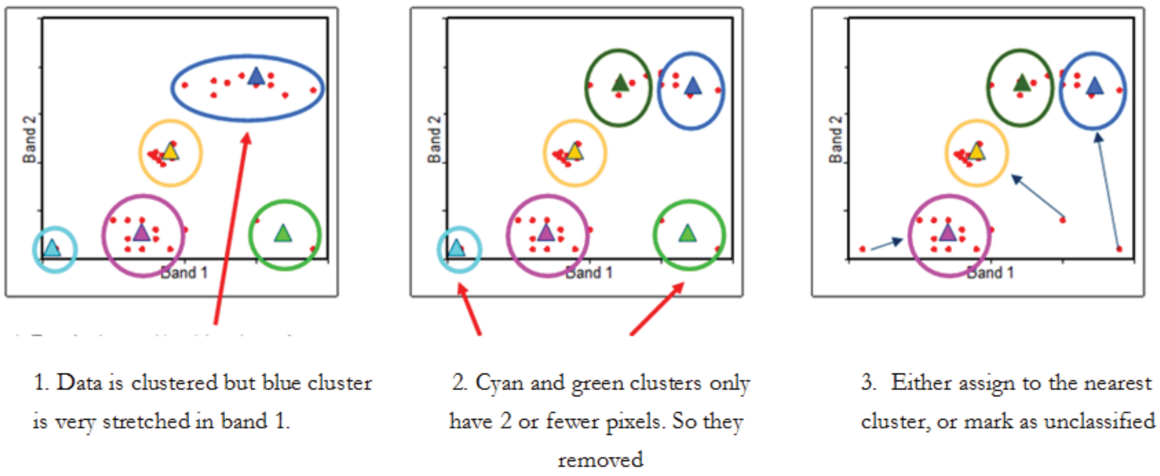

Figure 2.4: A diagram illustrating the iterative process of ISODATA: Source: (SPEAR, 2006)

Advantages of this method are:

- Limited knowledge about the data is required before hand.
- Interaction from the human operator is minimal.
- Effective in spectral identifying spectral clusters.
- Not-biased to top pixels in the image as against sequential clustering.
- Non-parametric, hence, data need not be normally distributed.
- Successful in finding “true” data when the number of iterations is sufficient.

- The saved cluster signature can be incorporated and used with supervised classification signature.

Disadvantages of the method are:

- Algorithm can spill out of control with unfavourable outcome.
- Can be time consuming when data is not well structured(Richards, 1993).

2.2.1.2. Supervised classifier-Maximum Likelihood classifier (MLC)

The supervised-Maximum Likelihood classifier (MLC) is a crisp classification algorithm. It is based on statistical principles and requires prior knowledge about the data, in order to determine the required number of classes. Samples of pixels are selected within all the classes defined to train the classifier to recognise the defined spectral patterns. During the process of classification, the spectral variance and covariance for each class is computed. The assumption in MLC, is that, it is a multivariate normally distribution function, hence each class is modelled to have a mean and covariance. The MLC builds a discriminant function for each class and uses this function to calculate the probability of each pixel, belonging to that class. Each pixel is therefore assigned to the class, in which its probability is highest (Memarsadeghi, et al., 2006; Richards, 1993).

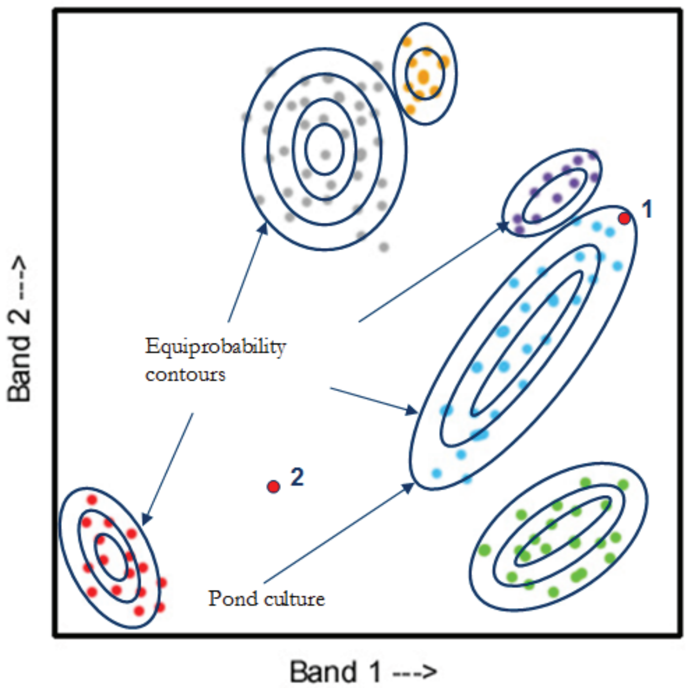

.

-Normal probability distributions are fitted to each training class.
-The lines in the diagram show regions of equal probability.
-Point 1 would be assigned to class 'pond culture' as this is most probable.
-Point 2 would generally be unclassified as the probabilities of fitting into one of the classes would be below threshold.

Figure 2.5: A diagram to illustrate MLC process. Source: (SPEAR, 2006)

Advantages of this method are:

- It is sophisticated and results in good separation of classes.
- It takes into account the size, shape and orientation of the clusters.
- It takes into account variability within the clusters.

Disadvantages of this method are:

- Requires training sets that truly reflects the variability within and between classes, before a meaningful mean and covariance can be computed.
- Requires lost of human interaction, especially during the training stage.
- It requires lost of computation time
- It based on normal distribution(Richards, 1993).

2.2.2. Fuzzy clustering

Fuzzy clustering method tends to be more natural when partitioning an image to form clusters. The resulting clusters are not mutually exclusive; hence, overlapping of clusters can take place. Each pixel belongs to all the clusters created to a certain degree expressed by its membership value. The membership value of a pixel is constrained to be real value between 0 and 1 and it is defined by a given membership function (non-linear). Thus, a pixel that lies close to the centre (or centroid) of a cluster has a high membership value in that cluster; conversely, a pixel that is far from a cluster has low membership value in that cluster. If the membership value of a pixel in a cluster is close to 1, it is an indication that the pixel has property that is similar to the property of that cluster and if it is low close to 0, it means the property of the cluster it has is low (Bezdek, Ehrlich, & Full, 1984).This is a more realistic way to describe Earth's related phenomenon. Earth's related phenomenon, interacts with its neighbours, hence it cannot be fully described if its relationship with its neighbours are not considered. Fuzzy clustering is formulated from fuzzy logic theory developed by (Zadeh, 1965). Mathematically, it can be expressed as follows:
The $\mathbf{R}^n$ (*n*-dimensional Euclidean space) defined in hard clustering section, still suffices here, equation (2.2), is now modified to reflect the relationship between one cluster and the as shown below;

$$Y_i \cap Y_j \neq \phi; \; 1 \leq i \neq j \quad \leq c, \qquad (2.9)$$

Equation (2.9), states the dependence between one cluster and the other. This statement shows cluster overlap; hence the intersection of two clusters will not result in null, this is not the same for hard clustering case. Also, equation (2.5) is modified to create the real values [0, 1] as shown:

$$\mu_{ik} \in [0, 1]; \; 1 \leq i \leq c; \; 1 \leq k \leq N; \qquad (2.10)$$

This expresses the fact that the membership value of a pixel can be any real value between 0 and 1. Equation (2.6) and (2.7) still holds in this instance. However, equation (2.8), does not apply in this case, because the function must not restrict the pixel from having membership values in other clusters, hence the membership value of a pixel in a cluster will be determined by the membership function (non-linear), chosen to describe the pixel in all cluster.

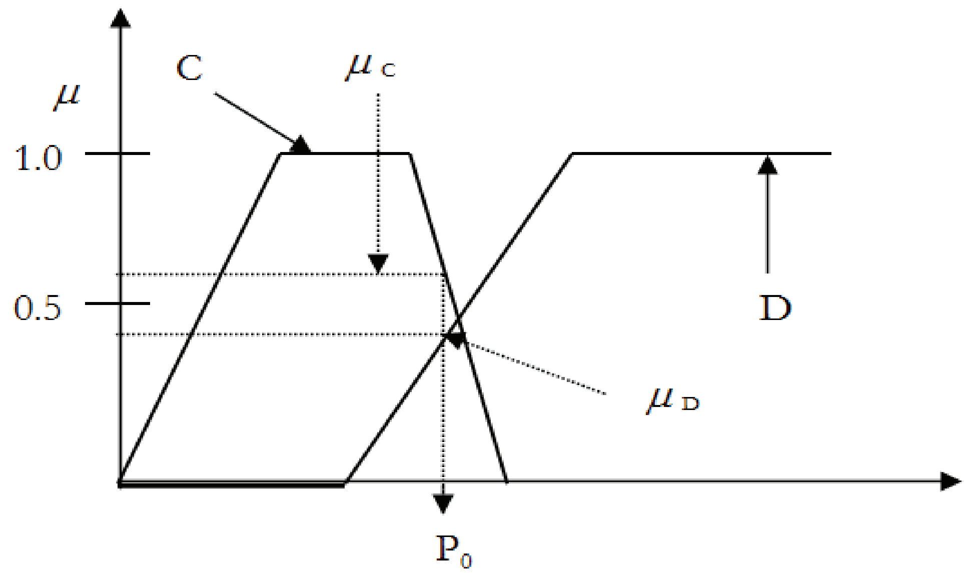

Figure 2.6: Fuzzy membership function

In figure 2.6, two clusters C and D are shown. The membership function of C and D, gives its pixels membership values μ_C and μ_D respectively. P_0 belongs to both C and D, hence its membership value in both clusters can be seen be to $\mu_C(P_0)$ 0.60 and $\mu_D(P_0) = 0.40$; Two clusters are defined, hence

$$\sum_{i=1}^{c} \mu_i = 1 = \mu_C(P_0) = 0.60 + \mu_D(P_0) = 0.40 \text{ condition is fulfilled.}$$

The entire space for the fuzzy cluster can be defined by their membership function as:

$$\mathbf{T}_{\mathbf{mfspace}} = \left\{ \mathbf{U} \in \mathbf{R}^{c \times N} \;\middle|\; \mu_{ik} \in [0, 1], \forall\, i,k;\ \sum_{i=1}^{c} \mu_{ik} = 1;\ \forall\, k;\ 0 < \sum_{k=1}^{N} \mu_{ik} < N,\ \forall\, i \right\}$$

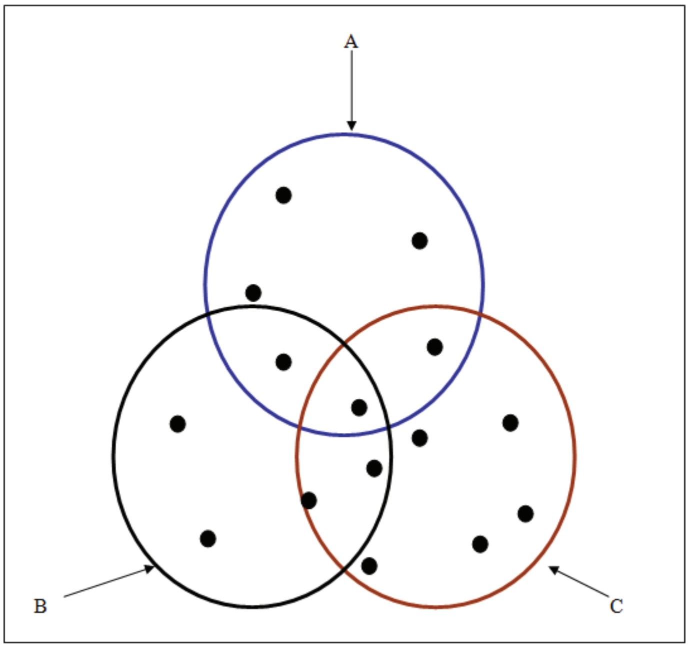

Figure 2.7: FCM clustering

Figure 2.7, depicts the boundaries of clusters A, B and C overlapping. Clearly it can be seen that a pixel belong to more than one cluster.

This fuzzy clustering method was applied to describe the burnt scar phenomenon, the fuzzy classifier used are:

- Fuzzy clustering classifier:
  - Unsupervised and supervised classifier-Fuzzy-c-means (FCM).

2.2.2.1. Unsupervised and supervised classifier-Fuzzy-c-means (FCM)

Fuzzy-c-means algorithm uses the concept of fuzzy logic theory (Zadeh, 1965) and the fuzzy clustering (Bezdek, 1981) to define a function referred to as an objective function. The function is an optimization function, in which the centroids (centres) of a given number of defined clusters will be iteratively updated until the desired minimum value for the objective function is attained, as this process is ongoing, pixels positions and their membership values in all the clusters continues to change and becomes constant when the desired minimum value for the objective function is attained, at this point the process is completed. The function is defined by a given number of parameters that influences the outcome of the pixel membership values. The mathematical process is shown below and adopted from (Bezdek, et al., 1984). The notations and explanation of variables remains the same from previous section.

$$J_m = \sum_{i=1}^{c} \sum_{k=1}^{N} (\mu_{ik})^m \| y_k - v_i \|_A^2 \qquad (2.11)$$

J_m = is the objective function; v_i = is an element of v, the vector of cluster centres i.e.

$$v = [v_1, v_2, \ldots, v_c] \quad v_i \in R^n \qquad (2.12)$$

c is the number of clusters in Y; $2 \leq c < n$ (2.13)

The fuzzy c-partition of Y is U; $U = [\mu_{ik}] \in M_f$ (2.14)

n = any arbitrary integer number

M_f = is the membership function

m = is the fuzziness parameter; $m \in [1, \infty)$ (2.15)

If m =1, it results in hard classification; fuzzy classification results when:

$$1 \leq m < \infty \qquad (2.16)$$

A= squared weight matrix; $\| \|$= norm

$\| y_k - v_i \|$ = is referred to as the positive difference between a pixel point y_k and a cluster centre v_i, this is usual calculated using the Euclidean distance, D_{ik}, when this is replaced, replacing equation $\| y_k - v_i \|$ with D_{ik} in equation 3.11, we obtain:

$$J_m = \sum_{i=1}^{c} \sum_{k=1}^{N} (\mu_{ik})^m (D_{ik})^2 \qquad (2.17)$$

To obtain the minimum objective function, two concurrent iterative processes are done to obtain new cluster centre v_i and new pixel membership value μ_{ik}, both equations are shown below (Dunn, 1974):

$$v_i = \frac{\sum_{k=1}^{N} (\mu_{ik})^m y_k}{\sum_{k=1}^{N} (\mu_{ik})^m} \quad ,1 \leq i \leq c \qquad (2.18)$$

and

$$\mu_{ik} = \frac{1}{\sum_{j=1}^{c} (D_{ik} / D_{jk})^{2/(m-1)}} \qquad (2.19)$$

The FCM algorithm works when the following parameters are defined:

- The number of clusters or classes c is defined.
- The measure of fuzziness m is defined, in this research m= 2. (Foody, 1996), suggested that 2, is an adequate measure of fuzziness.
- The number of iterations.

- The termination criterion ε .

Fuzzy-c-means algorithm can either be supervised or unsupervised. In supervised fuzzy-c-means, the estimated means of the clusters are determined by the human operator and imputed in the algorithm; these means will be used to determine the positions of all the pixels and their respective membership values in all the clusters; hence the cluster mean is determined by the human operator and not by the algorithm in the case of unsupervised fuzzy-c-means.

2.3. Accuracy assessment

Map production, is an important aspect of remote sensing. Maps contain information about the Earth which is needful for planning and decision making purposes. It is essential that the information in the map be 'judged' through an assessment technique in order to establish its accuracy. Accuracy statement is an indication of the quality information in the map and expresses the measure of uncertainty that the user should be aware of. When the accuracy information of a map or data is provided, the confidence of using the map or data is boosted; this is because, one is aware of its uncertainty. However, using a map or data without any accuracy information, might lead to unpleasant surprises(Congalton & Green, 2009). Accuracy assessment can be designed and implemented in various ways depending on some factors and limitations. It is essential that the producer's intended approach in implementing accuracy assessment is carefully and critically planned in order to obtain the optimum result.

2.3.1. Definition of accuracy assessment

Accuracy assessment was defined by (Stehman & Czaplewski, 1998), as the quantitative measure(s) applied in determining the quality of information derived from remotely sensed data. Map is used to represent the information and it is evaluated to establish its suitability for an intended purpose.

2.3.2. Need for accuracy assessment

Accuracy assessment is needful because it establishes the quality information in a map, thereby increasing knowledge. More so, it identifies the sources of errors in a map, this can be corrected to increase the quality information of the map. Furthermore, it is a basis for comparing algorithm, classifiers etc, to establish which is better, depending on the prevailing situations. Accuracy assessment report is useful in making decisions (Congalton, 2004).

2.3.3. Forms of accuracy assessment

Positional and thematic accuracy, are the two major forms of accuracy assessment. Positional accuracy assessment measures the spatial differences or mis-match between spatial features on the map and its corresponding features on the ground (Bolstad, 2005; Pontius, 2000). Thematic accuracy assessment measures the disagreement between the label or attributes of a map class and its corresponding reference class.

2.3.4. Developmental stages in accuracy assessment

Accuracy assessment technique started in the early days as a qualitative measure, in which a map is visually inspected and compared with what is on the ground (or reference) and statement of "it looks good" or "it looks bad" is ascribed to it. This method does not involve the identification of errors and its sources. A global accuracy is stated based on the appearance of the map only (Aronoff, 1982, 1985; Congalton & Green, 1993, 1999).

The next development in accuracy assessment was the non-site specific method; in this method, the overall acreages were compared between ground estimates and the map without taking into consideration the location (Meyer, Brass, Gerbig, & Batson, 1975; Van Genderen & Lock, 1977; Van Genderen, Lock, & Vass, 1978). One obvious flaw in the non-site specific method, is that, it can establish the area estimates between the class of interest and its ground equivalent with low spatial overlap between them(Meyer, et al., 1975); positional error in this method is high.

The third stage of accuracy assessment technological development, led to the creation of site specific approach; in this method, random areas (sites) within the classified map, are made comparable with their corresponding areas on the ground or reference data. A single global (overall) accuracy value in form of percentage can be calculated to establish matching areas and areas that do not match.

Presently, we are in the fourth stage of the technological developments in accuracy assessment techniques. In this stage, several accuracy assessment techniques have been developed for crisp and for fuzzy classification purposes.

In crisp classification, the error or confusion matrix is mostly used; it is referred to as the conventional error matrix. Error matrix is a square matrix, in which either the number of rows or the number of columns corresponds to the number of classes generated during classification. The element of the matrix represents the number of sampling units that either matches or mis-matches between the reference and classified map when they are compared on a site by site basis(matches and mis-matches are judged based on their corresponding locations). The diagonal elements represent correctly classified points, while off-diagonal elements represent in-correctly classified points. The assumption made in using the error matrix, is that the reference data is a true reflection of reality, hence samples generated from it have the correct class labels and that the errors generated during accuracy assessment comes from the classification processes and other sources. This assumption is erroneous, the reference data is as well prone to errors and affects the accuracy assessment results(Foody, 2009).Various measures can be computed from the error matrix, such as: the overall or global accuracy-this is computed by dividing the summation of all the diagonal elements with the total sample size ; errors of commission (this indicates the correspondence between correctly classified points in a row and the total sample points in the row) and omission (this establishes the correspondence between correctly classified sample points in a column and the total points in that column); user's accuracy (stating that a sample unit classified, corresponds to that on the ground)and producer's accuracy (indicates to the producer, how well an area can be classified) can be computed from the matrix(Card, 1982; Khorram et al., 1999). Kappa coefficient is another measure that can be derived from the error matrix, it is measure of chance agreement that compares the overall performance of the classification with a hypothetically generated random classification (Landis & Koch, 1977). The user, producer and overall accuracies can be determined from the conventional error matrix; their determinations are thus stated below using a simplified error matrix diagram.

Table 2.1: The conventional error matrix

3_classes						
	Conventional error for 3-classes				**Total**	**User accuracy (%)**
	Reference					
Classified data		A	B	C		
	a	25	1	5	31	81
	b	0	42	10	52	81
	c	3	7	57	67	85
	Total	28	50	72	**150**	
	Producer accuracy (%)	89	84	79		
		Overall (%)		**83**		

Table 2.1, represents a 3 by 3 error matrix used to depict three classes a, b and c; the corresponding reference is represented using A, B and C. In this case, pixels value (a pixel has only one value, this shows the class category it belongs) that match between reference and classified data are determined. The elements within the matrix, represent sampled units (pixels), from the table a total of 150 pixels were sampled; elements within the diagonal in blue (25, 42 and 57), represent pixels that correspond (correctly classified pixels) between the classified data and the reference. Off-diagonal elements represent mis-classification. Thus, the following measures can be determined from the matrix:

- Overall accuracy: This is a probability measure that expresses the percentage of correctly classified pixels (pixels value between classified data and reference that match). It is computed by the summation of the diagonal elements (25+42+57) divided by the total sampled pixels (150), the result is expressed as a percentage, for table 2.1, 83% was obtained as the overall accuracy. Overall accuracy is represented using a single value.
- User accuracy: This is a probability measure that expresses the percentage that the class of a sampled pixel, corresponds to the class of the reference. It is computed in each row, by taking the diagonal element in that row (taking the matching element between classified and reference data) divided by the sum of elements in the row. The values obtained, correspond to the number of rows, from the table three values were obtained, one for each row, they are:
  - User accuracy row 1: (25/31) * 100 = 81%
  - User accuracy row 2: (42/52) * 100 = 81%
  - User accuracy row 3: (57/67) * 100 = 85%
- Producer accuracy: This is a probability measure that expresses the percentage that the class of a sampled pixel corresponds to the class of the classified data. It is computed in each column, by taking the diagonal element in that column (taking the matching element between classified and reference data) divided by the sum of elements in the column. The values obtained correspond to the number of columns, from the table, three values were obtained, one for each column, they are:
  - Producer accuracy column 1: (25/28) * 100 = 89%
  - Producer accuracy column 2: (42/50) * 100 = 84%
  - Producer accuracy column 3: (57/72) * 100 = 79%

The conventional error matrix was designed to assess the accuracy of crisp classification; as a result, it has some limitations. According to (Knight, 2002), the assumption that the reference data selects data for comparison ascribing one class to a site, is not absolutely true, this is because defining reality can be vague (fuzzy) within the transition zones, hence a site can belong to more than one class, when it is represented in only one class, some information is lost. Furthermore, the off-diagonal errors are treated equally, which is not true in remote sensing classification. The need to improve on this limitations, led to the advent of fuzzy accuracy assessment.

Fuzzy accuracy assessment was developed to take into consideration, the vague nature of the Earth in image classification and as well as in assessing its accuracy. Hence, the sampling unit can be assigned to all the classes it belongs to; subject to its membership degree in all the classes. This was achievable by using the concept of fuzziness and fuzzy set theory designed by (Gopal & Woodcock, 1994; Wang, 1990; Zadeh, 1965). Various approaches have been developed for assessing the accuracy of fuzzy classifications; however, none has been standardized and globally accepted as a unique measure of fuzzy accuracy assessment; a given approach can involve defuzzification in which the classified output is hardened before its accuracy is assessed, this approach leads to lose of information (Okeke & Karnieli, 2006), other approaches intend to guide against information lost, amongst these, is the fuzzy error matrix (FERM).

The development of the fuzzy error matrix, is similar to that of the conventional error matrix discussed above, the difference lies in the fact that fuzzy error matrix accept real values unlike the conventional method. It is developed using "MIN" fuzzy operator, in which the membership values of pixels of the reference is compared with corresponding membership values of the pixels of the classified data, the minimum membership value between the corresponding pixels of the reference and the classified data is the intersection membership value that matches both pixel points, hence it becomes the element of the fuzzy matrix for both corresponding pixels(Binaghi, Brivio, Ghezzi, & Rampini, 1999). Like the conventional error matrix, overall, user and producer accuracies can be obtained, but in this context, as fuzzy overall, fuzzy user and fuzzy producer accuracies. The determinations of the measures are explained below using a simplified fuzzy error matrix.

Table 2.2: The fuzzy error matrix

3_classes						
Classified data	**Fuzzy error matrix for 3-classes** **Reference**				**Total**	**Fuzzy user accuracy (%)**
		A	B	C		
	a	45.11	13.98	5.76	64.85	69.56
	b	9.87	69.23	10.43	89.53	77.33
	c	21.56	7.65	80.65	109.86	73.41
	Total	76.54	90.86	96.84	**264.24**	
	Fuzzy producer accuracy (%)	58.94	76.19	83.28		
		Fuzzy overall (%)		**73.79**		

Table 2.2, represents a typical fuzzy error matrix, the matrix is similar to the conventional error matrix, the difference is that the elements of the fuzzy error matrix have real numbers generated from the membership values of pixels (a pixel belongs to all the classes to a certain degree, which is determined by the membership function). The depicted fuzzy error matrix, is a 3 by 3 matrix used to show three classes a, b and c; the corresponding reference is represented using A, B and C. The elements within the matrix, represent membership values of sampled units (pixels); from the table, the total membership values of all sampled pixels is 264.24; elements within the diagonal in blue (45.11, 69.23 and 80.65), represent the membership values that match between the classified data and the reference. Off-diagonal elements represent membership values that mis-match. Thus, the following measures can be determined from the matrix:

- Fuzzy overall accuracy: This is a probability measure that expresses the percentage of the total membership value that matches between the classified data and the reference. It is computed by the summation of the diagonal elements (45.11+69.23+80.65) divided by the total membership value (264.24), the result is expressed as a percentage, from table 2.2, 73.79% was obtained as the fuzzy overall accuracy. Fuzzy overall accuracy is represented using a single value.
- Fuzzy user accuracy: This is a probability measure that expresses the percentage that the membership value of a sampled pixel, corresponds to the membership value of the reference. It is computed in each row, by taking the diagonal element (membership value) in that row divided by the sum of the membership values in the same row. The values obtained, correspond to the number of rows, from the table three values were obtained, one for each row, they are:
  - Fuzzy user accuracy row 1: (45.11/64.85) * 100 = 69.56%
  - Fuzzy user accuracy row 2: (69.23/89.53) * 100 = 77.33%
  - Fuzzy user accuracy row 3: (80.65/109.86) * 100 = 73.41%
- Fuzzy producer accuracy: This is a probability measure that expresses the percentage that the membership value of a sampled pixel corresponds to the membership value of the classified data. It is computed in each column, by taking the diagonal element (membership value) in that column divided by the sum of the membership values in the same column. The values obtained correspond to the number of columns, from the table, three values were obtained, one for each column, they are:
  - Fuzzy producer accuracy column 1: (45.11/76.54) * 100 = 58.94%
  - Fuzzy producer accuracy column 2: (69.23/90.86) * 100 = 76.19%
  - Fuzzy producer accuracy column 3: (80.65/96.84) * 100 = 83.28%

Another measure of accuracy assessment used for both the crisp and fuzzy classification is the correlation coefficient. The correlation coefficient determines the linear association between the reference and the classified data (both are referred to as the variables in this instance). A common correlation coefficient is the Pearson's product moment; this computes the covariance between the reference and classified output and divides the result by the product of the standard deviation of the reference and that of classified output. The value ranges between -1 and 1; a value of 1 indicates both shows increases and decreases at the same time, a value of -1, indicates opposite association in which the increase of one variable decreases the other variable. A value of 0, indicates both are not correlated, values ranging between 0.5 and 1, indicates that the correlation between the two variables are high (Decoursey, 2003). The correlation for both the crisp and fuzzy classification is stated below:

- Correlation used for crisp classification: The Pearson's product moment was used in determining the linear association between the classified and the reference data as stated by (Denoeux & Masson, 2004). The classes of the reference data are compared with the classes of the classified data to determine their linear association. Each pixel of either the reference or classified data has only one class value, with this, the covariance of all pixels within the classified data and the reference was determined, the standard deviation of the classified data and as well as that of the reference were determined. To establish the correlation or linear association, the covariance value obtained was divided by the product of the standard deviation of the reference and classified data, the expression is stated below:

$$r_c = \frac{Cov(R_c, C_c)}{\sigma_{Rc} \quad \sigma_{Cc}} \qquad (2.20)$$

R_c= the class value of the reference (crisp)
C_c = the class value of the classified data (crisp)
Cov= covariance of both variables R_c and C_c
r_c = correlation coefficient
σ_{Rc} = standard deviation of variable R_c
σ_{Cc}= standard deviation of variable C_c

- Correlation used for soft classification: The Pearson's product moment was used in the same way to determine the linear association of the soft classification; however, the membership values of the pixels were used in this instance to generate the covariance and standard deviations(Denoeux & Masson, 2004), The above formula is thus modified as:

$$r_s = \frac{Cov(R_s, C_s)}{\sigma_{Rs} \quad \sigma_{Cs}} \qquad (2.21)$$

R_s= the membership value of the reference (soft)
C_s = the membership value of the classified data (soft)
Cov= covariance of both variables R_s and C_s
r_s = correlation coefficient
σ_{Rs} = standard deviation of variable R_s
σ_{Cs}= standard deviation of variable C_s

2.3.5. Factors to consider in designing an accuracy assessment scheme

There is no unique methodology to be adopted in designing an accuracy assessment scheme, this is because accuracy assessment scheme is multi-dimensional and depends on so many factors such as, the users and the purpose of the scheme, budget for the scheme, classifier(s) to be judged, the number of classes to be generated, sampling units, sampling size, sampling designs, reference data generations, sources of errors etc. The result obtained is dependent on the expert knowledge and as well as on how careful and critical the planning stage was carried-out (Congalton & Green, 2009). The following considerations are discussed.

2.3.5.1. Number of classes to generate

The number of classes to incorporate in the scheme depends on the geographic features of interest. It is not always possible to represent all classes in a given map; a form of generalization is usually done, this influences the outcome of the classification results and as well its accuracy measures. This phenomenon was studied and described in this research using two-class, three-class and four-class thematic maps.

2.3.5.2. Sampling units

Sampling is done to generate the subsets needed in the thematic map and its corresponding reference, for the accuracy assessment. In generating the samples, the unit of each sample should be determined. Sampling units can be a point or an areal unit (a single pixel, a cluster of pixels (usually of n by n square; for example 3 by 3 square can be adopted), a polygon or object and a cluster of polygons) (Fisher, 1997).

A single pixel is often used as sampling unit in most accuracy assessment method. (Congalton & Green, 2009) pointed out that the use of this method leads to poor results due to the following issue:

- Pixel represents an arbitrary rectangular delineation that might not correspond to the exact land cover or land use delineation.
- It is usually difficult aligning pixels on the map with that of the reference.
- It will lead to poor result when the minimum mapping unit specified by the classifier is larger than a pixel; this is because the sampling unit (a pixel) will be small and will not spatially match with the mapping unit of the classified output.

Using cluster of pixels as sampling units is becoming popular. This choice is based on the fact that it can help in reducing thematic and positional errors. Clusters of pixels can be easily registered to correspond between the map and reference data. Its usage is limited by the following:

- The level of details that can be investigated depends on the aggregated pixel sizes, hence a single pixel details cannot be reviewed.
- It produces poor result when used as sampling unit for vague regions; this is because, the individual pixels forming the cluster, might not have the same spectral information.
- The size of the clusters can be easily mistakenly and counted to represent single pixels: this is wrong.

Polygon or object based sampling unit, is created through image segmentation or through manual means by delineating a class from its edges, where much inter-class variations exists, creating a uniform label for a class. Its usage is growing by the day as an alternative method to single pixel sampling unit. It is more useful when the map to be created is of large scale.

Consequently, using clusters of polygon as sampling unit can be adopted when the issue of cost is to be considered and minimized.

2.3.5.3. Sample

Another consideration in accuracy assessment scheme is the issue of the size of the samples. Many equations have been proposed to be used for deriving the sampling sizes; still there is no unique method of achieving this(Congalton & Green, 2009). (Congalton, 1988) suggested as a rule of thumb, that the simple size should be chosen such that each class has a minimum of 50 sampled units. Furthermore, the sampling size should be large enough to adequately draw sufficient points for each class.

2.3.5.4. Sampling design

The method adopted in selecting the sampling unit is referred to as the sampling design. There are several sampling designs, with each having its own merits and demerits. The design was not necessary for the fuzzy accuracy assessment scheme, because the sample size used was equivalent to the total number of pixels in the map. However, considerations were made in choosing the sampling design for hard accuracy assessment scheme. A brief discussion is provided.

- Simple random sampling: In this method random pixels are chosen. It is an unbiased approach, because the probability of chosen any pixel to be part of the sample size is the same. This method can be easily designed but difficult to implement. Its major drawback lies in the fact that there is no guarantee that sufficient pixels will be chosen to represent rare classes.
- Systematic sampling: this design is spaced at regular interval in the area of study. It involves a random selection of a first point which is now used to generate regular intervals of points that will be sampled. This method guarantees that the selection of sampling pixels within the study area is done uniformly. However, if a phenomenon is of interest and lies outside the space of the generated random intervals, it will not be sampled. More so, the adequate representation of rare classes is not guaranteed(Stehman, 1997).

- Stratified random sampling: This method was developed to overcome the problem of not adequately representing rare classes in the sampling scheme, through formation of groups. Its main advantage is that, it provides a minimum number of samples for each group, ensuring that each group or class is adequately represented, hence improving the representation of the rare class. When adequate representation of the rare classes, results in the sparse representation of the other classes(Stehman & Czaplewski, 1998).
- Equal random sampling: in this method, the randomness is constrained to generate equal number of pixels for all classes, by so doing, rare classes are adequately represented, while other classes are not sufficiently represented.
- Cluster sampling: This method involves choosing a number of area samples of a fixed size and chosen samples in an exhaustive manner to describe the composition of each cluster. This reduces the number of areas to be visited by grouping the pixels. Calculating its standard error is very complex and it can under-represent rare classes(Cliff & Ord, 1973).
- Stratified systematic and unaligned sampling: This method combines the advantages of randomness and stratification in choosing the sampling pixels, this ensures that the area is adequately sampled. However, it can lead to under or over sampling of equally spaced points of interest.

Table 2.3: Summary of the various accuracy assessments sampling scheme

Sampling scheme	**Advantages**	**Disadvantages**
Simple Random	-Its selection is unbiased -Its statistical property is excellent	-Expensive, especially when field visit is required -No guarantee that each class will be adequately represented -Does not guarantee good distribution across the samples
Systematic	-It is easy to implement -less expensive when compared to random samples - ensures good distribution of samples across the landscape	-Can be biased, if sampling pattern is correlated with landscape pattern(periodicity) -It is weak statistically as each sample unit doesn't have equal probability of selection
Stratified Random	-It is an unbiased selection design -Ensures adequate representation of classes, because of the selection of a minimum number of selection in each class	-It requires knowledge about the map distribution before the strata can be created -It is very expensive, especially when field visit is required -Often difficult to find enough samples for rare classes
Cluster	-Least expensive as samples are closed to each other, hence reducing travelling time in field and or set up time in the office	- Can be affected by autocorrelation, resulting in the samples not being independent, if the samples are not different from each other, then they are not distinct samples, hence more independent samples should be taken.

Source: (Congalton & Green, 2009)

2.3.6. Generating reference data

Reference data generation, is a very important aspect in the implementation of an accuracy assessment scheme. The basic assumption is that the reference data is accurate and free from errors. (Foody, 2009) stated that there are several sources of errors prevalent in a reference data and the result of an accuracy assessment is not only influenced by the classifier and classified data, imperfection from the reference data as well contributes this. Furthermore, before assessment is carried out, there is need for the following to be done:

- The possible sources of errors associated with the reference data should be noted, this gives the indication that the accuracy assessment result obtained is also influenced by the errors in the reference data.
- The reference data should be collected in such a way that it will cover the mapped area.
- The reference data should be generated, bearing in mind the minimum spatial unit of the map (when the reference data is also a classified, its spatial support, should be made same as that of the map.)
- The same classification scheme as that of the map should be applied in the generating labels for the reference data.
- Reference data should be acquired as closely as possible to the date of the data used for classification, this will help in reducing temporal error.
- Reference data should be different from training data etc.

3. STUDY AREA, DATA, DATA PREPARATION AND SOFTWARE

3.1. Study area

The study area selected for the research is located within the Apalachicola National Forest in the western part of Florida in the United States of America. The Forest is the largest National forest in Florida; it occupies an estimated area of 2,286.3km2. Its coordinates as defined by the WGS84 ellipsoid are latitude 30°14'10"N and longitude 84°39'56"W. The forest contains the wilderness called Bradwell Bay and the Mudswamp (new river), which provides outdoor activities to people.

According to the Bureau of Land Management and the forest service southern coordination centre of the United States of America, the fire was caused by arson, affecting to a large extent, the Bradwell Bay wilderness. The fire is popularly referred to as the East Fork Fire. The fire broke out on April 4, 2004. The estimated area of the scar was put at 106.4km^2 (Rains, 2010).

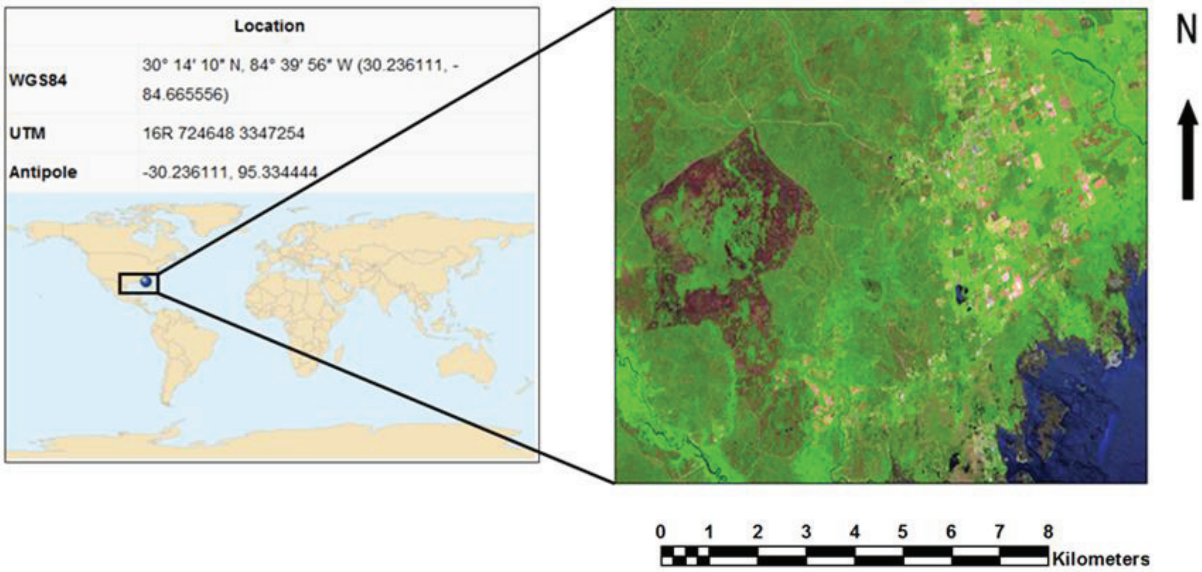

Figure 3.1: The study area. Source: (Przyborski, 2004)

3.1.1. Choice of study area

The study area was selected based on the fact that it is a natural reserve for tourism and provides income to the government. However, the area is constantly plagued by forest fire; this makes the area to be of concern to the government who are interested in understanding the extent of damage to the reserve which is a source of income to them. Proper damage assessment of the area will assist the government in decision making regarding the measures to control the spread of the fire and burn scar. Furthermore, the data needed for the research was freely available and downloadable (Rains, 2010).

3.1.2. Data availability and quality

The MODIS data acquired was the MOD9A1 product, which is referred to as the surface reflectance product. It is a 16 bit data and was captured in the hierarchical data format (HDF), having a pixel grid size of 500 m (it size was actually 463.31m.), its dimension is 2400 by 2400. It has a sinusoidal projection with; its upper left coordinates are -8895604.157, 4447802.079 and its lower right coordinates are -7783653.638, 3335851.559. The MODIS data is made up of 13 bands. The data was acquired on the 14th day of April

2004. The research was carried out using band 1 to band 7. However, band 5 and band 7, contained stripes, hence they were not used.

3.1.3. Sensor description

The research was carried out using two types of sensor; the MODIS sensor which captured the data used for classification and the ASTER sensor, which captured the data used for generating the reference. Both sensors are described below. Section 3.1.4 described the MODIS sensor, while section 3.1.5 was used to describe the ASTER sensor.

3.1.4. MODIS sensor and Image capture

The Moderate-Resolution Imaging Spectroradiometer (MODIS) instruments are part of the National Aeronautics and Space Administration's (NASA) Earth Observing System (EOS). The instrument has two sun-synchronous, near-polar orbiting satellites (Terra and Aqua). The Terra satellite was launched on the 18 December, 1999, while the Aqua satellite was launched on 4 May 2002. A summary of the description is shown below

Table 3.1: MODIS specification

Property	**Description**
Orbit	705km, 10:30 a.m descending node for Terra or 1:30 p/m ascending node for Aqua. It is circular, near –polar and sun-synchronous
Scan rate	20.3rpm across track
Swath wide	2330km across track and 10km along track at nadir
Telescope	17.78cm diameter
Size	1.0 * 1.6 * 1.0m
Weight	228.7Kg
Power	162.5W
Data rate	10.6 Mbps (peak daytime); 6.1Mbps (orbital average)
Quantization	12bits
Spatial Resolution	250m(bands1-2); 500m (bands 3-7); 1000m (bands 8-36)
Design Life	6 years

Source: http://modis.gsfc.nasa.gov/about/specifications.php; accessed 8/01/2010

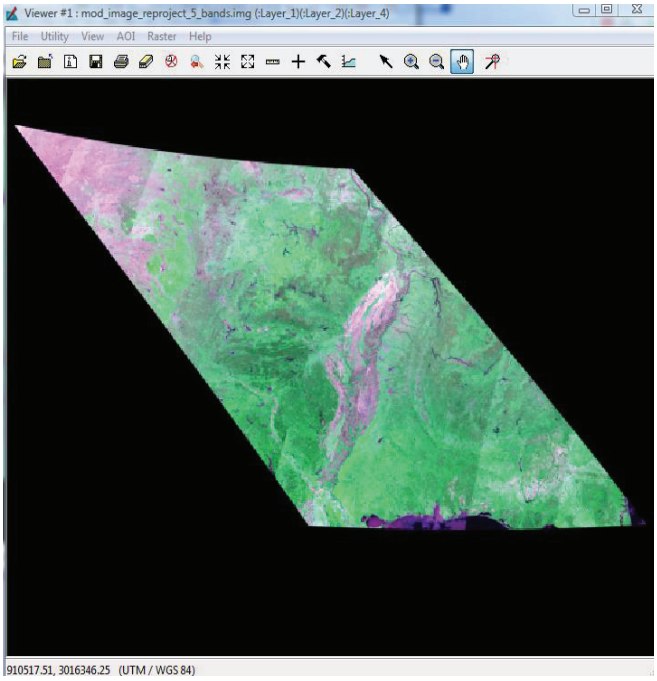

Figure 3.2: MODIS image

Figure 3.2: Represents the whole acquired image of MODIS, after it has been re-projected

3.1.5. ASTER sensor Image capture

The Advance Space borne Thermal Emission and Reflection (ASTER) instrument was acquired on 18 December, 1999. It is an instrument on-board NASA's EOS Terra satellite. It can be used in acquiring information relating to surface temperature, reflectance, elevation and emissivity at a relatively high resolution. It has three sub-systems, the visible and near infrared (VNIR(15m)), which is 8 bits and having a swath width of 60 Km, the second is the short wave infrared (SWIR(30m)) subsystem, which is 8 bits and swath width of 60 Km. The third is the thermal infrared (TIR(90m))subsystem, which is 12 bits and 60 Km swath width. The ASTER specifications are shown below.

Table 3.2: ASTER specification

Spectral coverage	0.53〜11.65μm
Spatial resolution	15m(Bands 1〜3) 0.52 - 0.86μm
	30m(Bands 4〜9) 1.60 - 2.43μm
	90m(Bands 10〜14) 8.125 - 11.65μm
Radiometric resolution	≦0.5% NEΔρ(Bands 1〜3)
	≦0.5〜1.3% NEΔρ(Bands 4〜9)
	≦0.3K NEΔT(Bands 10〜14)
Absolute radiometric accuracy	≦7 4%
Absolute temperature accuracy	≦3k(200〜240 K)
	≦2k(240〜270 K)
	≦1k(270〜340 K)
	≦2k(340〜370 K)

Signal quantization levels	8 bits(Bands 1～9)
	12 bits(Bands 10～14)
Base-to-height ratio of stereo capability	0.6(along-track)
Swath width	60km
Total coverage in cross-track direction by pointing function	232km
Mission life	5 years
MTF at Nyquist frequency	0.25(cross-track)
	0.20(along-track)
Peak data rate	89.2Mbps
Weight	406kg
Peak power	726W

Source: (ERSDAC)

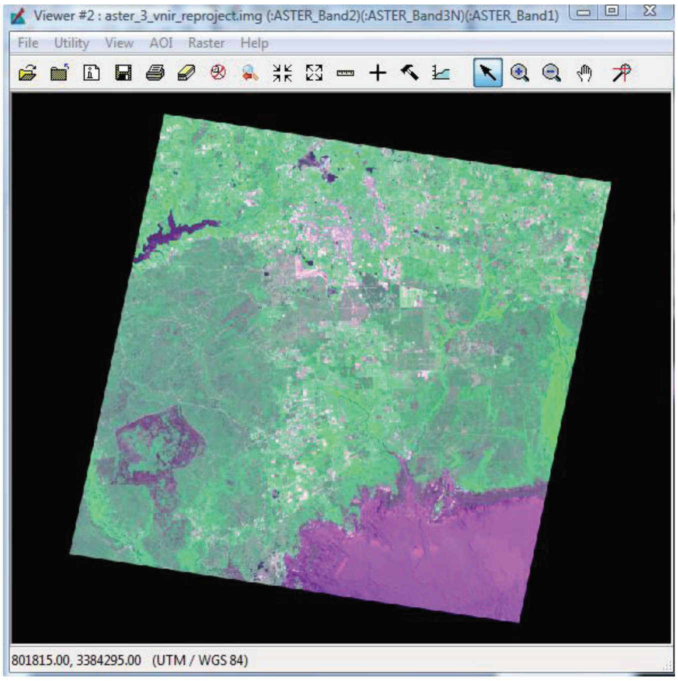

Figure 3.3: Whole image of ASTER

Figure 3.3 represents the whole ASTER image before it was subsetted

3.2. Data preparation

3.2.1. ASTER HDF data import and re-projection

The ASTER data was opened in ERDAS IMAGINE software, using the Red-Green-Blue band combination respectively as 2-3-1. Data exploration reviewed the ASTER was in the HDF file format., geo-referenced and geo-coded in the WGS 84, UTM zone 16 projection systems, having metric coordinates. The data was now imported in ERDAS IMAGINE for the convenience of working in IMAGINE format and for the ease of creating subsets of the image; this resulted in the transformation of the metric coordinate system to its geographical equivalent; however the metric coordinate was restored by re-projection and nearest neighbour resampling method. The pixel size was 15 m; this was not changed during the re-projection and resampling stage. The three visible to near infrared band of the sub-system contained three bands and were used in this research. The ASTER HDF data file was now converted to IMAGINE file.

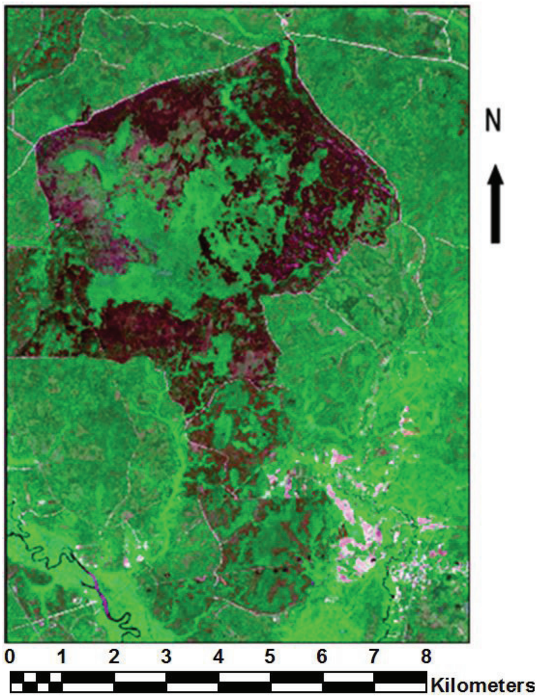

Figure 3.4: ASTER subsetted image in 2-3-1 band combination

3.2.2. MODIS HDF data import, DN-conversion and re-projection

MODIS data was opened in ERDAS IMAGINE using Red-Green-Blue band combination respectively as 1-2-3. Data exploration, reviewed that the MODIS data was in HDF and geo-referenced to sinusoidal datum projection. The data format was re-projected to the same datum system of the reference data. To achieve this, it was necessary to import the MODIS HDF file into ERDAS IMAGINE. The image is a signed 16 bit surface reflectance product, having real DN values between 0 and 1. ERDAS IMAGINE doesn't support fractional DN values; hence it converted the DN values of the pixels into integers by a scale of 10,000. the image was now re-projected to UTM, Zone 16, with Datum WGS 84 (hence corresponding to the projection of the ASTER data). The pixel size was 463.31 m, and was resampled using the nearest neighbour resampling method to 495 m, this made the ratio formed between the pixel of MODIS and that of ASTER to correspond to 1:33. The format of the MODIS file was also changed to Imagine format.

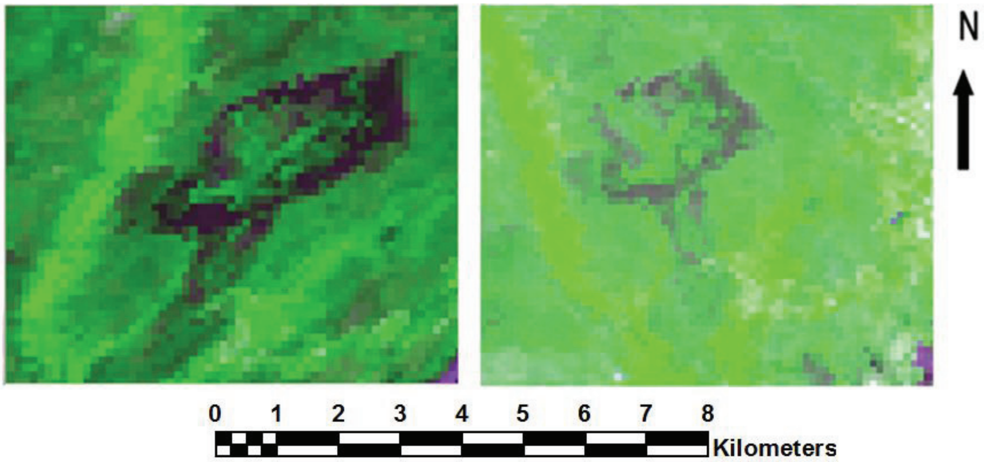

Figure 3.5: MODIS Image; **A** represents the Image before re-projection and **B** represents the image after re-projection

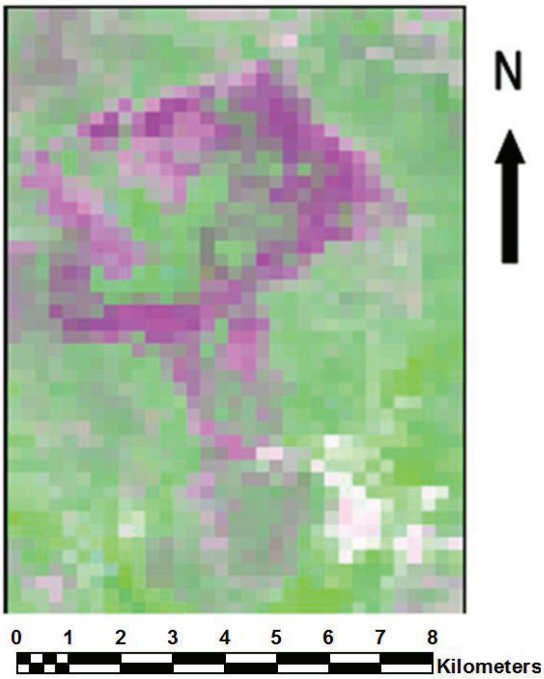

Figure 3.6: MODIS subset in 1-2-3 band combination

3.2.3. Images overlay

To verify if both images match within the areas of common scene, their corresponding re-projected and re-sampled forms were overlaid. The ASTER was placed on the top of the MODIS. A screen capture is shown below: It can be inferred that both images matched when overlaid.

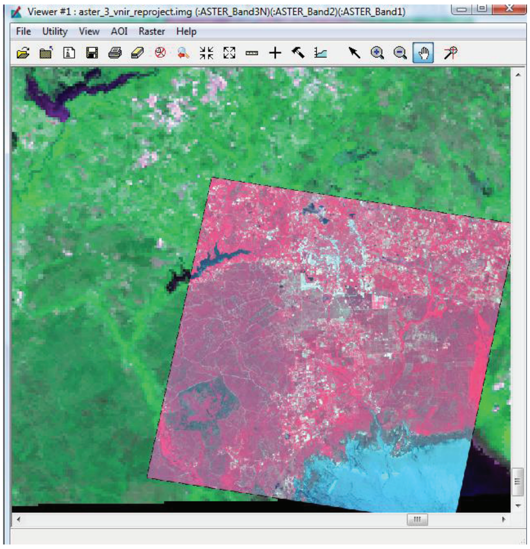

Figure 3.7: MODIS and ASTER overlay

3.3. Software

The research was carried out using image processing software (ERDAS Imagine and ENVI) and as well as a statistical software (R-software). A brief discussion of each of the software is done in the following section.

3.3.1. ERDAS Imagine

ERDAS Imagine software is a powerful geospatial application tool having a blend of both GIS and remote sensing analysis capabilities. It is designed primarily to handle raster data processing, which can allow the user prepare, display and enhance digital images for mapping use. It has flexible, easy to use toolboxes, which can be used to increase the accuracy of our work and as well as our productivity output. In this research ERDAS Imagine was used as image processing software in combination with ENVI.

3.3.2. ENVI

The ENVI software like the ERDAS Imagine is software used for the processing and analysing of geospatial imagery. It was used in combination with ERDAS Imagine to process the MODIS and as well as the ASTER data.

3.3.3. R-software

The R software is free downloadable software used in the research to perform image processing activities. The imaging processes are written as program codes and ran in R to generate the desired results. R software can be used to perform graphical as well as statistical image operations. The software was used for further analysis of the images after it has been converted to ASCII format, stored as arrays and matrices. FCM was performed using R and as well as accuracy assessment

4. RESEARCH METHODOLOGY

4.1. Introduction

The research proceeded with the acquisition of MODIS (image to be classified) and ASTER (reference, produced as well as classified output) images; both images were opened, explored and imported into ERDAS IMGINE software. The images were made ready for further processing after the data preparation stage, described in Chapter 3 was completed. The research was carried out in a sequential and orderly manner by following the methodology flow chat as shown below.

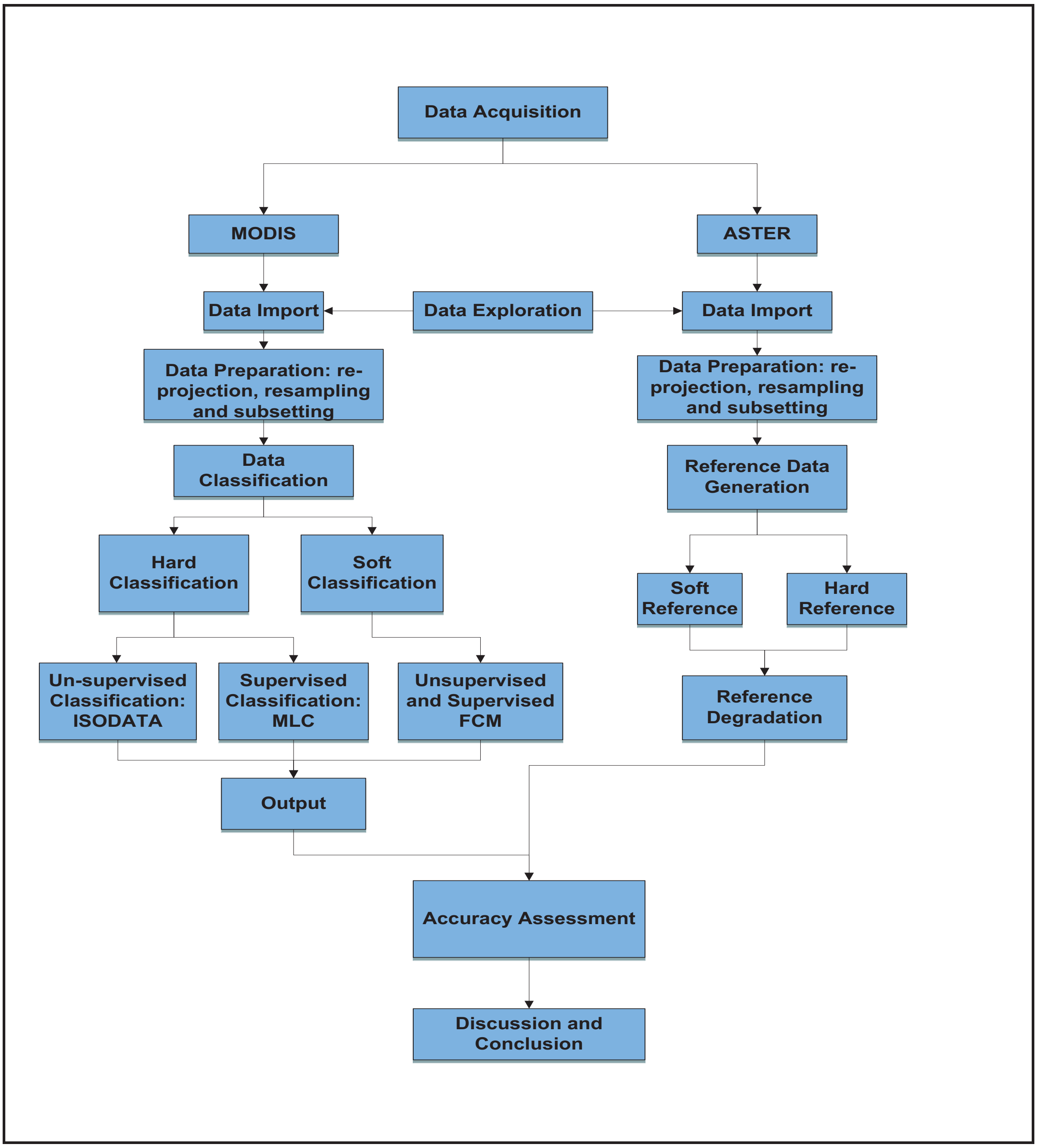

Figure 4.1: Research methodology flow chat

4.2. Classification

This research focused on the prevailing issues that should be considered right from the start, as an attempt is made to assess the accuracy of fuzzy images. The steps taken determine how efficiently or otherwise the fuzzy images phenomena can be described. The most important consideration is the classification method chosen and the method for generating the reference data. Every step taken contributes its own success rate to the eventual result achieved; hence no step should be downplayed. As the stages begin, errors are generated and propagated (the process is challenged by uncertainties); this gets compounded to the end stage, where the accuracy of the fuzzy object is assessed, this stage also generate errors; possible sources of errors can be identified, modelled and used to correct the process in order to improve the description of the phenomenon. The Land cover classes were identified in which the pixels were categorized based on their spectral information to create thematic maps(Lillesand & Kiefer, 1994) and the accuracy of the produced thematic map judged. In classifying the east fork fire burn scar, hard and soft classifications were used for the basis of comparison, bearing in mind the associated vagueness (or fuzziness) within the region of transition and how each handles the situation.

4.2.1. Three cases unsupervised classification using ISODATA

Three different cases (case A= 2-number-of-classes; case B=3-number-of-classes and case C=4-number-of-classes) were studied to investigate the influence of the number of classes on the classification output and to guide in the selection of the appropriate number of classes to defined, depending on the level of details of interest. The whole acquired MODIS image was processed and used for the classification purpose before sub-setting was done in order to incorporate the variability within the entire image. The class separabilty was determined by using transformed divergence. The convergence threshold was set at 0.950, while the number of iteration was set at 1,000. The classifier's signature editor was saved to determine the training pixels used automatically by the software. The class statistics were computed, with the mean value for each class plotted against their respective bands.

4.2.1.1. Case A

Two classes were determined as burnt scar and un-burnt area, the automatically generated training pixels are shown in the table below:

Table 4.1: Software generated training pixels for 2-classes unsupervised ISODATA-MODIS

	Software Training pixels	
Class	**Value**	**Number of Training pixels**
Burnt scar	1	488
Un-burnt area	2	1063

4.2.1.2. Case B

Three classes were determined as burnt scar, grasses and shrubs and trees, the automatically generated training pixels are shown in the table below.

Table 4.2: Software generated training pixels for 3-classes unsupervised ISODATA-MODIS

	Software Training pixels	
Class	Value	Number of Training pixels
Burnt scar	1	327
Grasses and Shrubs	2	919
Trees	3	305

4.2.1.3. Case C

Four classes were determined as burnt scar, built-up area, grasses and shrubs and trees, the automatically generated training pixels are shown in the table below

Table 4.3: Software generated training pixels for 4-classes unsupervised ISODATA-MODIS

	Software Training pixels	
Class	Value	Number of Training pixels
Burnt scar	1	238
Built-up area	2	407
Grasses and Shrubs	3	687
Trees	4	219

4.2.2. Three cases supervised classification using MLC

The same approach as discussed in section 4.2.1 was applied in this case; supervised MLC was used as the classifier in which some pixels within the entire image were selected for training. A screen capture is shown to represent the training sites selected. Subsequently the training pixels for three cases are tabulated as well below.

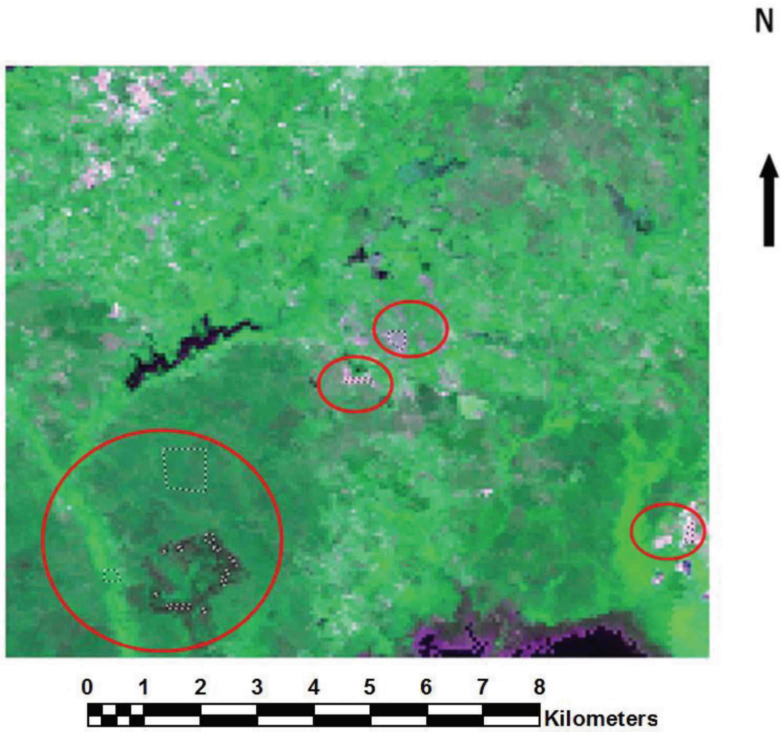

Figure 4.2: Screen capture of the area selected as training pixels-3-classes

4.2.2.1. Case A

Two classes were determined as well in this case; burnt scar and un-burnt area (all other land information aside burnt scar were merged together as un-burnt area), the number of training pixels are shown below.

Table 4.4: Training pixels for 2-classes-Supervised MLC-MODIS

	Training pixels supervised MLC	
Class	**Value**	**Number of Training pixels**
Un-burnt area	2	73
Burnt scar	1	56

4.2.2.2. Case B

Three classes were determined as well in this case; however, the class labels and training pixels were selected in order to represent the desired land information of interest. The grasses and shrubs class was merged with the tree class to form the vegetation class. The three classes depicted are burnt scar, vegetation and built-up area. The training pixels for the classes are shown below.

Table 4.5: Training pixels for 3-classes-Supervised MLC-MODIS

	Training pixels	
Class	**Value**	**Number of Training pixels**
Burnt scar	1	57
Vegetation	2	149
Built-up area	3	70

4.2.2.3. Case C

Four classes were determined in this case; just like in section 4.2.1.3. Training pixels were selected to depict area of interest. The classes defined are burnt scar, trees, grasses and shrubs and built-up areas. A screen shot of the training site is shown below as well as the number of training pixels selected.

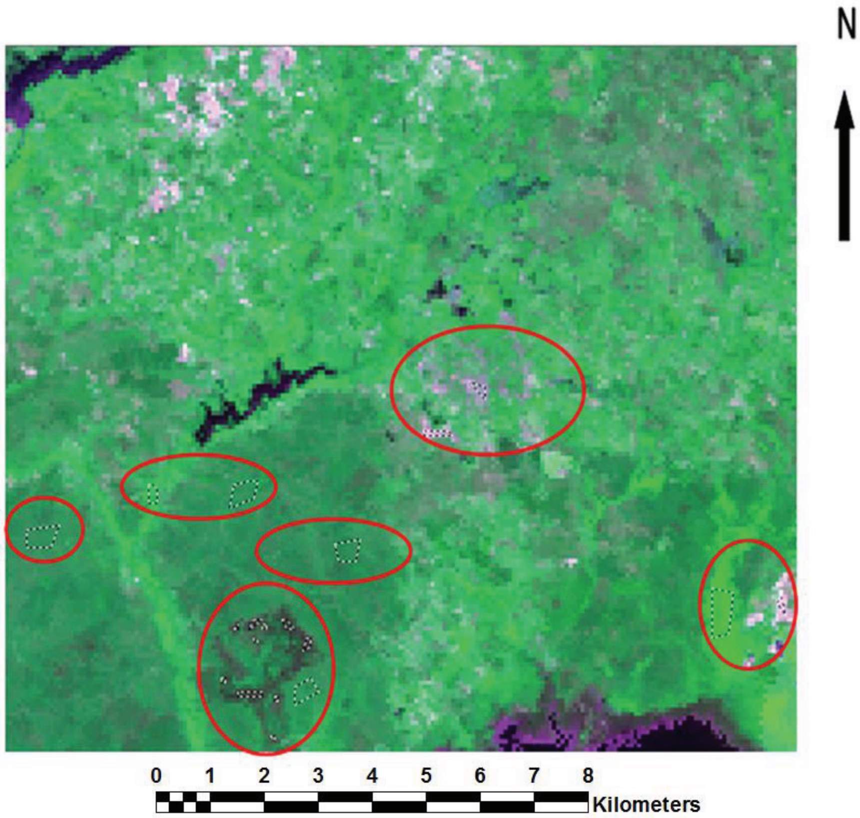

Figure 4.3: Screen capture of the area selected as training pixels-4-classes

Table 4.6: Training pixels for 4-classes-Supervised MLC-MODIS

	Training pixels	
Class	Value	Number of Training pixels
Burnt scar	1	57
Trees	2	113
Grasses and Shrubs	3	143
Built-up area	4	79

4.2.3. Three cases un-supervised classification of MODIS using Fuzzy-c-means (FCM)

The MODIS image was also classified using the un-supervised fuzzy-c-means algorithm. Three cases were also defined: case A, case B and Case C, representing 2, 3 and 4 classes respectively. The MODIS data was converted to ASCII format using the ENVI software. 5 bands of the MODIS data were imported one after the other into R-statistical software. The FCM algorithm code was now used to classify the image; however the following parameters were defined:

- The fuzziness parameter, m=2; this was recommended by (Foody, 1996), as an appropriate measure for FCM classification.
- The number of classes, (2, 3 and 4 representing each case respectively).
- The termination criterion represented as epsilon, this was set to 0.01.
- The number of iteration= 1,000.
- The number of bands =5

The FCM algorithm was initialized by randomly assigning pixels to classes and computing the mean of the classes. Iteration progresses in which more iterations led to the continuous update of the value of the mean of each class and as well as the membership values of each pixel; the update continued until the termination point was reached. The termination point could be reached either when the defined number of iteration is reached or the termination criterion epsilon, 0.01 is reached (Bezdek, 1981). In this research, the algorithm stopped only when the threshold termination point 0.01, was reached. The membership values for all the pixels in all the classes were computed and stored for further processing. The initial mean, final mean and the number of iterations reached for the three cases are shown below. In every case, the values obtained, were multiplied by a scale factor of 0.0001 in order to restore its original DN value, since this was converted initially by ERDAS using a scale of 10,000.

4.2.3.1. Case A

In case A, two classes were defined: the burnt and un-burnt classes. The FCM algorithm, assigned initial mean values to the classes. The process converged after reaching the termination criteria in 13 steps iterations. The membership values of the pixels for all classes were obtained and saved. The final mean values were also obtained. Two tables are shown below, to depict the initial and final class means obtained.

Table 4.7: Initial mean values for 2-classes-unsupervised FCM

Initial mean values in all bands and classes					
	Band (mean values $\times 0.0001$)				
Class	**1**	**2**	**3**	**4**	**5**
Burnt scar	338.91	2080.06	173.63	436.62	1506.96
Un-burnt area	339.58	2107.02	174.14	440.03	1510.67

Table 4.8: Final mean values for 2-classes-unsupervised FCM

Final mean values in all bands and classes					
	Band (mean values $\times 0.0001$)				
Class	**1**	**2**	**3**	**4**	**5**
Burnt scar	366.06	1563.96	187.87	385.63	1538.82
Un-burnt area	326.43	2299.62	167.09	457.43	1486.82

4.2.3.2. Case B

In case B, three classes were defined: the burnt scar, the grasses and shrubs and trees. The same procedure in section 4.2.3.1 was applied. After 16 iterative steps, the process converged. Membership values of the pixels were obtained and saved as well as the initial and final mean values of the classes. Tables of the mean values are shown below.

Table 4.9: Initial mean values for 3-classes-unsupervised FCM

Initial mean values in all bands and classes					
	Band (mean values $\times$ 0.0001)				
Class	1	2	3	4	5
Grasses and Shrubs	339.80	2098.78	174.64	439.22	1511.84
Burnt scar	339.67	2091.74	174.06	438.44	1509.99
Trees	336.95	2101.55	172.25	437.64	1501.69

Table 4.10: Final mean values for 3-classes-unsupervised FCM

Final mean values for all bands and classes combination					
	Band (mean values $\times$ 0.0001)				
Class	1	2	3	4	5
Grasses and Shrubs	330.70	2133.74	169.13	442.36	1465.78
Burnt scar	369.98	1401.12	190.22	367.00	1529.97
Trees	319.73	2552.77	164.23	478.97	1543.63

4.2.3.3. Case C

In this case, four classes were defined: the burnt scar, the grasses and shrubs, trees and the built-up area. The same procedure in section 4.2.3.1 was applied. After 15 iterative steps, the process converged. Membership values of the pixels were obtained and saved as well as the initial and final mean values of the classes. Tables of the mean values are shown below.

Table 4.11: Initial mean values for 4-classes-unsupervised FCM

Initial mean values in all bands and classes					
	Band (mean values $\times$ 0.0001)				
Class	1	2	3	4	5
Trees	342.54	2112.57	175.03	441.78	1521.79
Burnt scar	338.42	2073.75	173.58	435.72	1501.99
Built-up area	339.87	2081.63	174.70	437.29	1504.78
Grasses and Shrubs	337.49	2096.29	172.89	437.75	1504.93

Table 4.12; Final mean values for 4-classes-unsupervised FCM

Final mean values in all bands and classes					
	Band (mean values $\times$ 0.0001)				
Class	1	2	3	4	5
Trees	317.9489	2631.926	163.6541	485.5873	1565.202
Burnt scar	369.4671	1268.018	190.5354	350.4734	1511.441
Built-up area	354.6369	1892.1	181.3898	422.9087	1539.034
Grasses and Shrubs	322.0848	2225.407	164.6134	448.4607	1444.122

4.2.4. Three cases supervised classification of MODIS using FCM

The approach used in section 4.2.3, was also applied in this section to generate the membership values of the pixels in all the classes; however, this was done in a supervisory mode. The supervisory mode of FCM, involves imputing the desired class means by the human operator into the algorithmic process. The FCM algorithm uses this information to compute the membership values of every pixel in every class. The estimated class means corresponds to the spectral means of the classes obtained during supervised MLC classifications. Three cases were also studied in this instance. The mean values for each class in the threes cases are tabulated and shown below.

4.2.4.1. Case A

In case A, two classes were defined: the burnt and un-burnt classes. The class means were estimated to run the process and obtained the membership values of the pixels. The class means used are shown below.

Table 4.13: Mean values for 2-classes-supervised FCM

Mean values in all bands and classes					
	Band (mean values × 0.0001)				
Class	**1**	**2**	**3**	**4**	**5**
Burnt scar	382.36	1136.52	198.70	340.29	1553.00
Un-burnt area	378.99	2424.99	195.64	502.81	1600.14

4.2.4.2. Case B

In case B, three classes were defined: the burnt scar, vegetation and built-up area. The class means were imputed to generate the pixel membership values. The class means used are shown below.

Table 4.14: Mean values for 3-classes-supervised FCM

Mean values in all bands and classes					
	Band (mean values × 0.0001)				
Class	**1**	**2**	**3**	**4**	**5**
Burnt scar	371.14	1104.21	192.04	330.05	1507.11
Vegetation	338.36	2233.58	173.46	462.66	1499.15
Built-up area	1354.04	2774.03	731.61	1181.37	3416.29

4.2.4.3. Case C

In this case, four classes were defined: the burnt scar, trees, grasses and shrubs and built-up area. The class means were imputed to generate the pixel membership values. The class means used are shown below.

Table 4.15: Mean values for 4-classes-supervised FCM

Mean values in all bands and classes					
	Band (mean values × 0.0001)				
Class	1	2	3	4	5
Burnt scar	382.86	1139.60	196.83	338.16	1555.16
Trees	202.79	3354.62	103.98	420.40	1434.32
Grasses and Shrubs	336.62	2237.62	171.55	459.60	1464.41
Built-up area	1461.65	2827.13	768.03	1212.30	3920.56

4.3. Reference data generation

ASTER image was acquired along side the MODIS image to serve as the reference image for comparing the classification output of MODIS. To fairly judge the accuracy of the thematic map produced by the MODIS image, it is necessary to bring the ASTER to the same state as the MODIS, i.e, using the same classification approach, the same resolution, the same sampling unit etc(Congalton & Green, 2009; Liang, Fang, & Chen, 2001). Based on this, the ASTER image was classified in similar fashion like the MODIS. The ASTER image is a fine resolution image of 15 m, it was degraded as well to obtain the same spatial resolution as MODIS. Similar classifications and cases discussed in the MODIS image were also applied in this area. They are briefly explained.

4.3.1. Three cases unsupervised classification using ISODATA

The same approach in section 4.2.1 was applied to generate similar three cases A, B and C. The parameters defined are also the same. The training pixels automatically generated by the method in all cases are tabulated and shown below.

4.3.1.1. Case A

Table 4.16: Software generated training pixels for 2-classes unsupervised ISODATA-ASTER

	Software Training pixels	
Class	Value	Number of Training pixels
Burnt scar	1	429358
Un-burnt area	2	1203990

4.3.1.2. Case B

Table 4.17: Software generated training pixels for 3-classes unsupervised ISODATA-ASTER

	Software Training pixels	
Class	Value	Number of Training pixels
Burnt scar	1	342077
Grasses and Shrubs	2	956307
Trees	3	334960

4.3.1.3. Case C

Table 4.18: Software generated training pixels for 4-classes unsupervised ISODATA-ASTER

Class	Software Training pixels Value	Number of Training pixels
Burnt scar	1	274315
Built-up area	2	418292
Grasses and Shrubs	3	739628
Trees	4	201109

4.3.2. Three cases supervised classification using MLC

In the supervised hard classification using MLC, the training pixels were chosen to cover the whole image area. Similar procedures for the hard the supervised hard classification were adopted, the training site is shown below, as well as the training pixels generated.

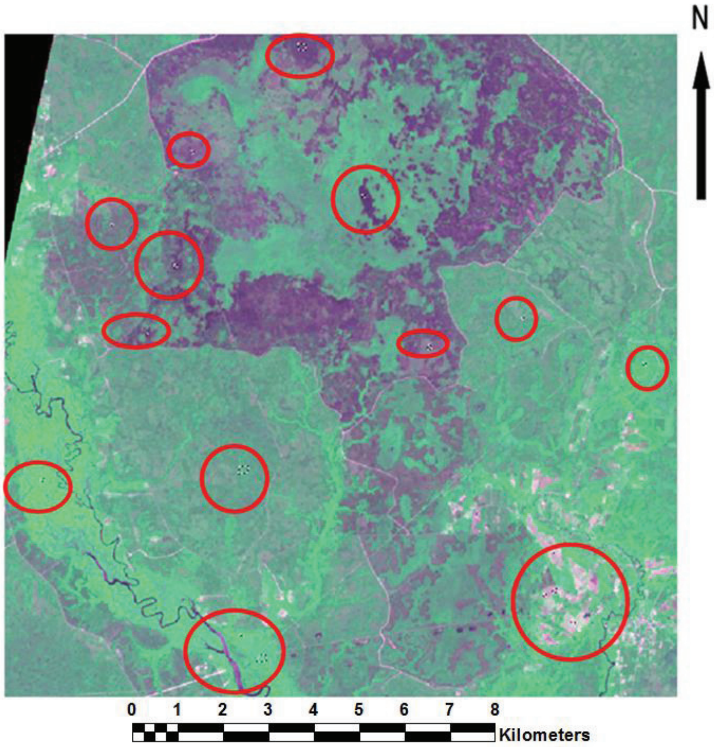

Figure 4.4: Site for selecting training pixels

4.3.2.1. Case A

This case is similar to that discussed in the MLC supervised classification. The class labels and the number of training samples are shown below.

Table 4.19: Training pixels for 2-classes-Supervised MLC-ASTER

	Training pixels	
Class	**Value**	**Number of Training pixels**
Burnt scar	1	695
Un-burnt area	2	1029

4.3.2.2. Case B

Table 4.20: Training pixels for 3-classes-Supervised MLC-ASTER

	Training pixels	
Class	**Value**	**Number of Training pixels**
Burnt scar	1	423
Vegetation	2	721
Built-up area	3	210

4.3.2.3. Case C

Table 4.21: Training pixels for 4-classes-Supervised MLC-ASTER

	Training pixels	
Class	**Value**	**Number of Training pixels**
Burnt scar	1	57
Trees	2	113
Grasses and Shrubs	3	143
Built-up area	4	79

4.3.3. Three cases un-supervised and supervised classification of ASTER using FCM

The FCM algorithm was also applied in generating the soft reference data, just like that of the MODIS. Three cases were also considered in the supervised and unsupervised FCM. The following parameters were defined; the fuzziness parameters m=2, the number of classes (2, 3 and 4), the termination criterion was set at 0.01, the number of iterations was set a 1,000, the number of bands equals 3.

4.3.4. Generalization

By visual inspection of the un-classified ASTER image, more features could be easily identified, which are not visible in the MODIS image, for example, a water body can be easily distinguished in the ASTER, but not visible in the MODIS, this was merged to belong to other classes, to establish the same number of classes for both the ASTER and MODIS. This was noted as well as a possible source of error.

4.3.5. Importation of classified Hard-output in R

The classified output of the hard classification of both the MODIS and ASTER were opened in ENVI, then saved in ASCII format before they were imported into R-statistical software for further analysis and accuracy assessment.

4.3.6. Reference data degradation

The classified outputs (hard and soft classifications) of the ASTER data were degraded to make it of the same spatial resolution as that of the MODIS, this was necessary to have the same basis for comparison (Congalton & Green, 1999; Liang, et al., 2001). The classified ASTER was initially 15m, while that of the MODIS was 495m; the ratio formed between the MODIS and ASTER pixel is 1:33. The classified output of the ASTER was degraded using a 33 by 33 window size of the pixels of the ASTER. The degradation (aggregation) was done to make a 33 by 33 pixels of the reference, correspond to a 1 by 1 MODIS classified output. This was done for both the hard and soft reference.

4.3.6.1. Reference Aggregation in the hard Case

To achieve aggregation in this case, the values of the proportions of each class within a 33 by 33 window pixels of the reference was determined; the aggregation resulted in assigning the whole 33 by 33 pixels with the value of the class with the highest frequency (Maselli, Gilabert, & Conese, 1998) .

4.3.6.2. Reference Aggregation in soft case

In this case, the aggregation was done using the mean of the grades of membership for all pixels within 33 by 33 window size of the reference to correspond to a 1 by 1 MODIS classified pixel.

4.3.6.3. Reference data dimension

The degraded ASTER's dimension (row by column) was 32 by 45, against the MODIS which was 33 by 47. Both were overlaid to determine if they matched or not; it was observed both matched, but the MODIS overshot by a 1 by 2(row by column) dimension. Visual investigation of the positions of the pixels was done, to determine the exact row and columns to remove from the MODIS output. The 33rd row was removed as well as the 47th and 46th column of this MODIS; this was done to make the whole mapped area comparable.

4.3.7. Accuracy assessment measures

The accuracy of both the hard and soft MODIS outputs, were compared with the degraded reference obtained. The whole mapped area was used for accuracy assessment; i.e. sampling size is the all area covered by both dataset. The sample size corresponds to the size of the classified MODIS, which is equivalent to the size of the reference (45 by 32 in rows and columns dimension); this was necessary to overcome the problems associated with sampling generation. The sampling unit (the minimum mapping unit) was maintained at the pixel level (Congalton & Green, 1999).

The confusion matrix was used to compare the reference and the classified MODIS for the hard classification; the overall, producer and user accuracy measures were determined; furthermore, the kappa coefficient was also determined.

In the soft classification, its accuracy was determined using the fuzzy error matrix (Binaghi, et al., 1999). This method is very similar to the hard confusion matrix; the difference is that, the fuzzy error matrix computes accuracy using grades of membership. The measure uses the 'MIN' operator from the fuzzy theory to determine the maximum intersection between the classified and reference datasets. The measures that are derivable are the fuzzy overall accuracy, fuzzy user accuracy, fuzzy producer accuracy.

Another measure determined was the correlation coefficient using Pearson's-product-moment-correlation coefficient, it is a measure that shows the linear association between the classified and the reference datasets (Decoursey, 2003)this was used as a measure both for the hard and soft cases.

5. RESULTS

The various results produced in the research are presented in this chapter. The presentation followed this adopted: unsupervised hard classification, supervised hard classification, unsupervised and supervised FCM classification, reference data results and accuracy assessments.

5.1. Result obtained for the unsupervised hard classification

Unsupervised classification results were obtained for three cases: case A, case B and case C, having 2, 3 and 4 classes respectively. The results are:

5.1.1. Class separability-unsupervised hard classification (ISODATA)

The separabilty of a given pair of classes in the three cases were computed using the transformed divergence (TD), this was done in ERDAS IMAGINE. The transformed divergence ranges between 0 and 2000, having a separabilty value of 2000, shows that the pair of classes are distinct, i.e. the inter-class variations are very high. When inter-class variations are low, separability values is low. Also, the increase in intra class variability reduces class separabilty values with low variability results in low separable, having a hard classification (Zhang, Marszalek, Lazebnik, & Schmid, 2007).

Table 5.1: Class separability (Transformed Divergence) for unsupervised hard classification of MODIS classification (ISODATA)

Transformed divergence for unsupervised 3 cases(TD)		
Cases	**Classes**	**TD value**
2 classes	Burn scar	1681
	Un-burnt area	
3 classes	Burn scar	1814
	Grasses and shrubs	
	Burn scar	1997
	Trees	
	Grasses and shrubs	1778
	Tress	
4 classes	Burn scar	1765
	Built-up area	
	Burn scar	1999
	Grasses and shrubs	
	Burn scar	2000
	Trees	
	Built-up area	1456
	Grasses and shrubs	
	Built-up area	1991
	Trees	
	Grasses and shrubs	1827
	Trees	

5.1.2. Plot of mean value against Bands-unsupervised hard classification (ISODATA)

The mean value of each class was plotted against the number of bands, for the three cases. The plot reviewed that the mean for all classes was highest in band 2, while the mean value of all classes was lowest in band 3, the plots are shown below:

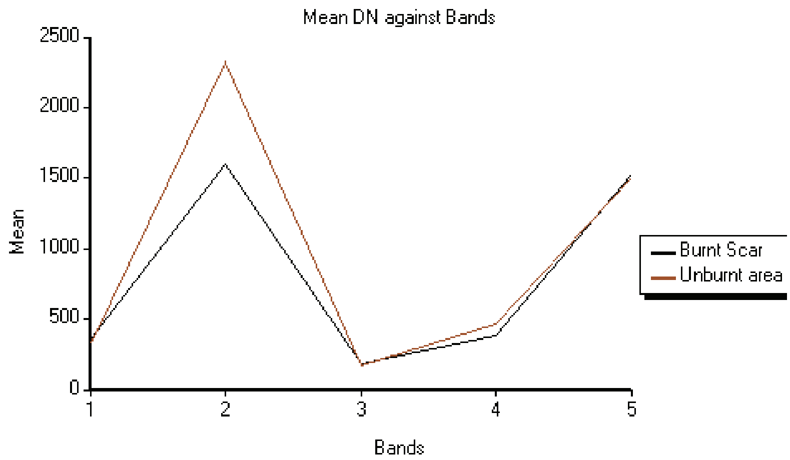

Figure 5.1: Mean value of class against Bands_2_classes_unsupervised hard classification(ISODATA)

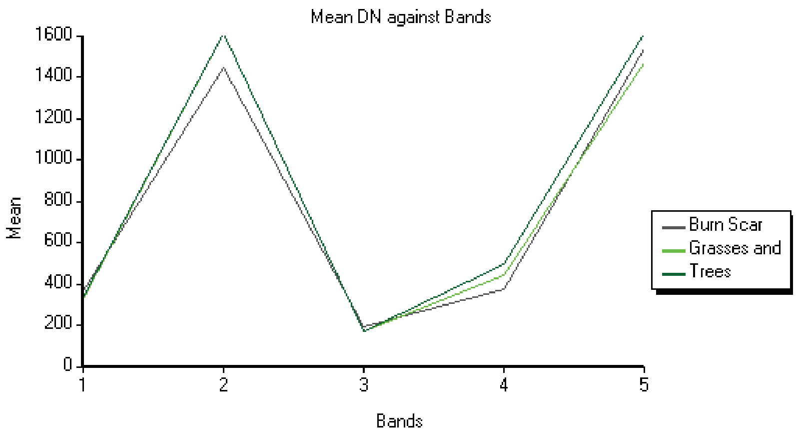

Figure 5.2:Mean value of class against Bands_3_classes_unsupervised hard classification(ISODATA)

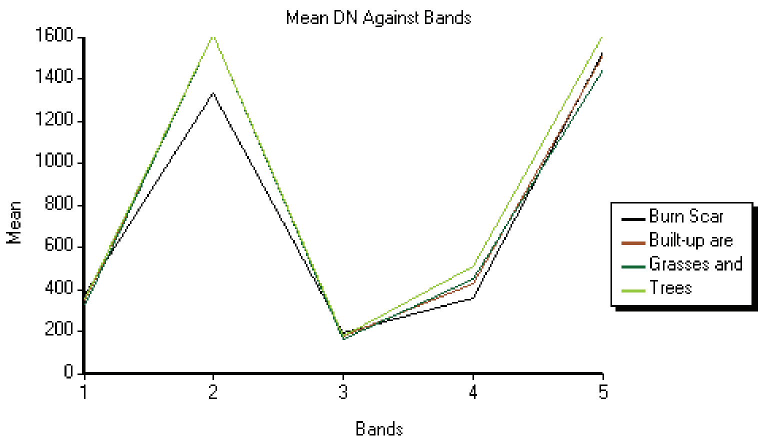

Figure 5.3: Mean value of class against Bands_4_classes_unsupervised hard classification (ISODATA)

5.1.3. Thematic map produced-unsupervised hard classification (ISODATA)

The thematic maps for 2, 3 and 4 classes were produced. In 2 classes more generalization was done, in which other features aside the burnt scar were categorized as un-burnt area. As the number of classes increased, the extent of the burnt scar class reduces. The area named as built-up area in the 4 classes case, was not a true representation of the built-up area in reality. This is one of the limitations of unsupervised classification; it might not represent reality the way expected. There is an abrupt change from one class to another, an indication that the zones of transitions were not considered. The maps are shown below for the three cases

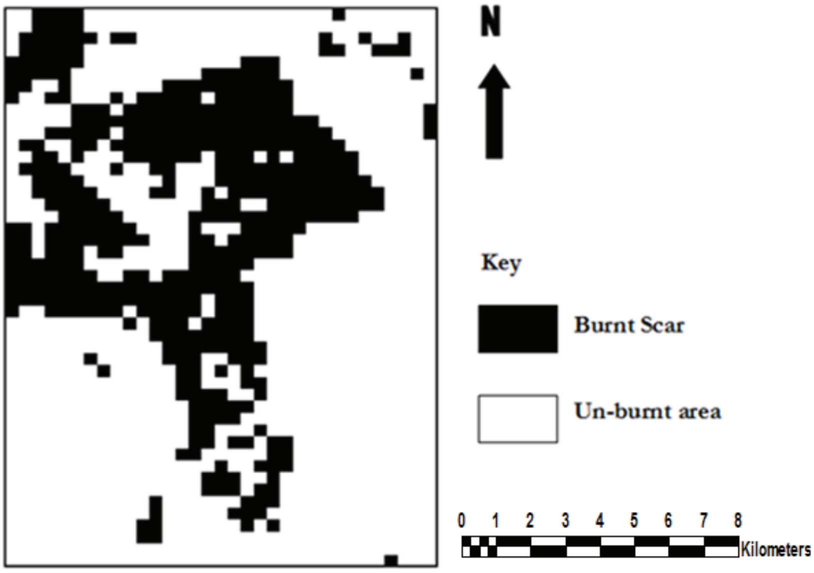

Figure 5.4: Classification result for 2-classes-unsuperviseed hard classification (ISODATA)

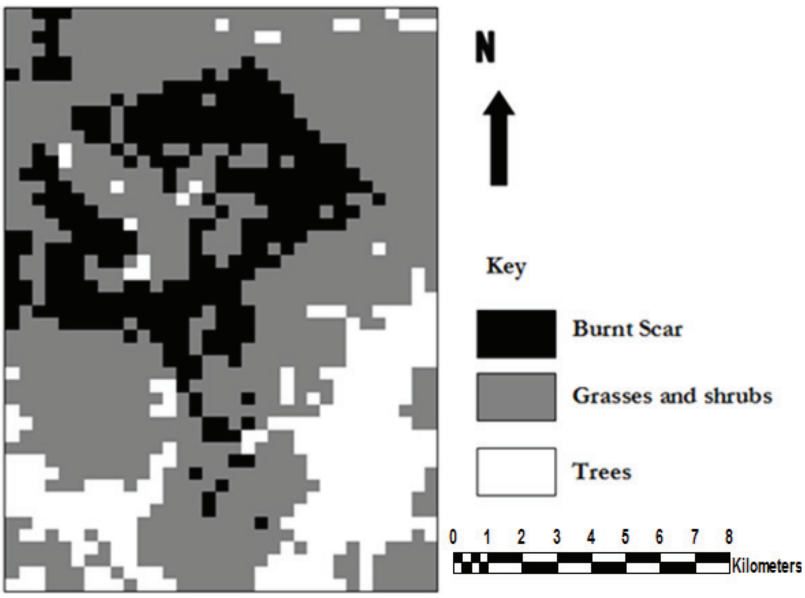

Figure 5.5: Classification result for 3-classes-unsuperviseed hard classification (ISODATA)

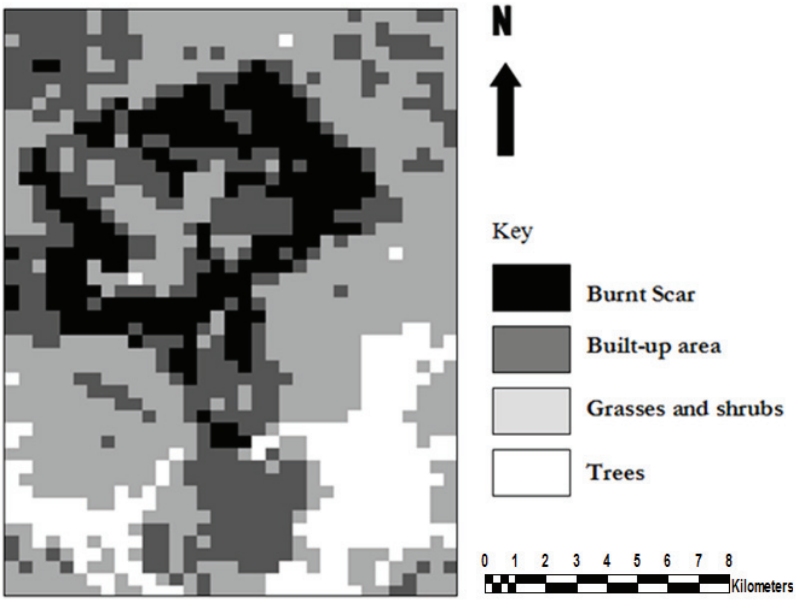

Figure 5.6: Classification result for 4-classes-unsuperviseed hard classification (ISODATA)

5.1.4. Class statistics-unsupervised hard classification (ISODATA)

The class statistics for all the cases were computed, however, the statistics. In both classes shown, the mean was lowest in band 3, while band 5, has the highest mean. The least covariance values were between 1 and 2.

Table 5.2: Class statistics-Burnt scar class-in-2-classes- unsupervised hard classification (ISODATA)

	Statistics of Burnt scar-2-classes-hard-unsupervised ISODATA($\times$0.0001)				
Bands	**Minimum**	**Maximum**	**Mean**	**Std. Dev.**	
1	266	486	361.279	42.706	
2	806	2003	1601.551	311.406	
3	136	253	185.371	23.53	
4	293	498	388.672	41.907	
5	1211	2006	1527.719	145.887	
	Covariance of bands ($\times$0.0001)				
Bands	**1**	**2**	**3**	**4**	**5**
1	1823.807	-2762.045	968.773	533.617	5280.109
2	-2762.045	96973.525	-1735.322	10947.616	2094.65
3	968.773	-1735.322	553.679	286.836	2738.014
4	533.617	10947.616	286.836	1756.176	2631.22
5	5280.109	2094.65	2738.014	2631.22	21283.13

Table 5.3: Class statistics-Un-burnt area class-in-2-classes- unsupervised hard classification (ISODATA)

	Statistics of Un-Burnt area-Unsupervised ISODATA(×0.0001)				
Bands	**Minimum**	**Maximum**	**Mean**	**Std. Dev.**	
1	203	736	329.412	62.971	
2	2000	3066	2320.94	225.53	
3	96	361	168.699	31.919	
4	373	727	461.319	39.845	
5	1102	2943	1500.47	195.699	
	Covariance of bands(×0.0001)				
Bands	**1**	**2**	**3**	**4**	**5**
1	3965.333	-167.007	1972.777	1951.222	11012.991
2	-167.007	50863.834	21.892	4884.52	14039.34
3	1972.777	21.892	1018.849	1004.963	5490.901
4	1951.222	4884.52	1004.963	1587.592	6755.906
5	11012.991	14039.34	5490.901	6755.906	38298.125

5.2. Result obtained for the supervised hard classification

The supervised classification results (Maximum likelihood (MLC)) were obtained for three cases: case A, case B and case C, having 2, 3 and 4 classes respectively. The results are:

5.2.1. Class separability-supervised hard classification (MLC)

The separability values of all combination of classes were done in all the three cases, the result indicated the maximum value of class separabilty was obtained in all pair of possible class combinations; this statement meant that the classes are distinct from each other. The result is shown below.

Table 5.4: Class separability (Transformed Divergence) for supervised hard classification of MODIS classification (MLC)

Transformed divergence for unsupervised 3 cases(TD)		
Cases	**Classes**	**TD value**
2 classes	Burn scar	2000
	Un-burnt area	
3 classes	Burn scar	2000
	Grasses and shrubs	
	Burn scar	2000
	Trees	
	Grasses and shrubs	2000
	Tress	
4 classes	Burn scar	2000
	Built-up area	
	Burn scar	2000
	Grasses and shrubs	
	Burn scar	2000
	Trees	

	Built-up area	2000
	Grasses and shrubs	
	Built-up area	2000
	Trees	
	Grasses and shrubs	2000
	Trees	

5.2.2. Plot of mean value against Bands-supervised hard classification (MLC)

The mean value of each class was plotted against the number of bands, for the three cases. The plot reviewed that the mean for all classes was highest in band 2, while the mean value of all classes was lowest in band 3, the plots are shown below

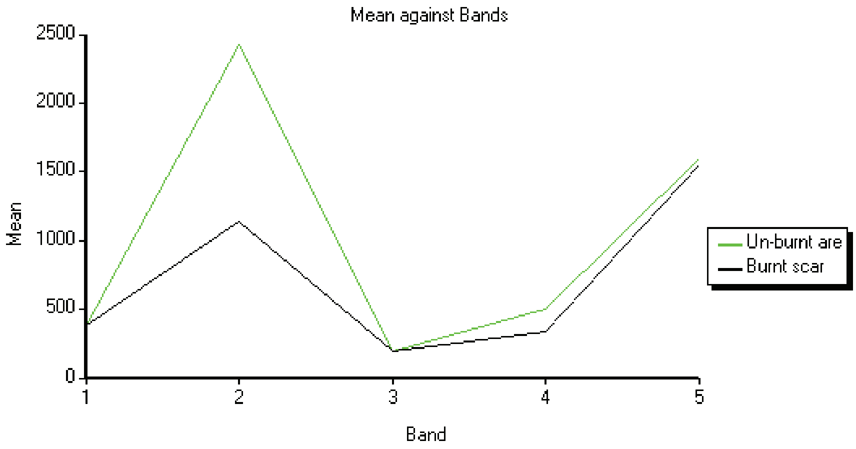

Figure 5.7: Mean value of class against Bands_2_classes_supervised hard classification (MLC)

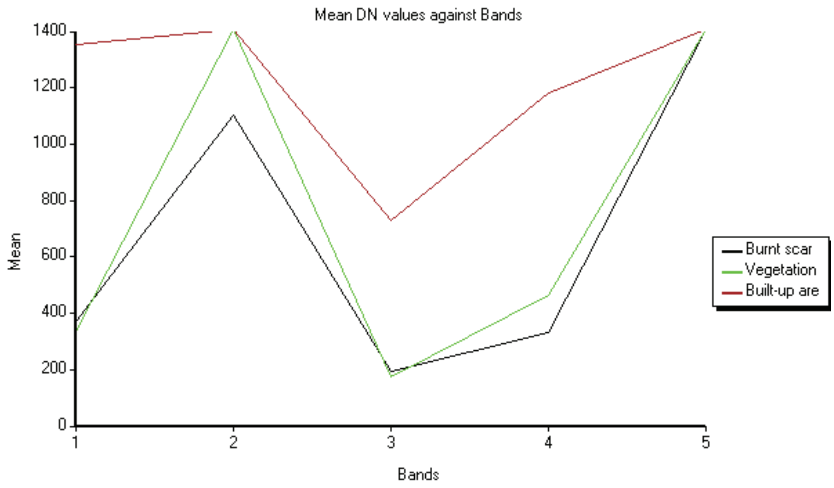

Figure 5.8:Mean value of class against Bands_3_classes_unsupervised hard classification(MLC)

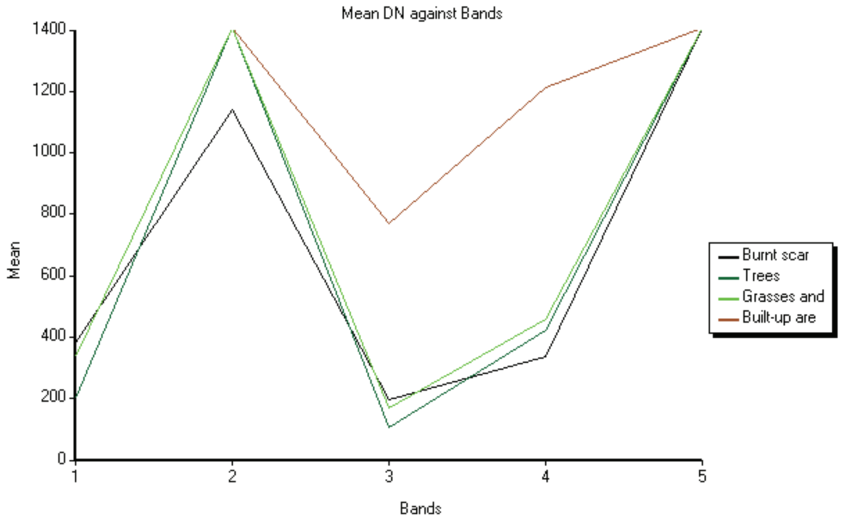

Figure 5.9: Mean value of class against Bands_4_classes_unsupervised hard classification (MLC)

5.2.3. Thematic map produced-supervised hard classification (MLC)

The thematic map using the MLC supervised hard classification was done for three cases as defined in section 6.2.2. This was done to obtain features of interest. In case A, we have burnt scar and un-burnt areas; this was the category for other features other than the burn scar. In case B, trees, grasses and shrubs were now merged and categorized as vegetation, with the built-up area separated, this was not possible in case B of the unsupervised classification(ISODATA). Case C was used to depict the four classes of interest, comparing the classification results for case C in both supervised and unsupervised hard classification, it was observed that the class definition for built-up area reflects reality in supervised than in un-supervised hard classification. The results are shown below:

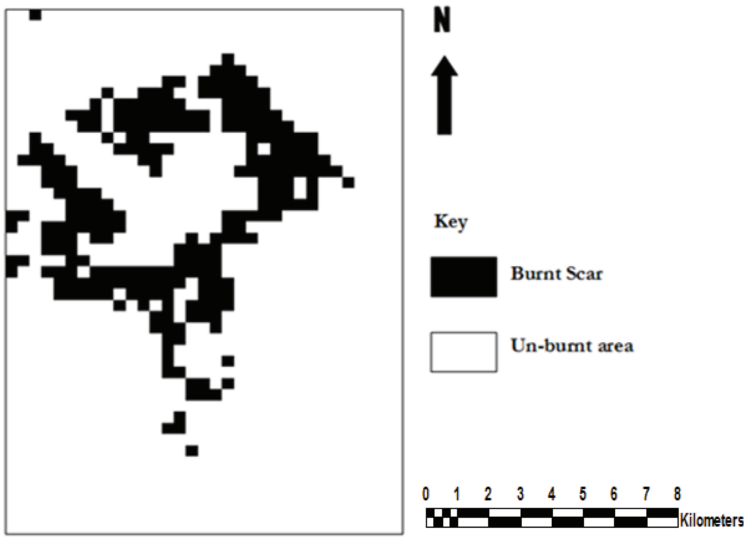

Figure 5.10: Classification result for 2-classes-superviseed hard classification (MLC)

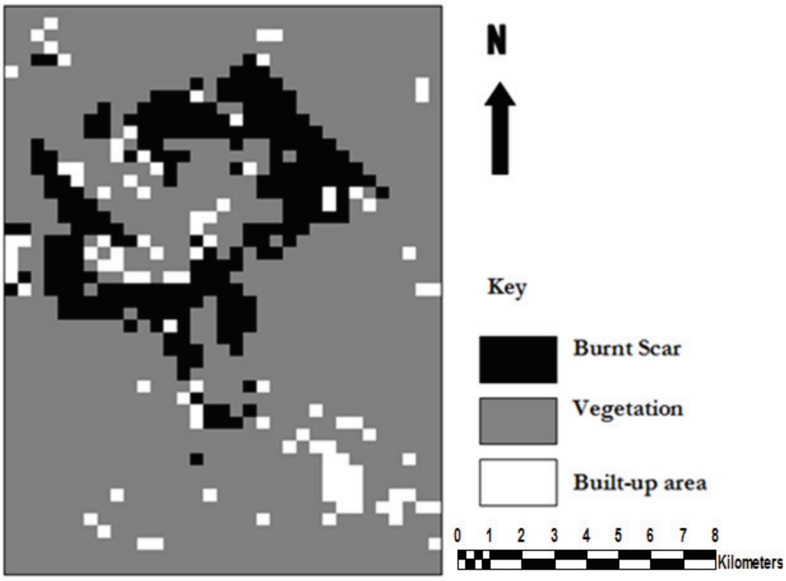

Figure 5.11: Classification result for 3-classes-superviseed hard classification (MLC)

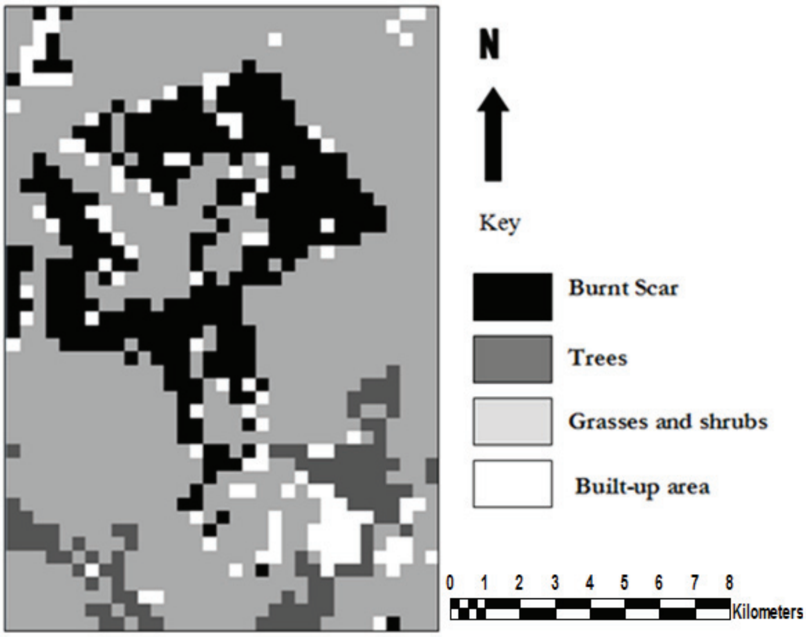

Figure 5.12: Classification result for 4-classes-superviseed hard classification (MLC)

5.2.4. Class statistics-supervised hard classification (MLC)

The class statistics for all the cases were computed. In both classes shown, the mean was lowest in band 3 in both classes. However, in the burnt scar class, the least covariance was obtained between band 3 and band 3 combination, for the un-burnt area, this was obtained between band 2 and band 3 combination.

Table 5.5: Class statistics-Burnt area class-in-2-classes- supervised hard classification (MLC)

	Statistics of Burnt scar-supervised MLC(×0.0001)				
Bands	**Minimum**	**Maximum**	**Mean**	**Std. Dev.**	
1	331	464	382.357	34.054	
2	806	1647	1136.518	211.665	
3	167	250	198.696	19.183	
4	293	438	340.286	38.699	
5	1315	1823	1553	136.084	
	Covariance of bands(×0.0001)				
Bands	**1**	**2**	**3**	**4**	**5**
1	1159.652	3873.866	603.019	1018.06	4018.455
2	3873.866	44802.181	1914.578	7258.068	15258.764
3	603.019	1914.578	367.997	582.761	2037.164
4	1018.06	7258.068	582.761	1497.626	3447.673
5	4018.455	15258.764	2037.164	3447.673	18518.8

Table 5.6: Class statistics-Un-burnt area class-in-2-classes- supervised hard classification (MLC)

	Statistics of Un-burnt scar-supervised MLC(×0.0001)				
Bands	**Minimum**	**Maximum**	**Mean**	**Std. Dev.**	
1	213	1669	378.986	278.633	
2	2064	3429	2424.986	398.565	
3	109	897	195.644	151.645	
4	415	1372	502.808	186.403	
5	1265	4005	1600.137	553.879	
	Covariance of bands(×0.0001)				
Bands	**1**	**2**	**3**	**4**	**5**
1	77636.18	11259.153	42211.745	50813.803	149048.182
2	11259.153	158854.403	6711.578	21885.761	64322.905
3	42211.745	6711.578	22996.149	27713.528	81184.466
4	50813.803	21885.761	27713.528	34746.018	100957.096
5	149048.182	64322.905	81184.466	100957.096	306781.453

5.3. Result obtained for the unsupervised and supervised soft classification(FCM)

Various results were obtained from using the fuzzy-c-means (FCM) algorithm. They are shown below.

5.4. Unsupervised soft classification(FCM)

The results for the unsupervised classification FCM classifications are presented here; this was done for all the three cases. The following were presented: the separability value between band 2 and band 3, classification and the membership values of all pixels were presented.

5.4.1. Class separability –unsupervised soft classification (FCM)

The class separability for different band combinations were investigated to determined the distinct nature of each class. The results presented the band combination of 2 and 4 are shown below for every of the 3 cases. In all the cases, there is no clear distinction between the various classes; this because there is no abrupt change from a class to another, there is the existence of a zone of transition, referred to as the zone of transition, within this zone, the pixels changes from one class to another, hence having values for all classes. In case A, the pixels for the un-burnt area were more closely clustered, compared to that of the burnt scar. In case B, the grasses and shrubs class were more clustered together, as shown below.

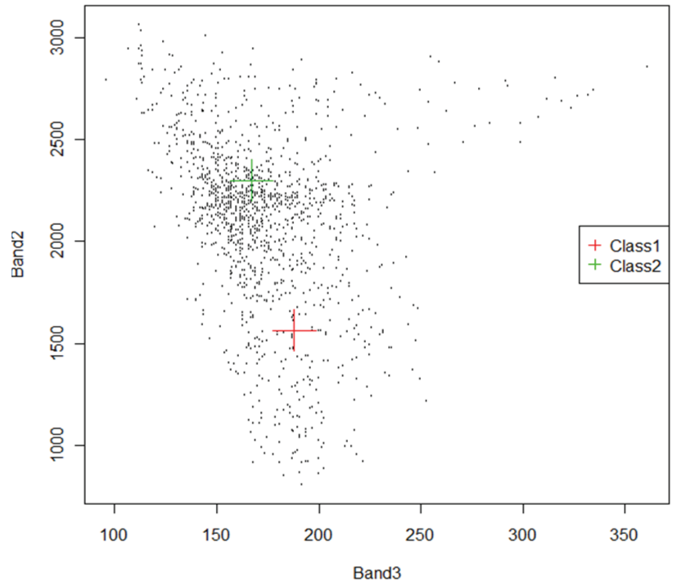

Class	Name
1	Burnt scar
2	Un-burnt area

Figure 5.13-: Feature space-2-classes_unsupervised FCM

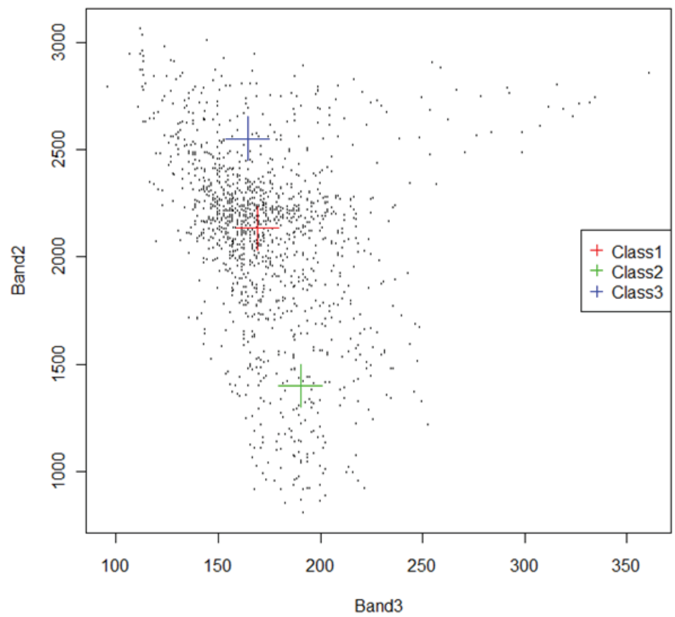

Class	Name
1	Grasses & shrubs
2	Burnt scar
3	Trees

Figure 5.14: Feature space-3-classes_unsupervised FCM

5.4.2. MODIS unsupervised FCM classification

The outputs of the unsupervised FCM classification for all the cases are shown below. The membership values of the pixels continue to change as the number of classes increase, these changes are gradual unlike in the hard classification. Membership values ranges between 0 and 1, also the summation of the membership values of a given pixel in all the defined classes is constrained to be equal to 1. The unsupervised FCM does not represent the true nature of the built-up area, just like the case of the unsupervised hard classification.

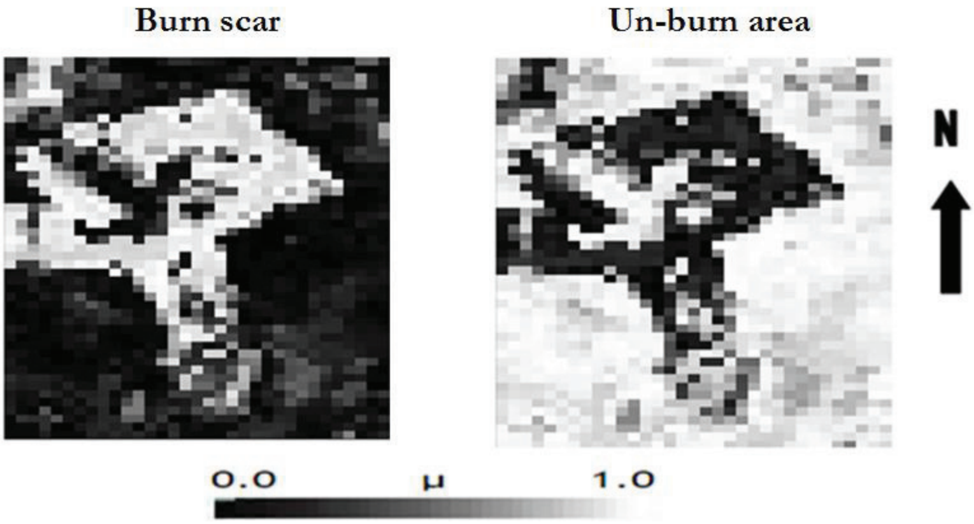

Figure 5.15: MODIS unsupervised FCM_2_classes

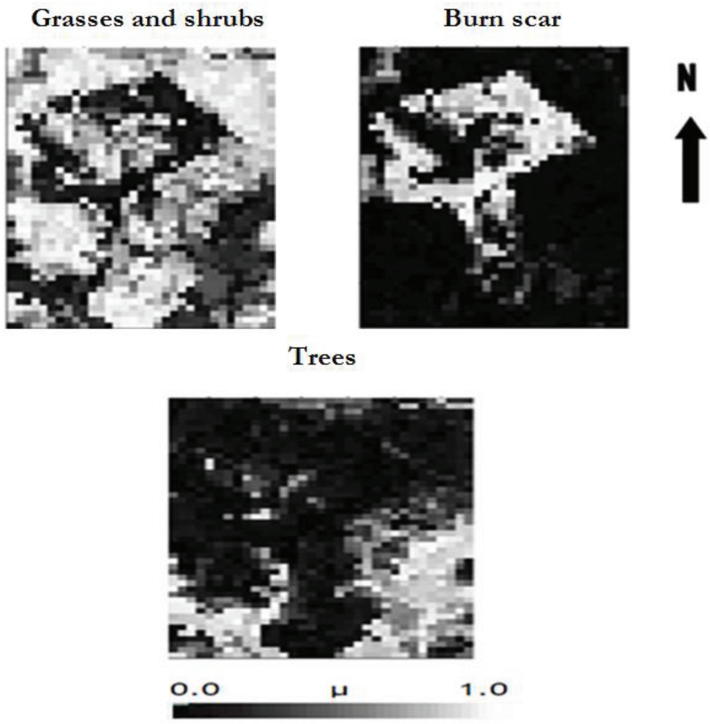

Figure 5.16: MODIS unsupervised FCM_3_classes

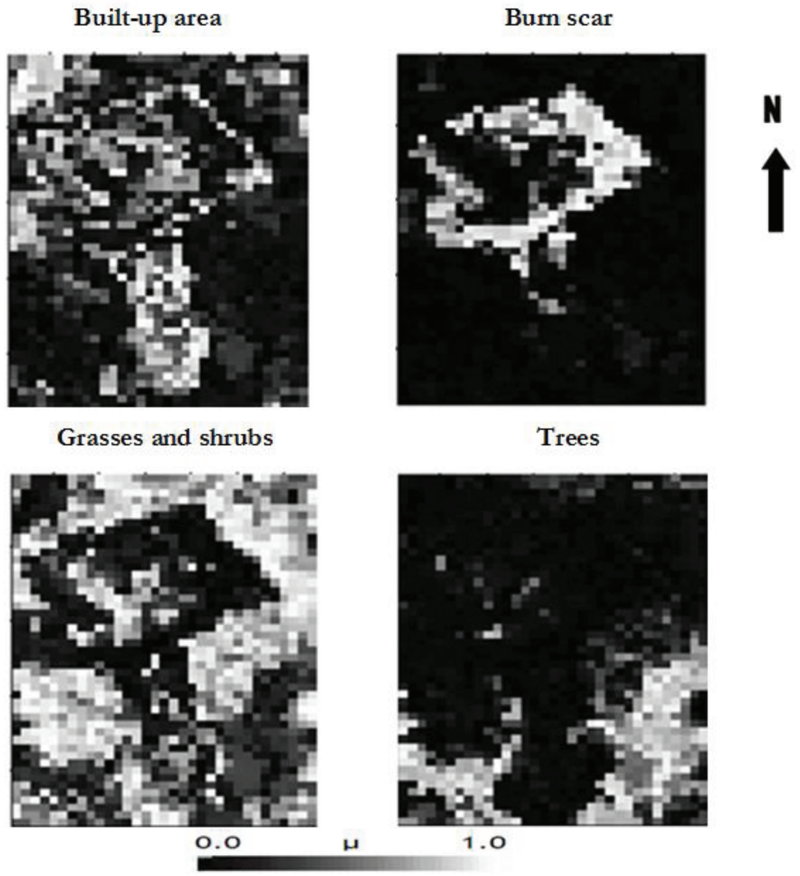

Figure 5.17: MODIS unsupervised FCM_4_classes

5.5. Supervised soft classification(FCM)

The results for the supervised classification FCM classifications are presented here; this was done for all the three cases. The classification and the membership values of all pixels were presented.

5.5.1. MODIS supervised FCM classification

The outputs of the unsupervised FCM classification for all the cases are shown below. The membership values of the pixels continue to change as the number of classes increase, these changes are gradual unlike in the hard classification. Membership values ranges between 0 and 1, also the summation of the membership values of a given pixel in all the defined classes is constrained to be equal to 1. The supervised FCM, allows the classes that are of interest to be defined before the algorithm is ran, this is not possible with the unsupervised FCM, for instance, getting the built-up area class was not possible in the in case B of the unsupervised FCM, when it was seen in case C, it didn't reflect reality. The supervised FCM can be used to show the classes of interest which will reflect reality. The results generated using the supervised FCM for the three cases are shown below.

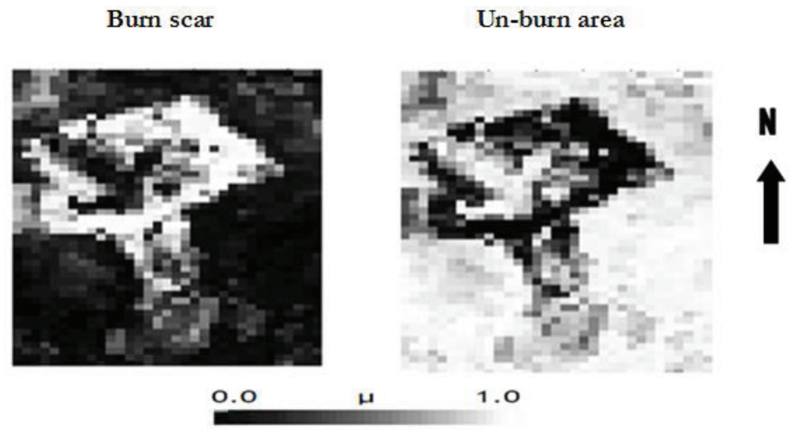

Figure 5.18: MODIS supervised FCM_2_classes

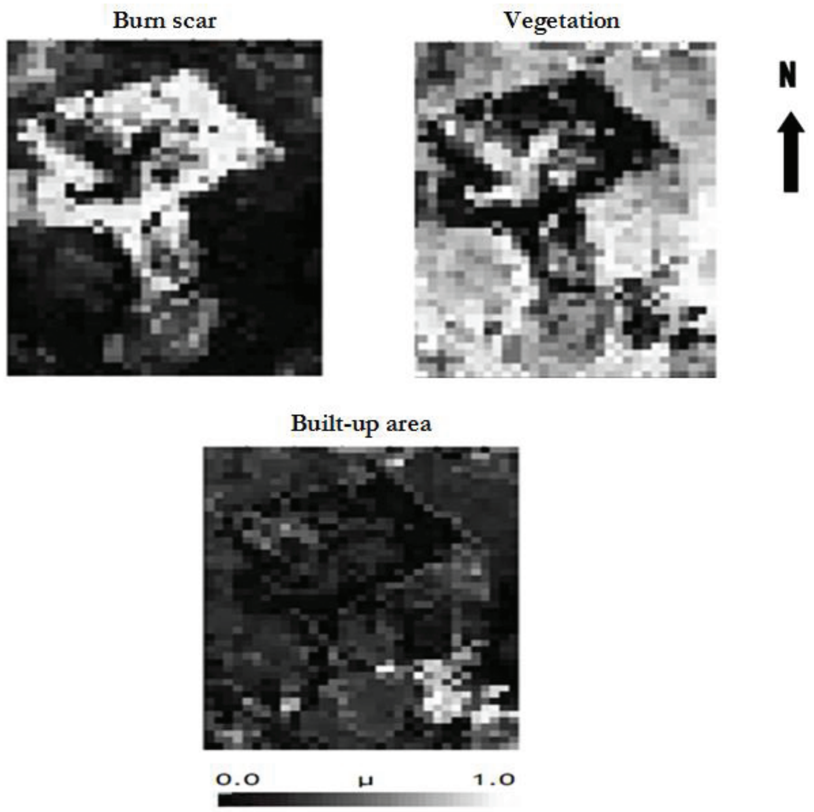

Figure 5.19: MODIS supervised FCM_3_classes

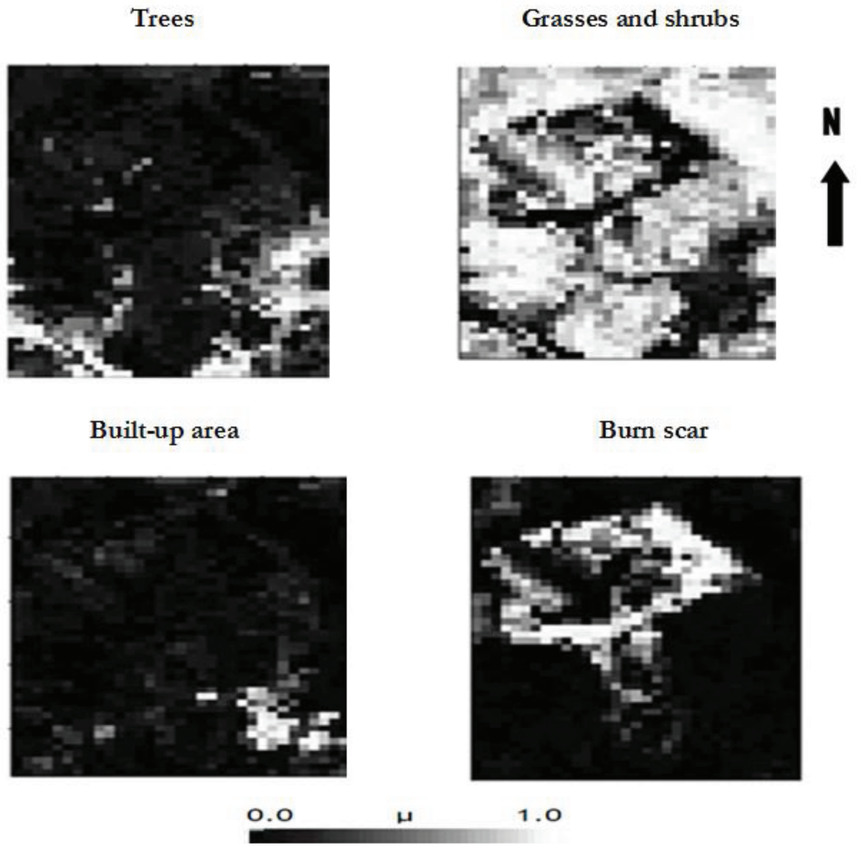

Figure 5.20: MODIS supervised FCM_4_classes

5.6. Reference data results

The ASTER data was used as the reference, it is a high resolution image (15 m), this resolution is very high when compared to the MODIS data (approximately 500 m). Before the ASTER data was used to compare the results of the classification produced using the MODIS data, it was itself processed to make it of the same state as the classified MODIS datasets, to achieve this, the ASTER data was classified in the same manner as the MODIS. The ASTER data was classified in three cases for the unsupervised (ISODATA) and supervised (MLC) hard classification. It was also classified in three cases for the unsupervised and supervised using the fuzzy-c-means. The completion of the classification, led to the degradation stage, in which the classified ASTER results were degraded to correspond to the spatial resolution of the classified MODIS, before accuracy of both datasets were compared. The results of the classifications for the reference datasets (ASTER) as well as the degradation results are shown below.

5.6.1. Classification result for ASTER unsupervised hard classification (ISODATA)

The three cases were applied to generate hard unsupervised classification (ISODATA) for the ASTER data. The highest level of generalisation was done in case A, this produces only two classes, burnt scar and un-burnt area (every other feature resulted in un-burnt area aside the burnt scar). In the case C, the built – up area was not clearly defined, the same resulted in the unsupervised classification of MODIS data. As the number of classes increase, the extent of the burnt scar class reduces. Also, another class referred to as water body could be easily defined in the ASTER image; this was not visible in the MODIS image, defining four classes for the ASTER image, concealed information that can still be easily identified. More generalization was done on the ASTER data than on the MODIS when classification results are compared. There is an abrupt change from one class to another, an indication that the zones of transitions were not considered. The maps are shown below for the three cases

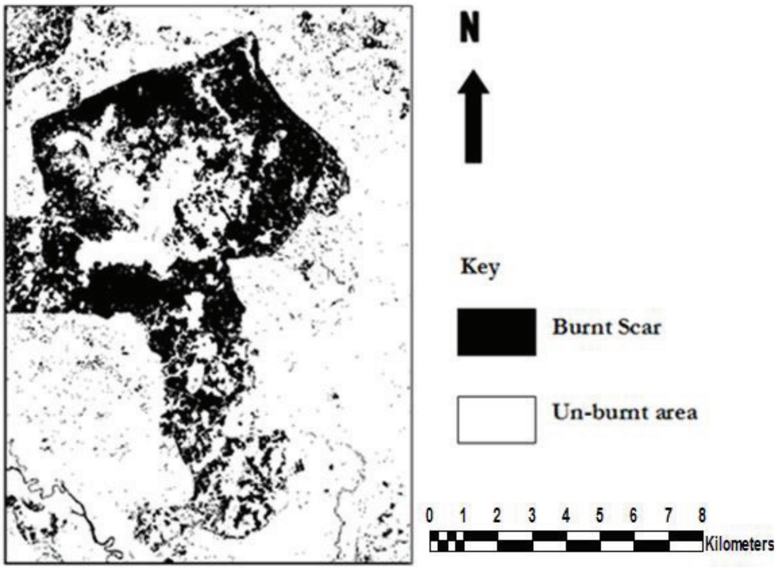

Figure 5.21: ASTER unsupervised hard classification_2_classes (ISODATA)

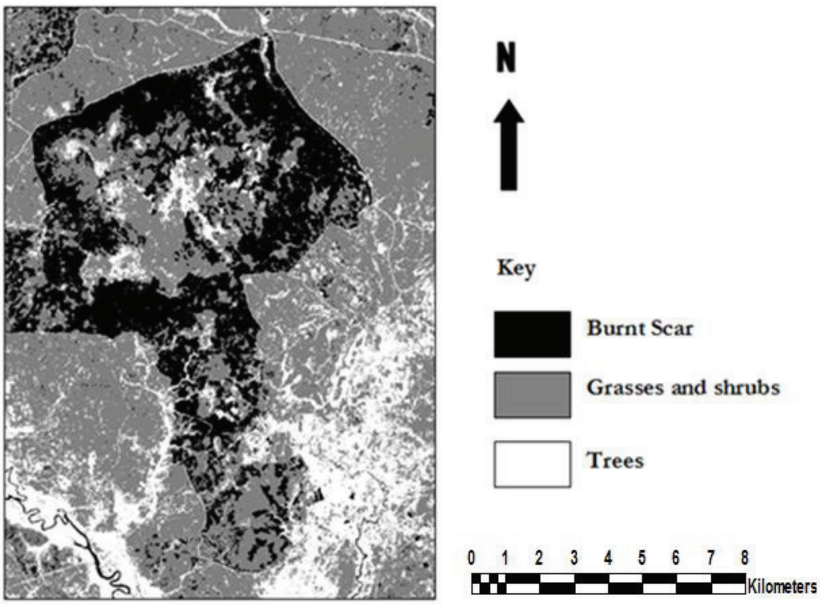

Figure 5.22: ASTER unsupervised hard classification_3_classes (ISODATA)

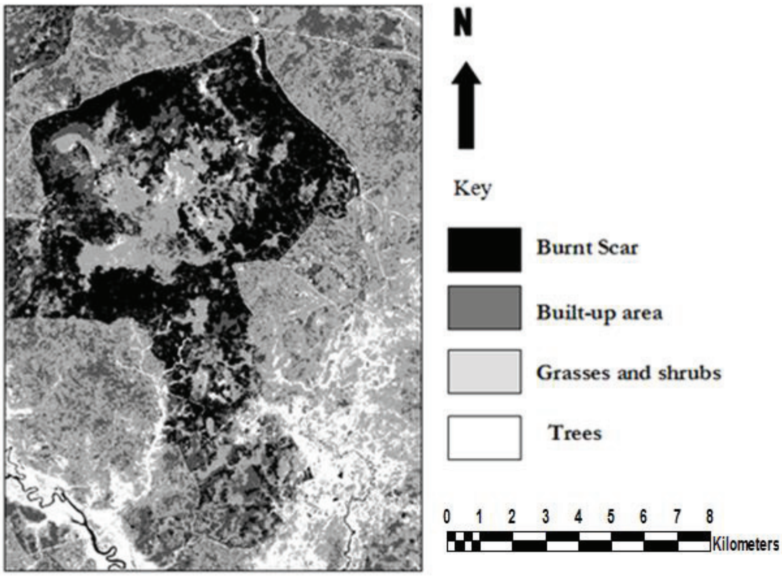

Figure 5.23: ASTER unsupervised hard classification_4_classes (ISODATA)

5.6.2. Classification result for ASTER supervised hard classification (MLC)

The thematic map using the MLC supervised hard classification was also done for the ASTER image so as to make it comparable with the corresponding MODIS classified output. Three cases were also defined. It was possible to obtain the features of interest by taking the appropriate training pixels. In case A, we have burnt scar and un-burnt areas; this was the category for other features other than the burn scar. In case B, trees, grasses and shrubs were now merged and categorized as vegetation, with the built-up area separated, this was not possible in case B of the unsupervised classification(ISODATA). Case C was used to depict the four classes of interest, comparing the classification results for case C in both supervised and unsupervised hard classification, it was observed that the class definition for built-up area reflects reality in supervised than in un-supervised hard classification. The results are shown below:

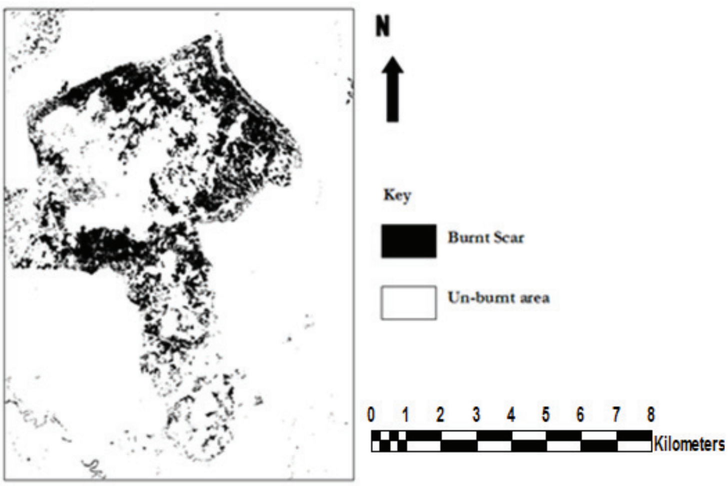

Figure 5.24: ASTER supervised hard classification_2_classes (MLC)

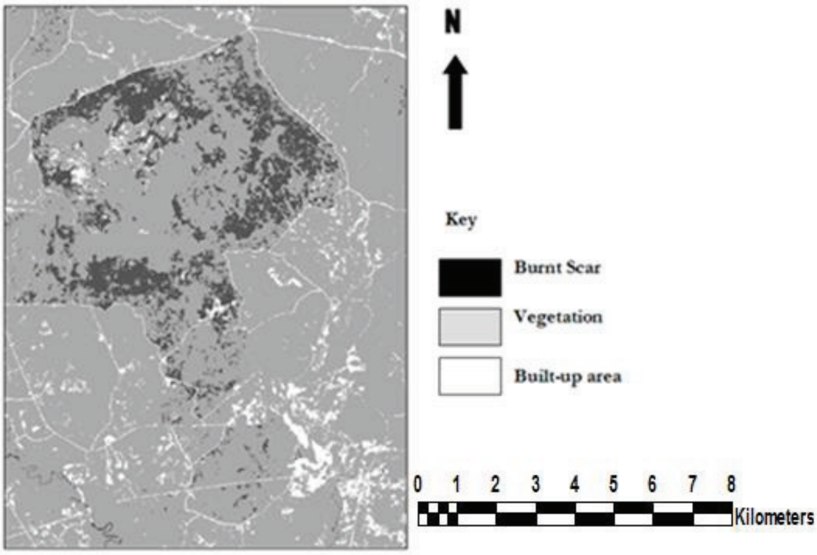

Figure 5.25: ASTER supervised hard classification_3_classes (MLC)

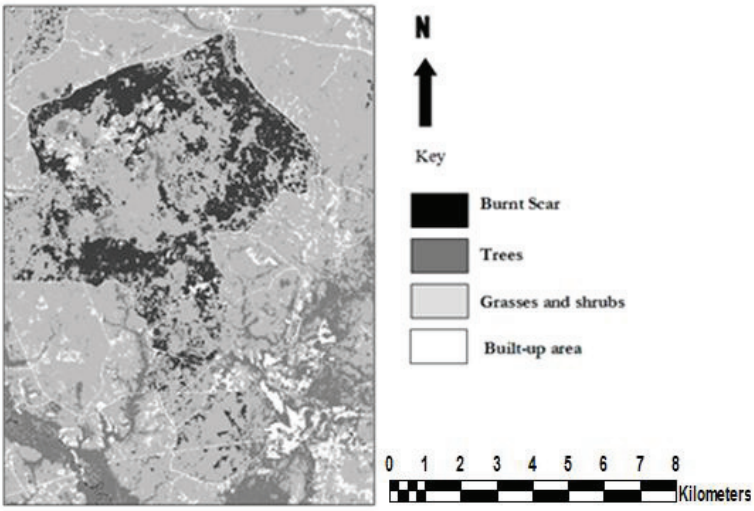

Figure 5.26: ASTER supervised hard classification_4_classes (MLC)

5.7. Result obtained for the unsupervised and unsupervised soft classification(FCM)

Various results were obtained in this regards for unsupervised and supervised FCM, three cases each were investigated for 2, 3 and 4 classes respectively and they are discussed below.

5.7.1. Unsupervised soft classification (Fuzzy-c-mean (FCM))-ASTER

The methods adopted in this instance has been explained in section 5.4.2, the difference is in the fact that we are talking of ASTER and not MODIS. The membership values are shown below for the three cases.

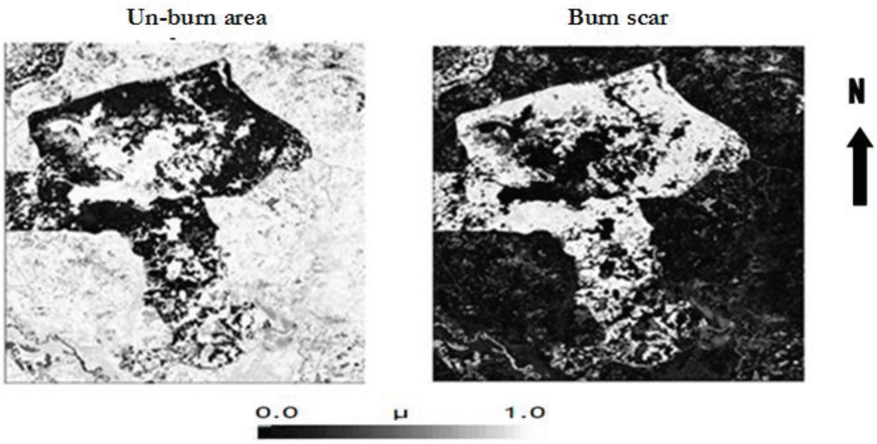

Figure 5.27: Unsupervised soft classification_2_classes_FCM-ASTER

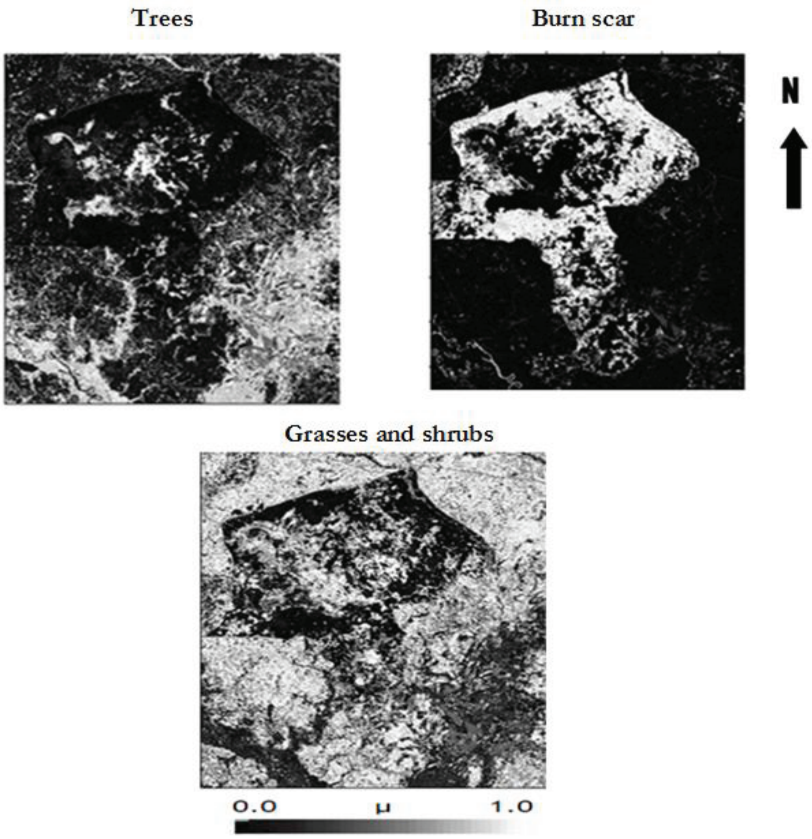

Figure 5.28: Unsupervised soft classification_3_classes_FCM-ASTER

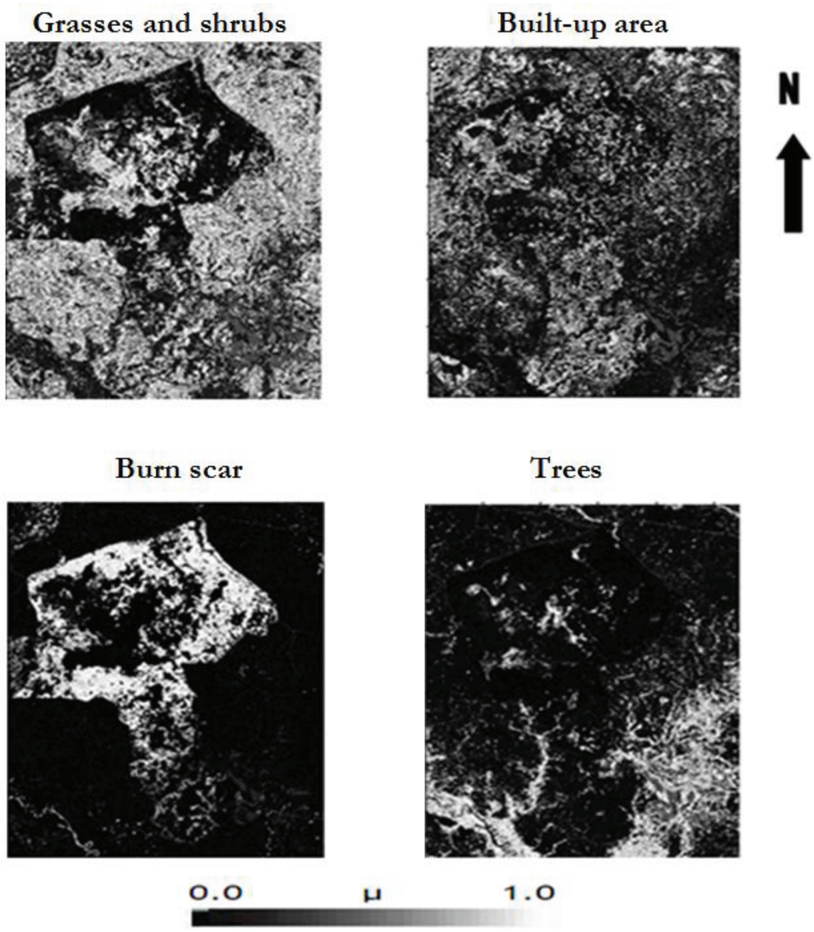

Figure 5.29: Unsupervised soft classification_4_classes_FCM-ASTER

5.7.2. Supervised soft classification (Fuzzy-c-mean (FCM))-ASTER

Again the same explanation for the section 5.4.3 suffices, the results are shown below

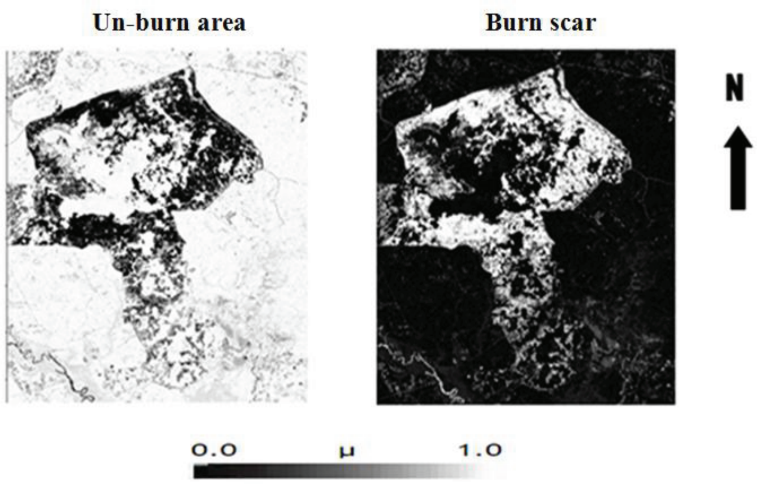

Figure 5.30: Supervised soft classification_2_classes_FCM-ASTER

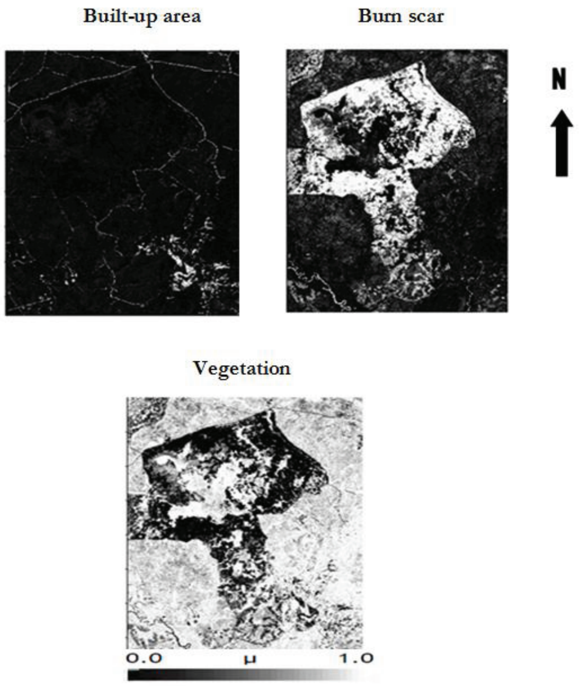

Figure 5.31: Supervised soft classification_3_classes_FCM-ASTER

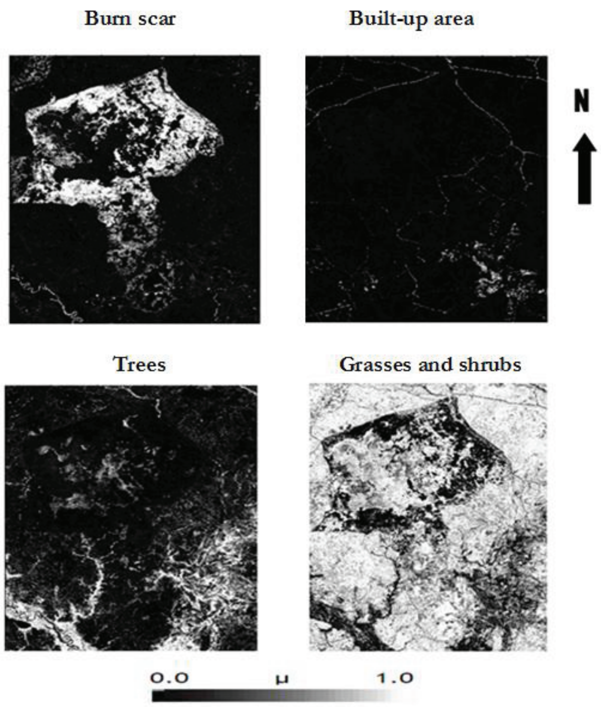

Figure 5.32: Supervised soft classification_4_classes_FCM-ASTER

5.8. Hard aster degradtion

The classified output of the ASTER was degraded to make it comparable with the MODIS data set, the degradation was done for the hard and soft cases, however the result here is presented for the hard case.

5.8.1. Un-supervised hard degradation aster

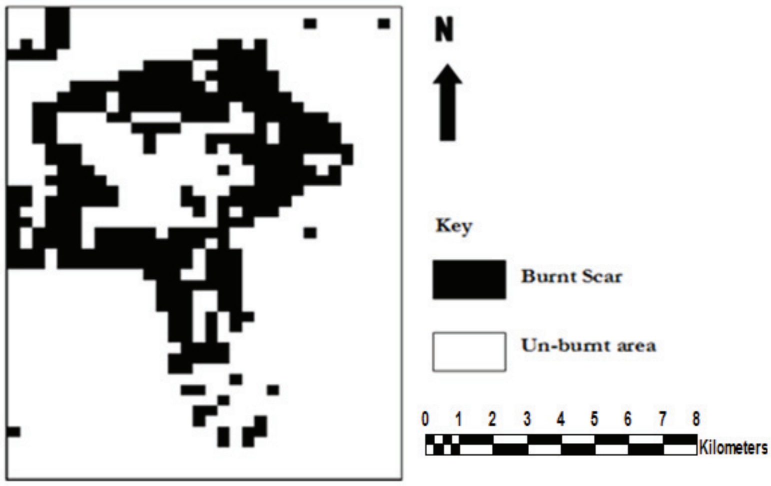

Figure 5.33: Degraded_aster_hard_2__unsupervised

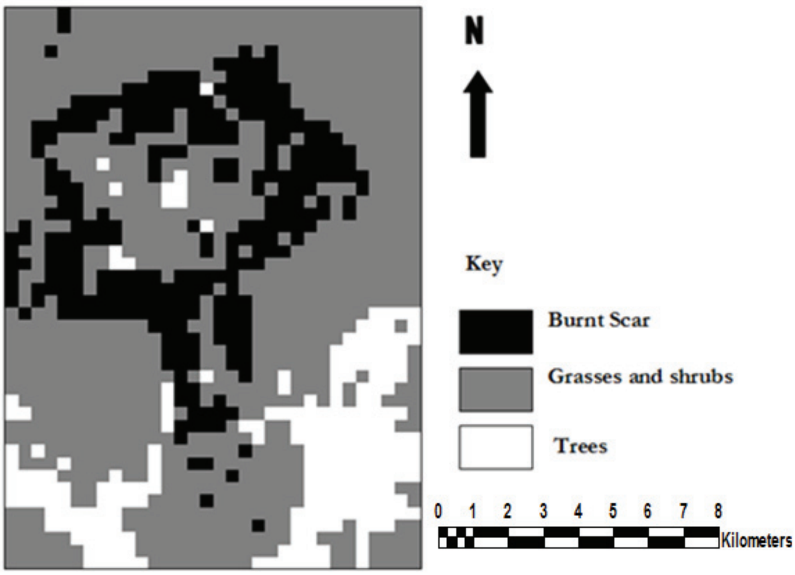

Figure 5.34:Degraded_aster_hard_3__unsupervised

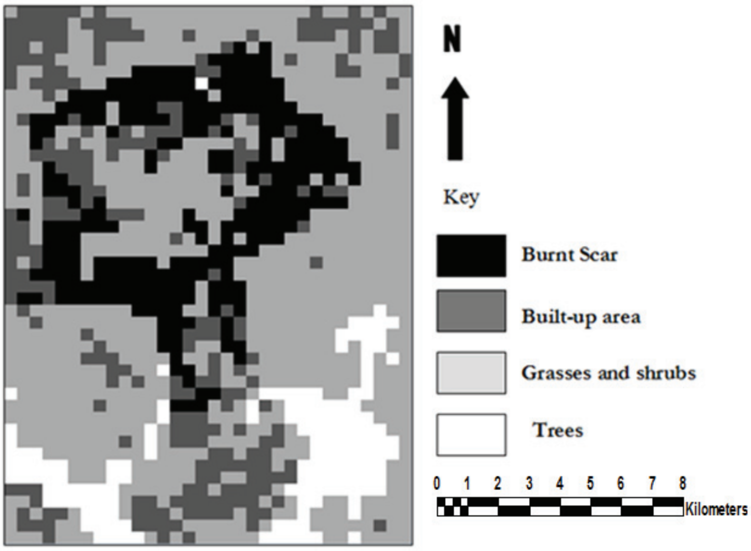

Figure 5.35: Degraded_aster_hard_4__unsupervised

5.9. Degradation of Supervised FCM output (ASTER)

The output of the degraded ASTER for the supervised FCM is shown below for 3 cases, 3 classes. The correlation between the FCM and the corresponding MODIS was done; it must prove that both correlate to a certain degree, the values are presented in the accuracy table.

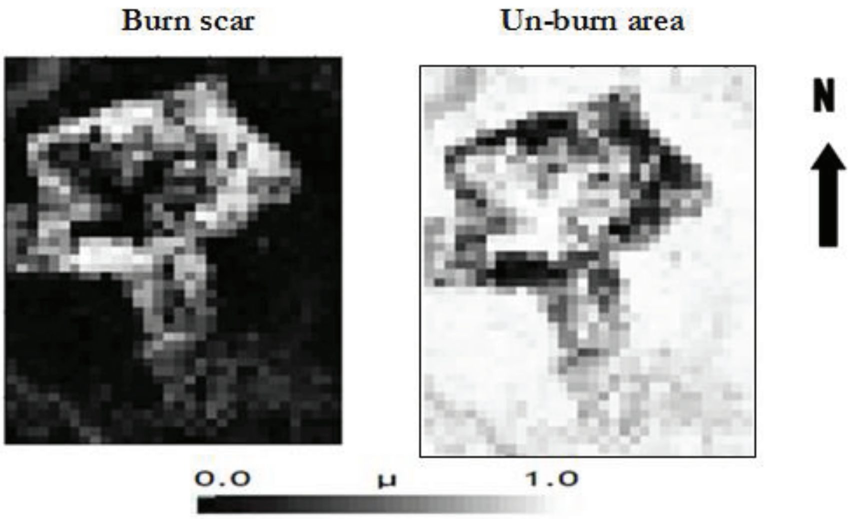

Figure 5.36: Degraded ASTER_2_classes_Supervised FCM

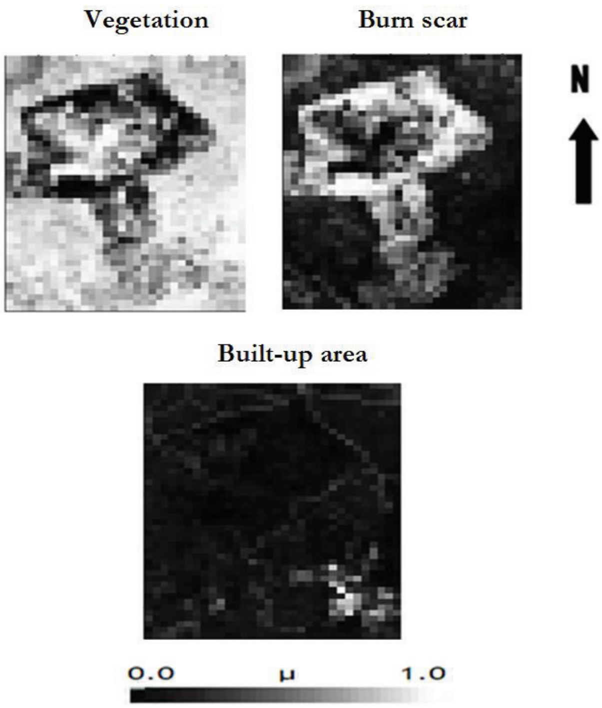

Figure 5.37: Degraded ASTER_3_classes_Supervised FCM

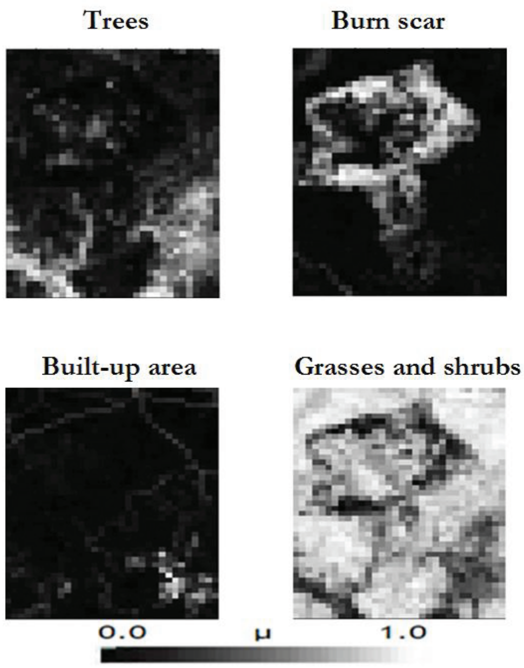

Figure 5.38: Degraded ASTER_4_classes_Supervised FCM

5.10. Accuracy assessment results

The accuracy results obtained are shown in the table below, this was done for hard and soft classification, and the results were discussed in the discussion section. The blue colour represents the diagonal values that show the relationship between corresponding classes.

5.10.1. Hard accuracy assessment unsupervised

Table 5.7: ISODATA_2_classes_confusion matrix

2_classes					
Classified data	Confusion matrix_2_classes_unsupervised_hard(ISODATA) — Reference			Total	User accuracy (%)
		Burnt scar	Un-burnt area		
	Burnt scar	329	150	479	69
	Un-burnt area	27	934	961	97
	Total	356	1084	1440	
	Producer accuracy (%)	92	86		
	Overall accuracy (%)		**88**		

Table 5.8: ISODATA_2_classes_correlation and kappa coefficient

Classified data	Correlation_coefficient_2_classes_unsupervised_hard(ISODATA) — Reference			Kappa coefficient
		Burnt scar	Un-burnt area	
	Burnt scar	0.72	-0.72	
	Un-burnt area	-0.72	0.72	**0.63**

Table 5.9: ISODATA_3_classes_confusion matrix

3_classes						
Classified data	Confusion matrix_3_classes_unsupervised_hard(ISODATA) — Reference				Total	User accuracy (%)
		Burnt scar	Grasses and shrubs	Trees		
	Burnt scar	241	82	1	324	74
	Grasses and shrubs	58	757	26	841	90
	Trees	0	78	197	275	72
	Total	299	917	224	**1440**	
	Producer accuracy (%)	81	83	88		
		Overall accuracy (%)		**83**		

Table 5.10:ISODATA_3_classes_correlation and kappa coefficient

Classified data	Correlation_coefficient_3_classes_unsupervised_hard(ISODATA)				Kappa coefficient
	Reference				
		Burnt scar	Grasses and shrubs	Trees	
	Burnt scar	0.71	-0.43	-0.23	
	Grasses and shrubs	-0.41	0.65	-0.41	
	Trees	-0.25	-0.36	0.75	**0.63**

Table 5.11:ISODATA_4_classes_confusion matrix

4_classes							
Classified data	**Confusion matrix_4_classes_unsupervised_hard(ISODATA)**					**Total**	**User accuracy (%)**
	Reference						
		Burnt scar	Built-up area	Grasses and shrubs	Trees		
	Burnt scar	196	26	16	0	238	82
	Built-up area	65	191	131	2	389	49
	Grasses and shrubs	8	46	544	13	611	89
	Trees	0	3	69	130	202	64
	Total	269	266	760	145	**1440.00**	
	Producer accuracy (%)	73	72	72	90		
		Overall accuracy (%)			**74**		

Table 5.12:ISODATA_4_classes_correlation and kappa coefficient

Classified data	Correlation_coefficient_4_classes_unsupervised_hard(ISODATA)					Kappa coefficient
	Reference					
		Burnt scar	Built-up area	Grasses and shrubs	Trees	
	Burnt scar	0.73	-0.09	-0.41	-0.15	
	Built-up area	-0.03	0.48	-0.23	-0.19	
	Grasses and shrubs	-0.38	-0.24	0.62	-0.23	
	Trees	-0.19	-0.18	-0.15	0.73	**0.56**

5.10.2. Hard accuracy assessment_supervised

Table 5.13: MLC_2_classes_confusion matrix

2_classes				
Confusion matrix_2_classes_supervised_hard(MLC)			Total	User accuracy (%)
Reference				
	Burnt scar	Un-burnt area		
Burnt scar	129	129	258	50
Un-burnt area	19	1163	1182	98
Total	148	1292	**1440**	
Producer accuracy (%)	87	90		
Overall accuracy (%)		**90**		

Table 5.14:MLC_2_classes_correlation and kappa coefficient

Correlation_coefficient_2_classes_supervised_hard(MLC)			Kappa coefficient
Reference			
	Burnt scar	Un-burnt area	
Burnt scar	0.61	-0.61	
Un-burnt area	-0.61	0.61	**0.52**

Table 5.15: MLC_3_classes_confusion matrix

3_classes					
Confusion matrix_3_classes_supervised_hard(MLC)				Total	User accuracy (%)
Reference					
	Burnt scar	Vegetation	Built-up area		
Burnt scar	201	39	1	241	83
Vegetation	68	992	42	1102	90
Built-up area	20	53	24	97	25
Total	289	1084	67	**1440**	
Producer accuracy (%)	70	92	36		
	Overall accuracy (%)	**85**			

Table 5.16:MLC_3_classes_correlation and kappa coefficient

Correlation_coefficient_3_classes_supervised_hard(MLC)				Kappa coefficient
Reference				
	Burnt scar	Vegetation	Built-up area	
Burnt scar	0.71	-0.61	-0.09	
Vegetation	-0.63	0.62	-0.07	
Built-up area	0.00	-0.13	0.26	**0.54**

Classified data

Table 5.17: MLC_4_classes_confusion matrix

4_classes							
Classified data	**Confusion matrix_4_classes_supervised_hard(MLC)**					**Total**	**User accuracy (%)**
	Reference						
		Burnt scar	Trees	Grasses and shrubs	Built-up area		
	Burnt scar	177	0	77	56	310	57
	Trees	0	92	0	5	97	95
	Grasses and shrubs	17	108	766	28	919	83
	Built-up area	8	18	58	30	114	26
	Total	202	218	901	119	**1440**	
	Producer accuracy (%)	88	42	85	25		
		Overall accuracy (%)			**74**		

Table 5.18: MLC_4_classes_correlation and kappa coefficient

	Correlation_coefficient_4_classes_supervised_hard(MLC)					**Kappa coefficient**
Classified data	**Reference**					
		Burnt scar	Trees	Grasses and shrubs	Built-up area	
	Burnt scar	0.65	-0.22	-0.41	0.19	
	Trees	-0.11	0.60	-0.35	-0.03	
	Grasses and shrubs	-0.47	-0.13	0.57	-0.25	
	Built-up area	-0.06	0.01	-0.07	0.19	**0.50**

5.10.3. Soft accuracy assessment_unsupervised

Table 5.19: Unsupervised_FCM_2_classes_fuzzy confusion matrix

2_classes					
Classified data	**Fuzzy confusion matrix_2_classes_unsupervised_soft(FCM)**			**Total**	**Fuzzy user accuracy (%)**
	Reference				
		Un-burnt area	Burnt scar		
	Un-burnt area	890.84	242.85	1133.70	78.58
	Burnt scar	264.19	368.45	632.64	58.24
	Total	1155.03	611.31	**1766.34**	
	Fuzzy producer accuracy (%)	77.13	60.27		
	Fuzzy overall accuracy (%)		**71.29**		

Table 5.20: Unsupervised_FCM_2_classes_correlation coefficient

Classified data	**Correlation_coefficient_2_classes_unsupervised_soft(FCM)**		
	Reference		
		Un-burnt area	Burnt scar
	Un-burnt area	0.84	-0.84
	Burnt scar	-0.84	0.84

Table 5.21: Unsupervised_FCM_3_classes_fuzzy confusion matrix

3_classes						
Classified data	**Fuzzy confusion matrix_3_classes_unsupervised_soft(FCM)**				**Total**	**Fuzzy user accuracy (%)**
	Reference					
		Trees	Burnt scar	Grasses and shrubs		
	Trees	299.88	84.34	238.75	622.97	48.14
	Burnt scar	83.18	238.47	152.72	474.38	50.27
	Grasses and shrubs	272.07	169.72	616.50	1058.28	58.25
	Total	655.14	492.53	1007.97	**2155.64**	
	Fuzzy producer accuracy (%)	45.77	48.42	61.16		
		Fuzzy overall accuracy (%)		**53.57**		

Table 5.22: Unsupervised_FCM_3_classes_correlation coefficient

Classified data	**Correlation_coefficient_3_classes_unsupervised_soft(FCM)**			
	Reference			
		Trees	Burnt scar	Grasses and shrubs
	Trees	0.83	-0.42	-0.30
	Burnt scar	-0.48	0.84	-0.53
	Grasses and shrubs	-0.26	-0.43	0.76

Table 5.23: Unsupervised_FCM_4_classes_fuzzy confusion matrix

4_classes							
Classified data	**Fuzzy confusion matrix_4_classes_unsupervised_soft(FCM)**					**Total**	**Fuzzy user accuracy (%)**
	Reference						
		Built-up area	Trees	Grasses and shrubs	Burnt scar		
	Built-up area	251.12	98.91	233.62	131.87	715.51	35.10
	Trees	96.34	185.73	158.36	44.18	484.61	38.33
	Grasses and shrubs	252.44	164.45	466.98	83.70	967.58	48.26
	Burnt scar	90.66	38.95	68.88	163.29	361.77	45.13
	Total	690.55	488.04	927.85	423.03	**2529.47**	
	Fuzzy producer accuracy (%)	36.36	38.06	50.33	38.60		
		Fuzzy overall accuracy (%)			**42.19**		

Table 5.24: Unsupervised_FCM_4_classes_correlation coefficient

Classified data	**Correlation_coefficient_4_classes_unsupervised_soft(FCM)**				
	Reference				
		Built-up area	Trees	Grasses and shrubs	Burnt scar
	Built-up area	0.58	-0.35	-0.21	0.12
	Trees	-0.47	0.84	-0.10	-0.31
	Grasses and shrubs	-0.05	-0.10	0.75	-0.54
	Burnt scar	-0.08	-0.32	-0.62	0.83

5.10.4. Soft accuracy assessment_supervised FCM

Table 5.25: Supervised_FCM_2_classes_fuzzy confusion matrix

2_classes					
Classified data	**Fuzzy confusion matrix_2_classes_supervised_soft(FCM)**			**Total**	**Fuzzy user accuracy (%)**
	Reference				
		Burnt scar	Un-burnt area		
	Burnt scar	269.53	286.47	556.00	48.48
	Un-burnt area	166.00	980.18	1146.18	85.52
	Total	435.53	1266.65	**1702.18**	
	Fuzzy producer accuracy (%)	61.89	77.38		
	Fuzzy overall accuracy (%)			**73.42**	

Table 5.26: Supervised_FCM_2_classes_correlation coefficient

Classified data	Correlation_coefficient_2_classes_supervised_soft(FCM)		
	Reference		
		Burnt scar	Un-burnt area
	Burnt scar	0.85	-0.85
	Un-burnt area	-0.85	0.85

Table 5.27: Supervised_FCM_3_classes_fuzzy confusion matrix

3_classes						
Classified data	**Fuzzy confusion matrix_3_classes_supervised_soft(FCM)**				**Total**	**Fuzzy user accuracy (%)**
	Reference					
		Burnt scar	Vegetation	Built-up area		
	Burnt scar	353.65	247.22	65.40	666.27	53.08
	Vegetation	207.27	721.49	76.68	1005.43	71.76
	Built-up area	167.70	255.12	80.65	503.48	16.02
	Total	728.62	1223.83	222.73	**2175.18**	
	Fuzzy producer accuracy (%)	48.54	58.95	36.21		
		Fuzzy overall accuracy (%)		**53.14**		

Table 5.28: Supervised_FCM_3_classes_correlation coefficient

Classified data	Correlation_coefficient_3_classes_supervised_soft(FCM)			
	Reference			
		Burnt scar	Grasses and shrubs	Built-up area
	Burnt scar	0.88	-0.86	-0.21
	Grasses and shrubs	-0.77	0.82	-0.15
	Built-up area	-0.28	0.15	0.69

Table 5.29: Supervised_FCM_4_classes_fuzzy confusion matrix

4_classes							
Classified data	**Fuzzy confusion matrix_4_classes_supervised_soft(FCM)**					**Total**	**Fuzzy user accuracy (%)**
	Reference						
		Burnt scar	Trees	Grasses and shrubs	Built-up area		
	Burnt scar	182.55	45.98	144.48	26.10	399.11	45.74
	Trees	72.61	172.69	178.66	36.16	460.13	37.53
	Grasses and shrubs	142.71	159.08	766.67	36.98	1105.43	69.35
	Built-up area	61.31	86.16	98.18	37.19	282.84	13.15
	Total	459.17	463.91	1187.99	136.43	2247.50	
	Fuzzy producer accuracy (%)	39.76	37.23	64.53	27.26		
		Fuzzy overall accuracy (%)		**51.57**			

Table 5.30: Supervised_FCM_4_classes_correlation coefficient

	Correlation_coefficient_4_classes_supervised_soft(FCM)				
Classified data	**Reference**				
		Burnt scar	Trees	Grasses and shrubs	Built-up area
	Burnt scar	0.87	0.80	-0.54	-0.16
	Trees	-0.26	0.80	-0.37	0.11
	Grasses and shrubs	-0.11	-0.38	0.81	-0.26
	Built-up area	-0.19	0.32	-0.25	0.74

6. DISCUSSION, CONCLUSIONS AND RECOMMENDATIONS

6.1. Discussion

Fuzzy object results when there is uncertainty associated with the description of an object (Fisher, 1999). Uncertainties are of different types; hence there is need to be aware of the phenomenon that makes the description of the object of interest uncertain. In this research, the object of interest is the burn scar; its fuzziness is as a result of the presence of partially burnt pixels that lies between the boundary of a fully burnt pixels and un-burnt pixels. This zone is referred to as the transition zone, the boundary between the burnt scar and the un-burnt area is submerged within this zone making the delineation of the area described as burnt scar from that described as un-burnt very difficult, hence burnt scar definition is unclear or vague or fuzzy; this is why it is the choice for the study of fuzzy object. An attempt was made in this research to assess the accuracy of the burn scar phenomenon. In achieving this, several issues were considered: Are we interested only in the burnt scar or do we need as well some information about neighbouring features? Are we interested in a classification technique that will result in better description of the burnt scar phenomenon or we need a classification technique that will result in high accuracy? These issues where both considered by the classification methods used and as well as the number of classes generated. The steps taken and the results generated are explained below.

6.1.1. Re-projection

The acquired MODIS data was in the sinusoidal projection system, while the ASTER was in WGS 84, the MODIS data was re-projected to obtain the same coordinate as that of the ASTER, the reason for doing this, was to make sure both images overlay properly before further processing was carried out. Both images were overlaid and I can confirm both matched.

6.1.2. Re-sampling method

The acquired MODIS data had a pixel size of 463.31m, while that of the ASTER image was 15 m; the need to have an integer ratio between both datasets led to the resampling of the MODIS data to 495 m , using nearest neighbour resampling method. Nearest neighbour resampling method was chosen because it is simple to apply and preserves the DN values of the image, unlike other resampling method, however it can lead to positional errors (Jensen, 1996). The ratio formed between the MODIS and ASTER image was now 1:33.

6.1.3. Subsetting

A subset was created from the whole image that contains the area of interest in both images; this was used for studying the burn scar phenomenon. The dimension of the original MODIS data was 2400 by 2400 a subset of size 34 by 47 was created. The original ASTER image size was 4980 by 4200; the subset created was 1086 by 1506, all measurements were in meters. Both created subsets corresponded.

6.1.4. Classification methods

In order to meet the demand of several users, the research was conducted using both the crisp (unsupervised (ISODATA and supervised maximum likelihood)) and fuzzy classification (unsupervised and supervised fuzzy-c-means) methods; three cases involving 2, 3 and 4 classes respectively were experimented using each classifier.

6.1.5. Class separability

The separability of the classes were determined using the transformed divergence (crisp classification) because it takes into consideration the mean, variance and covariance of the clusters in determining the spectral distance or separaibilty between classes and represents them using a transformation scale (Swain & Davis, 1978). In ERDAS IMAGINE software, this scale is between 0 and 2000. A value of 2000 means the classes are completely separable, while a value of 0, means no separabilty. The fuzzy separabilty was investigated using the feature space plot of different combinations of bands.

6.1.6. Generating the reference

The ASTER image was used as the reference data. The reference data was generated from ASTER a fine resolution image, instead of using ground data or aerial photograph because of the following reasons:

- Ground data and aerial photographs were not readily available.
- Identification of pixel classes on the ground when ground data is used as reference can be very difficult.
- Acquisition of aerial photographs is usually expensive.
- Identification of classes on the ground is not objective, rather depends on expert knowledge(Okeke & Karnieli, 2006).

ASTER image as a reference data was also classified, before it was made comparable with the MODIS classified output. Various sources of error can plague the dataset and hence reduce the accuracy result. Some of the sources of these errors are:

- Errors generated from classification (Congalton & Green, 2009) - to reduce this effect, the same classification scheme was used for both the MODIS and ASTER datasets.
- Errors resulting from different date of data acquisition: The MODIS dataset was captured on the 14th of April 2004, while the ASTER was captured on the 16th April 2004, the acquisition date for both images is almost the same, this can help in reducing errors in the scheme.
- Another source of error results from the spatial difference between the two dataset,- both datasets; the MODIS dataset was resampled to become 495 m , while the ASTER is 15 m, both cannot be truly compared, unless they are of the same spatial resolution. To achieve this, the ASTER dataset was degraded to 495 m, by a scale window of 33 by 33 pixels; degrading the FCM output of the ASTER data was done by averaging the membership values of the pixels within the 33 by 33 window to obtain a mean value that corresponds to one MODIS pixel; degrading was also performed on the crisp ASTER output by determining the frequency of pixels with similar class label within a window size of 33 by 33, the class label with the highest frequency becomes the resultant class of the 33 by 33 window size pixels. Both method of degradation introduces error to the accuracy scheme, however, the error introduced was higher from the crisp approach than from the fuzzy approach, this was investigated by determining the correlation between the classified MODIS and the degraded ASTER output. In the fuzzy approach, the determined correlation value was between 0.58 - 0.84 for all the three cases in unsupervised FCM, in the supervised FCM, the correlation values obtained in all cases is between 0.69 - 0.85, comparing these values against that obtained in the crisp method, it was observed that the correlation value for ISODATA is between 0.48 – 0.75, for MLC, the value ranges between 0.32 – 0.71, this confirms the fact that the fuzzy degradation corresponds more to the MODIS classified output than that of the crisp degradation. However, users should be aware of this fact that the method of generating the reference data introduces error to the accuracy assessment scheme(Congalton & Green, 2009).
- The dimension of the degraded ASTER was 32 by 45, while that of MODIS was 33 by 47, to make both the ASTER and MODIS comparable, visual inspection led to the removal of 1 row and 2 columns from the MODIS, hence both datasets became fully comparable for accuracy assessment.

6.1.7. Sampling

In order to avoid the disadvantages of using samples discussed in table 2.3-1 and to possibly avoid the errors that can be introduced by this scheme, the whole dimensions of the reference data was completely compared with the whole MODIS classified output (both of dimension 32 by 45) this was done for both the crisp and fuzzy classification.

6.1.8. Training pixels

The numbers of pixels selected automatically by the software in the crisp unsupervised classification are larger than that obtained by the human operator during supervised classification. The number of pixels chosen and their relative position within the study area influences the variability achieved within class and interclass. The pixels obtained by the software were very large and less separable than that obtained by the human operator; hence, the classification results for both methods are influenced.

6.1.9. Classification results obtained

Different results were obtained for two, three and four classes for both the crisp and fuzzy classifications. The process started with the crisp classification, in which the un-supervised (ISODATA) and supervised (MLC) were performed, the accuracy was assessed using error matrix. Fuzzy classification was performed using unsupervised and supervised fuzzy-c-means; the accuracy of the classification was judged using the fuzzy error matrix. Another measure that was used in assessing the accuracy of both classified output and the reference is the Pearson's product moment correlation coefficient.

6.1.10. Classification results obtained- discussion for two classes obtained

2, 3 and 4 classes were each defined during the classification process in order to determine their effects on the accuracy measure that will be used. By visual assessment of the maps produced, for all the "2 classes", it was noticed that the unsupervised ISODATA classification and the unsupervised FCM produced maps in which the spatial extent of the burn scar were larger compared to their supervised counterparts, however, there is an abrupt change between the burnt scar and un-burnt area in the crisp classification, suggesting that the area of transition was not considered; in the FCM classification, the edges indicates a gradual change from burnt to un-burnt area, this explains the fact that the transitional zone was considered and the pixel belongs to either of the classes by their membership value, which was defined by the membership function; their accuracies were determined and it was observed that the overall accuracy for the ISODATA was 87.71%, the MLC was 89.72%, the unsupervised FCM was 81.19% and the supervised FCM was 80.57%. Also their correlation was determined with the supervised FCM, having the highest value of 0.85, the unsupervised reported 0.84, the MLC and ISODATA reported 0.61 and 0.72 respectively,; the supervised FCM, had the least overall accuracy and the highest correlation value, from this we can infer that supervised FCM gave a better description for the phenomenon, despite the fact that its overall accuracy was lowest, the reason is that, the uncertainty within the object was identified and modelled in describing the burnt scar, however, this value can either increase or decrease depending on the choice of training pixels used, this was seen from the low correlation value of 0.61 for supervised MLC, another human operator, can get either higher or lower values depending on the training samples. When supervised classification is used, the operator influences the choice of result and features to show. Kappa value of 0.63 was reported for ISODATA, while that of MLC was 0.52; largely the results obtained from supervised classification depend on the operator and the choice of training samples. From the separabilty value reported, the transformed divergence for MLC reported a value of 2000, indicating that the classes are distinct, hence other sources of error must have contributed to the low value, for example error from the reference data could have contribute to its low value. The producer and user accuracies were also determined in all cases. The supervised FCM reported the least user accuracy of 48.48% for the burn scar class and MLC reported the highest value of 98.39% for the un-burnt area. this means that 48.48% of the burn scar was actually identified as such in the FCM supervised classification, while that of

98.39% was actually truly un-burnt area as determined by MLC. In general, crisp classification indicates high accuracy value when compared to the fuzzy classification, however, it does not account for the transition boundary problems we are interested in. if the interest is to identify only burn scar and no neighbouring information is required, then definition of two classes is sufficient and suitable. needed, two classes definition is suitable in this regard.

6.1.11. Classification results obtained- discussion for three classes obtained

In a similar way like that of the "2 classes", the accuracy of the "3 classes" for all pixels were obtained, the MLC reported the highest overall accuracy value of 84.51%, the unsupervised FCM reported the least overall accuracy value of 74.46%, in this case, more variation was introduced in the supervised classification, by a slight change difference between class labels for supervised and unsupervised. In unsupervised (ISODATA), the labels are burn scar, trees and grasses and shrubs. For the supervised case(MLC) the labels are burn scar, vegetation and built-up area; the supervised method merged the grasses and shrubs class with the tree class to obtain the vegetation class, the training pixels were chosen in such a way that the rare class-(built-up area) can be extracted from the classification, this means with supervised method, rare classes can be easily made distinguishable because of the choice of training pixels we will collect.; hence we can create the desired class of interest. Visual assessment indicates that the sizes of the burn scar reduces as more classes are introduced, however, the supervised form of classification produced results that are more diverse because it included the rare class, which was submerged by the unsupervised classification. Uncertainties within the submerged boundary of the scar within the zone of transition were not considered by the crisp classification, the change from one class to the other is abrupt, and hence some information about the burn scar is lost. The FCM classification takes into consideration this transition zone problem by assigning grades of membership to the pixels as defined by the membership function, this result in better description of the burn scar phenomenon. From the defined three classes and comparing the overall accuracy of both the description of two classes and the description of 3 classes, it can be inferred that a more accurate result were obtained in the two classes in the tree classes definition, this means obtaining a better description for the burnt scar phenomenon can be best achieved when the map describes the burnt scar phenomenon and categorize other features as background.

6.1.12. Classification results obtained- discussion for four classes obtained

It is difficult accepting the class built-up area, created by the ISODATA and the un-supervised FCM, as a true reflection of the area on the ground, to have a better description, the MLC and supervised FCM were used, from the results obtained, we can see the intuitive form of the built-up area. Creating several undue classes can lead to errors; hence, the producer should be aware of this. In all the cases defined, the correlation values for fuzzy c means are high compared to the crisp cases. MLC produced the highest overall accuracy (77.29%), the least overall accuracy was reported by the un-supervised FCM (68.81%). The correlation value for the built-up area is highest in the supervised FCM, while the least correlation was reported in the MLC.

There is always a trade-off, between using a classification method that describes the fuzzy object better and using the one that leads to higher accuracy result. If the intention is to describe the fuzzy object, then the fuzzy approach should be adopted, but we need to be aware that the accuracy might not very high.

6.2. Conclusion

The objective of this research was to determine how the accuracy of a fuzzy object can be assessed, to determine this, there is need to establish the fuzziness associated with the word object. From literature review, it was identified that fuzziness is one type of uncertainty, that results when an object cannot be clearly defined(Fisher, 1999). An object is made of its interior and its boundary point, the easy delineation of the boundary of an object makes it definition clear, for example determining the boundary of a building, this can be done without difficulty; fuzzy objects are not easily defined, this is because their boundary points cannot be easily determined, they are submerged within the zone of transition between the object and its neighbours, the spatial extent of an object, corresponds to the totality of its interior touching the boundary point, when the boundary cannot be established the spatial extent cannot be established, hence the object cannot be fully defined. The forest fire burn scar that occurred in April 2004 at the Apalachicola national forest in Florida was chosen as the fuzzy object of interest. The definition of the forest fire burn scar was established as the damage or injury that results when forest fire occurs, it is characterised by the presence of dark or black patches within the area affected by fire, the area contains burnt pixels, partially burnt pixels and un-burnt pixels, the partially burnt pixels, contains the boundary of the burn scar and the un-burn area and it is within the zone of transition, between the two phenomena.

.

ASTER was obtained as a fine resolution image, which was used as the reference data. The ASTER data as a reference was classified like the MODIS data; this was done to make both comparable. Crisp and fuzzy methods were applied in creating the reference data; this was later degraded to make its resolution the same as that of the MODIS.

To determine the accuracy measure that is applicable, the crisp and fuzzy accuracy assessment measures were used, the crisp method used was the error matrix and the fuzzy method used fuzzy error matrix. The accuracy produced by the crisp method was higher than that of the fuzzy error matrix, however, the fuzzy approach provided a better description of the phenomenon because it takes into consideration, the uncertainty resulting from unclear boundary definition (vagueness).

6.3. Recommendation

This research was carried out to describe and determine the accuracy of the burn scar phenomenon as a fuzzy object; the issues to consider before assessing the accuracy of burn scar were discussed. This research is also a stepping stone on which further work can be done; hence I recommend that the work can progress further, by the consideration of the following:

- Adding contextual and or auxiliary information to improve the output of the fuzzy-c-means.
- Considering the use of another fuzzy classifier to determine which will produce a better result, such as possibility c means.
- Defining and modelling another form of uncertainty that will be investigated in defining the burn scar phenomenon, such as the mixed pixel problem.
- Consideration for generating soft reference from another approach other than from fine resolution images.

LIST OF REFERENCES

Ambrosia, V. G., & Brass, J. (1988). Thermal analysis of wildfires and effects on global ecosystem cycling. *Geocarto International, 1*, 29-39.

Aronoff, S. (1982). The map accuracy report: a user's view. *Photogrammetric Engineering and Remote Sensing, 48*(8), 1309-1312.

Aronoff, S. (1985). The Minimum Accuracy Value as an Index of Classification Accuracy. *Photogrammetric Engineering and Remote Sensing, 51*(1), 99-111.

Atkinson, P. M., & Foody, G. M. (2006). *Uncertainty in Remote Sensing and GIS: Fundamentals*: John Wiley & Sons, Ltd.

Bezdek, J. C. (1981). *Pattern Recognition with Fuzzy Objective Function Algoritms*. New York: Plenum Press, New York.

Bezdek, J. C., Ehrlich, R., & Full, W. (1984). FCM: The fuzzy c-means clustering algorithm. *Computers & Geosciences, 10*(2-3), 191-203.

Binaghi, E., Brivio, P. A., Ghezzi, P., & Rampini, A. (1999). A fuzzy set-based accuracy assessment of soft classification. *Pattern Recognition Letters, 20*(9), 935-948.

Bolstad, P. (2005). *GIS Fundamentals* (2nd ed.). White Bear Lake, MN: Eider Press.

Card, D. H. (1982). Using Known Map Category Marginal Frequencies to Improve Estimates of Thematic Map Accuracy. *Photogrammetric Engineering and Remote Sensing of Environment, 48*(3), 431-439.

Cheng, T. (2002). Fuzzy objects: Their changes and uncertainties. *Photogrammetric Engineering and Remote Sensing, 68*(1), 41-49.

Cheng, T., & Molenaar, M. (1999). Objects with fuzzy spatial extent. *Photogrammetric Engineering and Remote Sensing, 65*(7), 797-801.

Cheng, T., Molenaar, M., & Lin, H. (2001). Formalizing fuzzy objects from uncertain classification results. *International Journal of Geographical Information Science, 15*(1), 27 - 42.

Cliff, A. D., & Ord, J. K. (1973). *Spatial autocorrelation*. Pion: London.

Congalton, R. (1988). A comparison of sampling schemes used in generating error matrices for assessing the accuracy of maps generated from remotely sensed data. *Photogrammetric Engineering & Remote Sensing, 504*(5), 593-600.

Congalton, R. (2004). Putting the Map Back in Map Accuracy Assessment. In R. S. Lunetta & J. G. Lyon (Eds.), *Remote Sensing and GIS Accuracy Assessment* (pp. 1-11): Taylor & Francis Inc.

Congalton, R., & Green, K. (1993). A Practical Looks at the Sources of Confusion in Error Matrix Generation. *Photogrammetric Engineering and Remote Sensing of Environment, 59*(5), 641-644.

Congalton, R., & Green, K. (1999). Assessing the Accuracy of Remotely Sensed Data: Principles and Practices.

Congalton, R., & Green, K. (2009). *Assessing the Accuracy of Remotely Sensed Data* (2nd ed.): CRC Press Inc.

Decoursey, W., J. (2003). *Statistics and Probability for Engineering Applications*: Elseiver Science, USA.

Denoeux, T., & Masson, M. (2004). Principal component analysis of fuzzy data using autoassociative neural networks. *IEEE Transactions on Fuzzy Systems, 12*, 336-349.

Dunn, J. (1974). Well separated clusters and optimal fuzzy partitions. *Journal of Cybernetics, 4*, 95-104.

ERSDAC. ASTER SCIENCE PROJECT. Retrieved 2nd February, 2011, from http://www.science.aster.ersdac.or.jp/t/en/documnts/users_guide/part1/04_02_02_2.html

Fisher, P. F. (1997). The Pixel: A Snare and a Delusion. *Internation Journal of Remote Sensing of Environment, 18*, 679-685.

Fisher, P. F. (1999). Models of uncertainty in spatial data. In P. A. Longley, M. F. Goodchild, D. F. Maguire & D. W. Rhind (Eds.), *Geographical Information Systems: Principles and technical issues* (2nd ed., Vol. 1, pp. 191-205). New York: John Wiley & Sons, Ltd.

Fisher, P. F., Arnot, C., Wadsworth, R., & Wellens, J. (2006). Detecting change in vague interpretations of landscapes. *Ecological Informatics, 1*(2), 163-178.

Foody, G. M. (1996). Approaches for the production and evaluation of fuzzy land cover classifications from remotely-sensed data. *International Journal of Remote Sensing, 17*(7), 1317 - 1340.

Foody, G. M. (1999). The continuum of classification fuzziness in thematic mapping. *Photogrammetric Engineering and Remote Sensing, 65*(4), 443-451.

Foody, G. M. (2002). Status of land cover classification accuracy assessment. *Remote Sensing of Environment, 80*(1), 185-201.

Foody, G. M. (2008). Harshness in image classification accuracy assessment. [Proceedings Paper]. *International Journal of Remote Sensing, 29*(11), 3137-3158.

Foody, G. M. (2009). The impact of imperfect ground reference data on the accuracy of land cover change estimation. *International Journal of Remote Sensing, 30*(12), 3275-3281.

Fowler, A. D. (1991). The fractal geometry of nature (revised edition): by B. B. Mandelbrot, 1983, W. H. Freeman & Co., New York, 468p., ISBN 0-7167-1186-9. *Computers & Geosciences, 17*(7), 1065-1066.

Fuller, R. M., Groom, G. B., & Jones, A. R. (1994). The land-cover map of Great-Britain -an automated classification of landsat thematic mapper data. *Photogrammetric Engineering and Remote Sensing, 60*(5), 553-562.

Gopal, S., & Woodcock, C. (1994). Theory and methods for accuracy assessment of thematic maps using fuzzy sets. *Journal Name: Photogrammetric Engineering and Remote Sensing; (United States); Journal Volume: 60:2*, Medium: X; Size: Pages: 181-188.

Green, K., & Congalton, R. (2009). An Error Matrix Approach to Fuzzy Accuracy Assessment. *Remote Sensing and GIS Accuracy Assessment*: CRC Press.

Hammen, J. (1997). Introductory digital image processing: A remote sensing perspective. *Professional Geographer, 49*(3), 382-382.

Jensen, J. R. (1996). *Introductory Digital Image Processing: A Remote Sensing Perspective*: Upper Saddle River, NJ: Prentice-Hall.

Key, C. H., & Nate, C. B. (2004). Landscape Assessment: Sampling and Analysis Methods. *Alaska Park Science 4*(1).

Khorram, S., Biging, G., Chrisman, N. R., Colby, D. R., Congalton, R., Dobson, J. E., et al. (1999). Accuracy Assessment of Remote Sensing-Derived Change Detection. *American Society of Photogrammetry and Remote Sensing (ASPRS),*, 58.

Knight, J. F. (2002). *Accuracy Assessment of Thematic Maps Using Inter-Class Spectral Distances.* North Carolina State University.

Landis, J. R., & Koch, G. G. (1977). The Measurement of Observer Agreement for Categorical Data. *Biometrics, 33*, 159-174.

Lark, R. M. (1995). Components of accuracy of maps with special reference to discriminant-analysis on remote sensor data. *International Journal of Remote Sensing, 16*(8), 1461-1480.

Liang, S., Fang, H., & Chen, M. (2001). Atmospheric correction of Landsat ETM+ land surface imagery: I. Methods. *IEEE Transactions on Geoscience and Remote Sensing, 39*, 2490-2498.

Lillesand, T. M., & Kiefer, R. W. (1994). *Remote Sensing and Photo Interpretation* (3rd ed.). New York: John Wiley & Sons.

Lizarazo, I., & Barros, J. (2010). Fuzzy Image Segmentation for Urban Land-Cover Classification. *Photogrammetric Engineering and Remote Sensing, 76*(2), 151-162.

Maselli, F., Gilabert, M. A., & Conese, C. (1998). Integration of High and Low Resolution NDVI Data for Monitoring Vegetation in Mediterranean Environments. *Remote Sensing of Environment, 63*(3), 208-218.

McNicoll, G. (1997). Geographic objects with indeterminate boundaries - Burrough,PA, Frank,AU. *Population and Development Review, 23*(2), 437-438.

Memarsadeghi, N., Netanyahu, N. S., & LeMoigne, J. (2006). A Fast Implementation of the ISODATA Clustering Algorithm. *International Journal of Computational Geometry and Applications*.

Meyer, M., Brass, J., Gerbig, B., & Batson, F. (1975). *ERTS Data Applications to Surface Resource Surveys of Potential Coal Production lands in Southeast Montana,* : University of Minnesota.

Molenaar, M., & Cheng, T. (1998). Fuzzy spatial objects and their dynamics. *In: Proceedings of the ISPRS proceedings, Vol. XXII, pt. 4. GIS between visions and applications, Stuttgart, 1998. pp. 389-394*.

Okeke, F., & Karnieli, A. (2006). Methods for fuzzy classification and accuracy assessment of historical aerial photographs for vegetation change analyses. Part I: Algorithm development. [Article]. *International Journal of Remote Sensing, 27*(1), 153-176.

Pontius, R. G. (2000). Quantification error versus location error in comparison of categorical maps. *Photogrammetric Engineering and Remote Sensing, 66*(8), 1011-1016.

Przyborski, P. (2004). East Fork Fire Burn Scar. Retrieved 02 November, 2010, from http://earthobservatory.nasa.gov/IOTD/view.php?id=4411

Rains, D. (2010). Get to Know Your National Forests in Florida. www.fs.fed.us/r8/florida

Richards, J. (1993). *Remote Sensing Digital Image Analysis: An introduction* (2nd ed.). Berlin: Spring-Verlag.

Smits, P. C., Dellepiane, S. G., & Schowengerdt, R. A. (1999). Quality assessment of image classification algorithms for land-cover mapping: a review and a proposal for a cost-based approach. *International Journal of Remote Sensing, 20*(8), 1461-1486.

SPEAR. (2006). Remote Sensing and Land Classification (Remote_sensing_tutorial_mar06.PPT). Retrieved 15/02/2011, 2011, from http://www.biaoqiang.org/default.aspx?
Stehman, S. V. (1997). Selecting and interpreting measures of thematic classification accuracy. *Remote Sensing of Environment, 62*(1), 77-89.
Stehman, S. V., & Czaplewski, R. L. (1998). Design and Analysis for Thematic Map Accuracy Assessment: Fundamental Principles. *Remote Sensing of Environment, 64*(3), 331-344.
Swain, P. H., & Davis. (1978). *Remote Sensing: The Quantitative Approach*: McGraw-Hill.
Tso, B., & Mather, P. M. (2001). *Classification methods for remotely sensed data*. London etc.: Taylor & Francis.
Van Genderen, J. L., & Lock, B. F. (1977). Testing Land Use Map Accuracy. *Photogrammetric Engineering and Remote Sensing, 43*(9), 1135-1137.
Van Genderen, J. L., Lock, B. F., & Vass, P. A. (1978). Remote Sensing: Statistical Testing of Thematic Map Accuracy. *Remote Sensing of Environment, 7*, 3-14.
Wang, F. (1990). Fuzzy supervised classification of remote sensing images. *Geoscience and Remote Sensing, IEEE Transactions on, 28*(2), 194-201.
Weng, Q., & Lu, D. (2007). A survey of image classification methods and techniques for improving classification performance. *International Journal of Remote Sensing of Environment, 28*, 823-870.
Williams, J. K., Kessinger, C., Abernethy, J., & Ellis, S. (2009). Fuzzy Logic Applications (pp. 347-377).
Zadeh, L. (1965). Fuzzy Sets *Information and Control* (pp. 338-353).
Zhang, J., Marszalek, M., Lazebnik, S., & Schmid, C. (2007). Local features and kernels for classification of texture and object categories: A comprehensive study. *IJCV, 73*(2), 213-238.

APPENDIX

CODE FOR GENERATING ACCURACY ASSESSMENT FOR SUPERVISED FCM_2_CLASSES

```
require(MASS)
require(mvtnorm)
require(pixmap)

library(MASS)
library(mvtnorm)
library(pixmap)

Path <- 'D:\\Thesis_modis\\'

# Fuzzy parameter
m <- 2.0

# Number of classes
Ncl <- 1

# Number of bands
Nb <- 5

dir.create(Path, recursive = TRUE)

Outputfile <- 'FCM'


##############################################################
# Import image FCM for MODIS
##############################################################
##############################################################
# Import image
##############################################################

i<-1

Inputfile <- paste(Path, 'FCM_Membership_modis_2_classes_supervised_class_',i,'.txt', sep='')

temp <- read.table(Inputfile)

# Determine image dimension
d <- dim(temp)
M <- d[1]
N <- d[2]

x <- 1:M
y <- 1:N
```

```
D  <- array(0, c(Ncl,M,N))

D[i,,] <- as.matrix(temp)

for(i in 1:Ncl)
{
       Inputfile <- paste(Path, 'FCM_Membership_modis_2_classes_supervised_class_',i,'.txt', sep='')

       temp <- read.table(Inputfile)

       D[i,,] <- as.matrix(temp)
}

U<-D

#D[i,,] <- (D[i,,]-min(D[i,,]))*255/max(D[i,,]) #normalization but to confirm how????

# Remove ridiculous values

#D[D<0] <- 0
#D[D>1] <- 1


#
# Display bands

windows(title='Multispectral image: grayscale')
Nrow <- round(sqrt(Nb))
par(mfrow=c(3,3))

for(k in 1:Ncl) image(x,y, D[k,,], col=gray((0:255)/255), main = paste('Band ',k,sep=''), xlab='',ylab=''))


################################################################
#############################
# Display results
################################################################
##############################

windows(title='FCM result: membership values')
Nrow <- round(sqrt(Ncl))
par(mfrow=c(Nrow,round(Ncl/Nrow)))

for(k in 1:Ncl)
{
   image(x,y, U[k,,], col=gray((0:255)/255), main = paste('Class ',k,sep=''), xlab='',ylab='')
}
```

```
################################################################
# Import Fuzzy reference membership value for ASTER
################################################################

Path <- 'D:\\Thesis_aster\\'

dir.create(Path, recursive = TRUE)

S <- 33

ia <- 1
Nba <- 2
Ncla <- 2
Inputfile_aster <- paste(Path, 'FCM_Membership_aster_2_classes_supervised_class_',ia,'.txt', sep='')

temp_aster <- read.table(Inputfile_aster)

# Determine image dimension
da <- dim(temp_aster)
Ma <- da[1]
Na <- da[2]

xa <- 1:Ma
ya <- 1:Na

Da  <- array(0, c(Ncla,Ma,Na))

Da[ia,,] <- as.matrix(temp_aster)

for(ia in 1:Ncla)
{
	Inputfile_aster <- paste(Path, 'FCM_Membership_aster_2_classes_supervised_class_',ia,'.txt', sep='')

	temp_aster <- read.table(Inputfile_aster)

	Da[ia,,] <- as.matrix(temp_aster)
}




# Display bands

windows(title='ASTER FCM_MEMBERSHIP BEFORE DEGRADE: grayscale')
Nrow <- round(sqrt(Nba))
par(mfrow=c(3,3))

for(ka in 1:Ncla) image(xa,ya, Da[ka,,], col=gray((0:255)/255), main = paste('class ',ka,sep=''),
xlab='',ylab='')
```

```
##################################################################
#
#Degrade ASTER membership values
##################################################################
###
Mdeg <- floor(Ma/S)
Ndeg <- floor(Na/S)

xdeg <- 1:Mdeg
ydeg <- 1:Ndeg

UA <- array(0,c(Ncla,Mdeg,Ndeg))


for(i in 1:Mdeg)
for(j in 1:Ndeg)
for(l in 1:Ncla)
{
    UA[l,i,j]<- mean(Da[l,((i-1)*S+1):(i*S),((j-1)*S+1):(j*S)])
}

x11()
par(mfrow=c(2,2))
for(k in 1:Ncla)
{
  image(xdeg,ydeg, UA[k,,], col=gray((0:255)/255), main = paste('Degraded Aster Class ',k,sep=''),
xlab='',ylab='')
}

##################################################################
##############
# Reference creation
##################################################################
#############
F_Ref <- array(0,c(Ncla,Mdeg,Ndeg))
F_M <-   array(0,c(Ncla,Mdeg,Ndeg))

F_ref <- UA

dim(F_ref)


##################################################################
################################################
# REmoving pixels from modis to have corresponding points 2 rows and one colunm was removed from
the MODIS
##################################################################
#################################################
```

```
F_M <- U[,-47,-33]
F_M <- F_M[,-1,]
########################################
#Recode and sign classes
#F_rec <- F_M

#F_rec[1,,] <- F_M[2,,]
#F_rec[2,,] <- F_M[1,,]
##############################################

##################################################################
##
# check the correlation to see how the bands relate after degrading
#aster and removing 2 rows and one column from modis to have
#corresponding dimesions
##################################################################
####
#correlation



Z <- array(0,c(Ncl,Ncl))
for(k in 1:Ncl)
for(l in 1:Ncl)

{Z[k,l] <- cor(as.vector(F_M[k,,]),as.vector(F_ref[l,,]))
}
Z


#x11()
#par(mfrow=c(2,2))
#for(k in 1:Ncl)image(xdeg,ydeg,F_rec[k,,],col=gray((0:255)/255))
##########################################################




#F_ref <- array(0,c(Ncl,Mdeg,Ndeg))
#F_M <-   array(0,c(Ncl,Mdeg,Ndeg))

F_ref <- UA
F_M <- U[,-47,-33]
F_M <- F_M[,-1,]
########################################
#Recode and sign classes
```

```
#F_rec <- F_M

#F_rec[1,,] <- F_M[2,,]
#F_rec[2,,] <- F_M[1,,]
##############################################

#x11()
#par(mfrow=c(2,2))
#for(k in 1:Ncl)image(xdeg,ydeg,F_rec[k,,],col=gray((0:255)/255))


#################################################################
###############################
# Accuracy assessment: fuzzy error matrix
#################################################################
###############################

Ncl <- 2
Ferm <- array(0,c(Ncl,Ncl))
Fuser <- array(0,Ncl)
Fprod <- array(0,Ncl)

for(k in 1:Ncl)
for(l in 1:Ncl)
{
 Ferm[k,l]<- sum(pmin(F_M[k,,],F_ref[l,,]))
}

FOA <- sum(diag(Ferm))/sum(Ferm)
for(k in 1:Ncl)
{
  Fuser[k] <- Ferm[k,k]/sum(Ferm[k,])
  Fprod[k] <- Ferm[k,k]/sum(Ferm[,k])
}


Ferm
FOA
Fuser
Fprod
```